KWAME NKRUMAH UNIVERSITY OF SCIENCE AND TECHNOLOGY KUMASI, GHANA

FAST FOURIER TRANSFORM (FFT) ANALYSIS ON NDVI TIME SERIES FOR ASSESSMENT OF VEGETATION PATTERNS IN GHANA

BY

QUASHIE, GILBERT KOBLA

(PGD, GEOINFORMATICS, RECTAS, BSC GEOMATIC ENG., KNUST)

THESIS

A Thesis submitted to the Department of Geomatic Engineering, Kwame Nkrumah University of Science and Technology In partial fulfillment of the requirements for the degree of

MASTER OF SCIENCE
IN
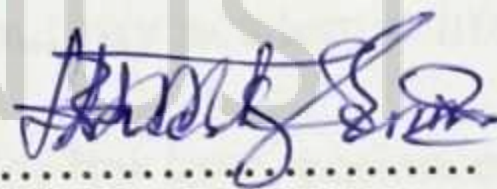### _ (GEOMATIC ENGINEERING)

College of Engineering

October 2013

DECLARATION

I Quashie Gilbert Kobla, declares that this thesis is my own work and that it contains

neither material previously published by any other person nor material which has been

accepted for the award of any other degree of any University, except where due

acknowledgement has been made in the text.
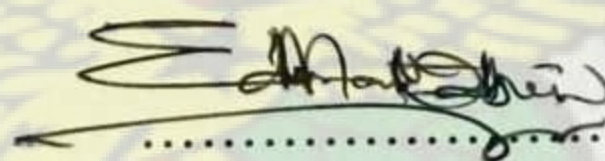
Quashie, Gilbert Kobla (PG 5871311) 31-10-2013

Student Name and ID   Signature   Date

Certified by:

Dr. Edward M. Osei Jnr 31/10/2013

Supervisor(s) Name   Signature   Date

Certified by:

Rev. John Ayer 31/10/2013

Head of Dept. Name   Signature   Date

DEDICATION

And we know that all things work together for the good to those who Love God and those who are called according to his purpose. Romans 8 : 28

This project is first and foremost dedicated to the Almighty God for his Divine Grace and Mercy that saw me through this course of study.

It is also dedicated to my Father, Mr. Johnson Kwame Quashie, for his unflinching fatherly support and encouragement throughout my academic life and to my beautiful and lovely wife Mrs. Catherine Yaa Quashie for her love, patience and understanding.
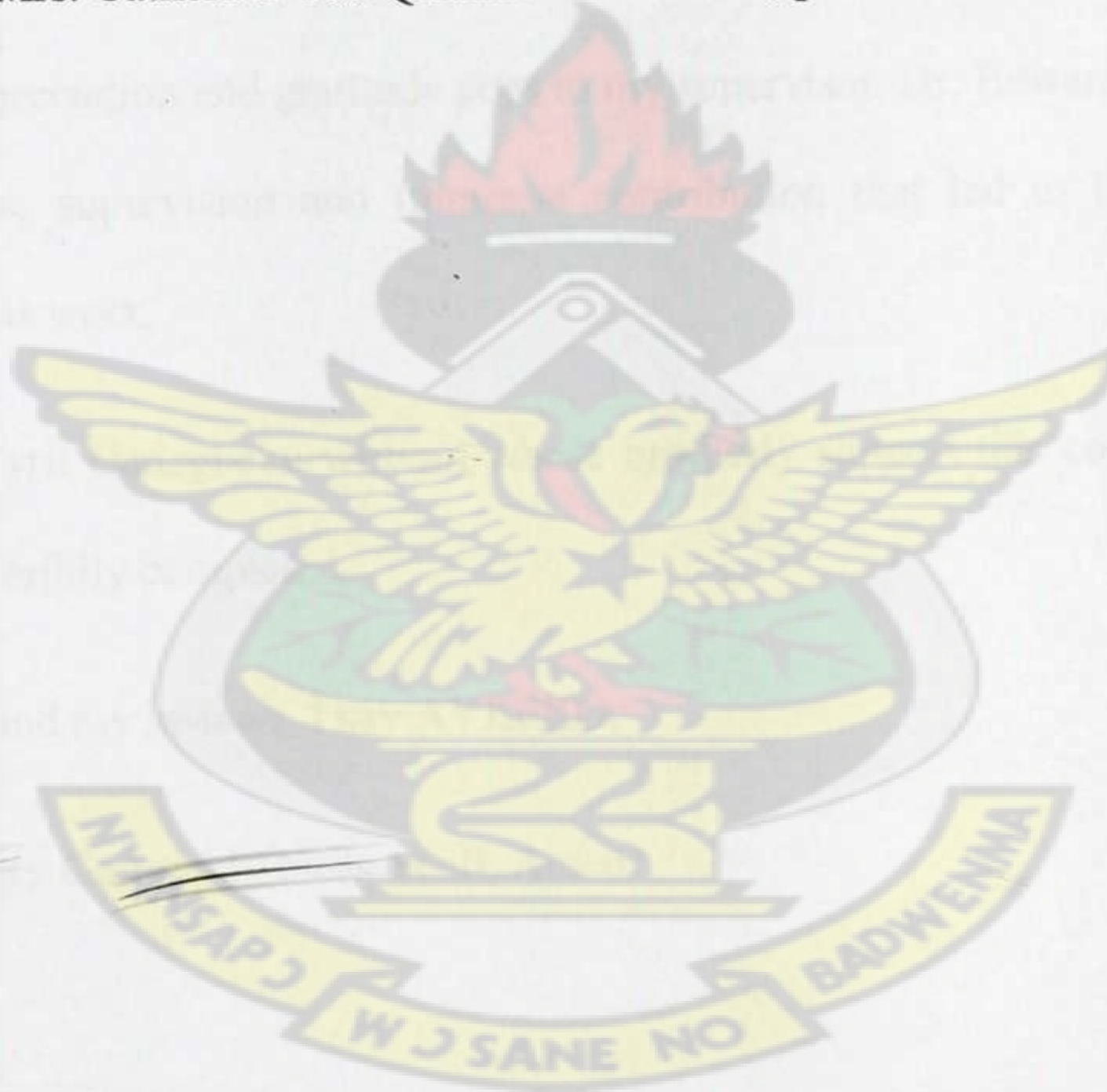
ACKNOWLEDGEMENTS

I wish to express my profound gratitude to the Almighty God who has made it possible for the successful completion of this course.

I wish to also express my immeasurable appreciation to the Government of Ghana, The Executive Director of Lands Commission, The Director, Survey and Mapping Division of Lands Commission, the Principal, Ghana School of Surveying and Mapping and the entire Staff of the Lands Commission, Accra, Ghana for assisting me throughout this course.

My sincerest appreciation and gratitude goes to my supervisor, Dr. Edward M. Osei Jnr. for his guidance, supervision and immense contribution that led to the successful completion of this work.

Kudos to Mr. Cyril Gadegbeku without whose brotherly support this course wouldn't have been successfully completed.

To my siblings and my in-laws, I say AYEEKO.

May the Almighty God richly bless us all, Amen.

TABLE OF CONTENTS

Content		Page

CHAPTER TWO: LITERATURE REVIEW - - - **11**

CHAPTER THREE: MATERIALS AND METHOD - - - **41**

LIST OF TABLES

LIST OF FIGURES

KNUST

Appendix I Figures

ABSTRACT

Time series analysis of Normalized Difference Vegetation Index (NDVI) imagery is a powerful tool in studying vegetation phenology in data scarce and inaccessible areas. Application of these datasets involves typically, per-pixel analysis of multi-temporal Vegetation Indices (VIs), which are frequently subject to high-frequency fluctuations (i.e. noise) caused by changing atmospheric conditions and varying sun-sensor-surface geometries. A broad range of NDVI noise-reduction strategies are applied in an effort to either reduce or if possible remove completely such embedded noise in these dataset. However, rarely are the benefits of applying such noise reduction techniques questioned. In light of this, the Fast Fourier Transform (FFT), a noise reducing algorithm in Erdas Imagine was applied to two averaged National Oceanic and Atmospheric Administration (NOAA) – Advanced Very High Resolution Radiometer (AVHRR) NDVI images acquired from Global Inventory Modeling and Mapping Studies (GIMMS) for Africa. The two averaged images were calculated from 792 NDVI images representing 1996 (i.e. 1986 -1996, 396 images) and 2006 (i.e. 1996 - 2006, 396 images). Although the FFT algorithm did offer statistically significant benefit, this occurred much less often than might be assumed. It therefore suggests that noise reduction techniques are not universally beneficial, and can, in fact, be detrimental in some situations especially when the extraction of phenological signatures is the ultimate goal. Six randomly selected scenes of TM images were classified into 6 different Vegetation pattern using supervised clustering and maximum likelihood classifications algorithm. This information was used for selecting training signatures in the NDVI images and vegetation maps representing 1996 and 2006 produced. These maps were visually assessed for land cover changes during the 10 year period, and the comparison shows an alarming rate of degradation over the 10-year period.

CHAPTER ONE

INTRODUCTION

1.1 Background

The study of recurrent vegetative, biophysical events such as springtime budburst, leaf-out, flowering and autumnal senescence is referred to as vegetation phenology (Badeck et al., 2004). Agricultural interests in vegetation phenology date back thousands of years, with more recent interests expanding considerably to include those of biologists, ecologists, climatologists and other researchers (Zhang et al., 2004). This interest stems from the recognition that close relationships exist between vegetation phenology and both biotic and abiotic environments. For instance, plant growth and development is affected by air and soil temperatures, solar illumination, moisture and photoperiod (Reed et al., 1994). Vegetation phenology is therefore one of the most responsive and easily observable environmental traits that varies in response to climate, rendering it of particular interest in global climate change research (Badeck et al., 2004). In addition, animal activity, movement and population dynamics including migratory patterns (Sanz et al., 2003), breeding behaviour (Loe et al., 2005) and species richness and distribution (Hurlbert and Haskell, 2003) can be closely linked to seasonal vegetative growth. Thus, not only does vegetation phenology provide a means of studying the terrestrial effects of climatic variation and change, but also, the effects of land use and land cover change on ecosystem processes and dynamics.

The need for regional to global scale datasets in support of contemporary earth science research initiatives continues to grow. The launch of the Landsat Multispectral Scanner in the early 1970s and the subsequent availability of satellite imagery with global coverage initiated the remote sensing of vegetation phenology. Beginning with applications in the enhancement of land cover classification and the development of

1

spectrally based crop calendars (MacDonald and Hall, 1980; Badhwar, 1982), remotely sensed phenological information has become increasingly attractive to researchers interested in large area earth and atmospheric dynamics. Over the past three decades a variety of multi spectral sensors have been employed to provide the data sources necessary for the remote sensing of vegetation phenology, particularly with the launch of the AVHRR sensor in the early 1980s. Some of these research initiatives include; mapping vegetative transitions in areas of intensive ranching (Dougill et al., 1999), detecting crop planting and harvesting dates (Sakamoto et al., 2005), linking phenology to other observable biophysical parameters like Leaf Area Index (LAI) or Gross Primary Production (GPP) (Turner et al., 2003; Wang et al., 2005a; Wang et al. 2005b), characterizing vegetation types (Xiao et al., 2002), studying vegetation response to ecological change (Pettorelli et al., 2005), and linking changes in phenological event timing and duration to climatological shifts (Yang et al., 1997).

Spectral vegetation indices (VIs) often form the basis for remote sensing-based phenological investigations (Townshend and Justice, 1986; Huete et al., 2002). VIs have been closely linked to the chlorophyll content and structural characteristics of green vegetation at the surface (Myneni et al., 1995) and are therefore particularly useful for studying vegetation health and development. Multi temporal datasets of the normalized difference vegetation index (NDVI) are particularly prevalent throughout the literature and continue to be the principal data source for numerous remote sensing based phenological studies (Pettorelli et al., 2005). Its ease of application, long tradition of use and a demonstrably close relationship with photosynthetic activity at the surface (Myneni et al., 1995) have contributed to the popularity of the NDVI over the past two decades. Notwithstanding the extensive use of VI time series in the remote sensing of vegetation phenology, the noise in these datasets continues to be an issue of importance.

2

Varying atmospheric conditions caused by cloud, ozone, dust, and other aerosols, and varying sun-sensor-surface angle geometries manifested in bidirectional reflectance, and sensor calibration and co-registration errors as shown if figure 1.1, all contribute to variations in the data that are unrelated to surficial vegetative phenology or conditions of interest, and are therefore considered noise (Goward *et al.*, 1991; Viovy *et al.*, 1992; Cihlar *et al.*, 1997; Huete *et al.*, 1999; Roerink *et al.*, 2000; Kang *et al.*, 2005; Sakamoto *et al.*, 2005).
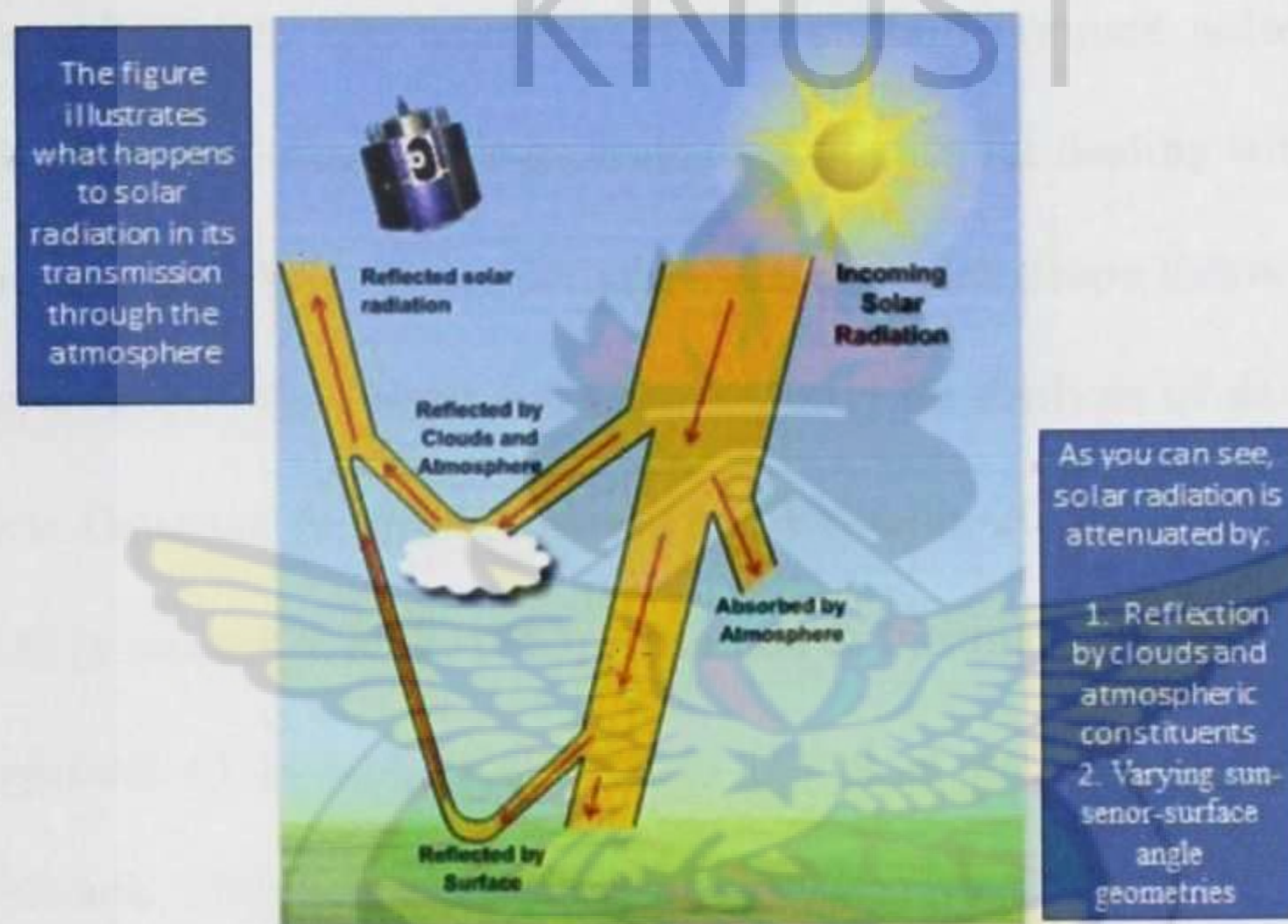
Figure 1.1: Causes of Noise in NDVI Datasets (Source: Sakamoto *et al.*, 2005)

This noise must be minimized before VI datasets can be used either efficiently or effectively for phenological investigations. Some pre-processing is possible, and in newer datasets it is a standard procedure before the data is released to the public (Huete *et al.*, 1999). However, precise and rigorous atmospheric and geometric corrections are neither practical nor feasible, both because of the size of modern satellite image datasets and generally the unavailability of necessary detailed ancillary information (Cihlar *et al.*, 1997). As an alternative, a multitude of techniques for further reducing noise in multi temporal VI datasets are found in the literature. These can range from simple

temporal compositing and moving average filters, to more complex techniques involving fourier analysis or wavelet transforms (e.g. van Dijk *et al.*, 1987; Menenti *et al.*, 1993; Sakamoto *et al.*, 2005). The benefits of temporal compositing for multi temporal VI datasets became apparent in the 1980s, and continue to be recognized as an important noise reduction method (Holben, 1986; Chen *et al.*, 2003).

Indeed, it is now standard procedure for many publicly available remotely sensed VI datasets to be composited before distribution. Despite the application of compositing, however, composited data sets nevertheless still contain remnant noise that requires further consideration, and there is a multitude of strategies for dealing with this remnant noise (Carreiras *et al.*, 2003). These include the Best Index Slope Extraction algorithm (BISE) (Viovy *et al.*, 1992; Lovell and Graetz, 2001) for analysis of daily NDVI data, the Asymmetric Gaussian function (Jonsson and Eklundh, 2002), Principal Component Analysis (PCA) (Eastman & Fulk, 1993; Anyamba & Eastman, 1996; Gurgel & Fereira, 2003), development of phenological metrics (Reed *et al.*, 1994; Lee *et al.*, 2002; Jönsson & Eklundh, 2004; Verbesselt *et al.*, 2006), change detection (Coppin *et al.*, 2004), a Savitzky- Golay filtering algorithm (Chen *et al.*, 2004), the Mean-Value Iteration filter (MVI) (Ma and Veroustraete, 2006), and the weighted least-squares linear regression to the temporal NDVI signal (Swets *et al.*, 1999), among others. Even though these algorithms have been successfully used in many different applications, limitations need to be mentioned. For instance, the length of the sliding window and threshold value in BISE method may need to be adapted to different phenological stages and for different plant species. The weighted least-squares linear regression and the Asymmetric Gaussian function could not capture the complex phenology of land cover characterized by two or more growth cycles in one year. PCA as a fusing technique for classification depends on the datasets being evaluated and also on the

4

analysts experience with using the technique. Although the use of PCA might result in good quality images, one of the limitations of this technique, as reported in many research papers is the concern over colour distortions and loss of spectral information (Nikolakopoulos, 2008). The reliability of the Savitzky-Golay filtering algorithm strongly depends on the assumption that the envelope of the original data gives the best description of vegetation growth, while this concept may lead to overestimate of the NDVI values, which are in most cases generated using the Maximum Value Composite (MVC) method.

1.2 Statement of the Problem

In the last few years, the scientific community has shown increasing interest in developing computational tools for extracting subtle signatures of the behavior of vegetation on the Earth's surface through monitoring time series of the NDVI determined from multichannel spectrometers on board earth orbiting satellites (Hermance et al., 2007). These observations provide a common base of self-consistent long-term time series, from local to global scales. The analysis of such data provides a significant insight into the response of vegetation to short and long term environmental forcing effects, both natural and anthropogenic (Hermance et al., 2007), and provide valuable information in assessing spatial distributed linkages between climate properties, vegetative phenological cycles and rain fed land use (Tucker, 1979).

Since different plant species tend to respond differently to fluctuations of environmental factors, their phenology can be used on a site by site (i.e., pixel by pixel) basis to identify particular land cover types and monitor their response to typical climate and weather conditions, as well as their response to anomalous conditions of extreme drought, storms, and wildfire (Hermance et al., 2007). However, the persistent noise

inherent in these data sets continues to be of great concern and to reduce these noises and generate a cloud-free NDVI time series data for analysis, a number of methods have been developed and have been successfully applied in some cases.

In this present study, the effectiveness of the FFT algorithm will be assessed and evaluated. In the FFT algorithm, the signal for each individual pixel can be decomposed into its Fourier components, such as series of harmonic sine or cosine waves, from which a cloud-free signal can be reconstructed (Menenti et al., 1993 and 1995; Verhoef, 1996; Azzali and Menenti, 2000). The term harmonic in the FFT implies that the time series is periodic and the assumption that the natural variation can be reproduced by a periodic model was inspired by the fact that time series of daily and yearly datasets of remotely sensed images often clearly displayed the influence of the daily and yearly courses of the sun on the earth's surface. The actual signals are not purely periodic, but the periodic model could be successfully applied to obtain useful insights in the dynamics of land surface processes.

The FFT has shown to be particularly useful for NDVI time series analysis to describe and quantify fundamental temporal characteristics, since the noise-affected NDVI time series are decomposed into simpler periodic signals in the frequency domain. By performing analysis in the frequency domain, a distinction can be made between frequency terms with daily frequencies, related to atmospheric and cloud contamination effects, and specific frequency terms related to vegetation in dynamic ecosystems (Juarez and Liu, 2001; Olsson and Eklundh, 2001; Jakubauskas et al., 2001 and 2002; Evans and Geerken, 2006;). So it has been widely used to study the linkages between climate and vegetation dynamic (e.g. Roerink et al., 2003; Wen et al., 2004; Immerzeel et al., 2005; Julien et al., 2006).

6

1.3 Justification for this Thesis

The UN Conference on the Human Environment, held at Stockholm in 1972, was a first milestone in the process of raising public awareness on environmental issues, a process that reached its maturity after the Rio Conference in 1992. As a result, most governments around the world now have ministries and regional agencies devoted to environmental protection. To pursue this goal, these institutions need reliable information on relevant themes of the territory under their control.

Consequently, the demand for geo-referenced environmental information has grown considerably in the last decades, at a pace akin to the development of the technologies that enable it. Based on this information, the authorities make decisions, and the public make up an opinion that in turn influences those decisions. Thus comprehensive up-to-date geographic information on the environment is a must for a wealthy society concerned with environmental quality.

This need is even more conspicuous in countries like Ghana (a developing country for that matter), where every year many infrastructures are built, land use changes from rural to urban and from forest to agriculture, and thousands of square kilometres are burnt by wild fires. Furthermore, natural resource managers, policy makers and researchers demand knowledge of phenological dynamics over increasingly large spatial and temporal extents for addressing pressing issues related to global and local environmental change such as biodiversity, primary production and carbon emissions (White and Nemani, 2003; Cleland *et al.*, 2007). Changes in the timing and length of the growing season may not only have consequences for plant and animal ecosystems, but persistent increase in length may lead to long-term increase in carbon storage and changes in vegetation cover (Linderholm, 2006). Causal attribution of recent biological

trends to climate change however is complicated because non-climatic influences, such as land use change, dominate local short term biological changes (Parmesan and Yohe, 2003). Long term observations of plant phenology have been used to track vegetation responses to climate variability but are often limited to particular species and locations (Schwartz, 1999).

Vegetation influences markedly the productivity, vulnerability and biodiversity of ecosystems, and has a crucial impact on biogeochemical cycles, albedo, and ultimately global climate. Thus information on vegetation is essential for a proper management, monitoring and preservation of our environment. Satellite data possess significant potential for the production of such vegetation map and for monitoring vegetation dynamics at regional to global scales (Anyamba and Eastman 1996; Azzali and Menenti 2000).

However, as mentioned earlier, these datasets contains contaminated values which must be dealt with and several methods have been presented to identify and interpolate these contaminated values in these dataset (van Dijk *et al.*, 1987; Viovy *et al.*, 1992; Roerink *et al.*, 2000; Jönsson and Eklundh, 2002, and 2004; Chen *et al.*, 2004; Beck *et al.*, 2006; Ma and Veroustraete, 2006), the latest methods usually performing better than the previous ones (Hird and McDermid, 2009).

The aim of this thesis is therefore to contribute to the ongoing effort aimed at solving this dilemma in respect of inherent noise in these dataset by applying the Fast Fourier Transform algorithm on time series NDVI dataset for the assessment and production of vegetation maps and its trend in Ghana.

8

1.4 Research Objectives

1.4.1 Main Objective

This study aims to produced and assess vegetation maps of Ghana, applying FFT noise reduction technique on NDVI time series datasets.

1.4.2 Specific Objectives

The specific objective of this work includes the following;

> Extract Ghana, from the Africa NDVI dataset and produce two average NDVI images representing 1996 (i.e. 1987 -1996, 360 images) and 2006 (i.e. 1997 - 2006, 360 images).

> Apply the FFT noise reduction algorithm to these two averages of NDVI dataset for Ghana.

> Perform a supervised classification on the two average NDVI datasets of Ghana in relation to the six agro-ecological zones.

> Finally, produce two vegetation maps of Ghana representing 1996 and 2006, and investigate the probable future trend.

1.5 Research Questions

- Is it practical to extract and average an NDVI dataset for Ghana from an Africa NDVI time series dataset?

- Is it beneficial to apply the FFT technique? Under what circumstances is it beneficial, or not beneficial? What is the demonstrated success of the FFT technique?

- Is it reliable to produce vegetation maps using NDVI time series dataset?

- What is the trend of the vegetation pattern within the stipulated period?

9

1.6 Thesis Organization

Chapter one introduces the importance of vegetation phenology to a wide variety of research interests, and the use of satellite remote sensing imagery in its study. The main objective, four specific objectives and their corresponding associated research questions are listed in this chapter. This is followed by a literature review in Chapter two which emphasizes the remote sensing of vegetation phenology, the reduction of noise in the multi-temporal NDVI datasets employed in the research, and the extraction of phenological measures from these datasets. Chapter three outlines the methods and procedures followed in carrying out this research. It begins with a comprehensive description of the study area Ghana, the extraction and averaging of NDVI for Ghana from the Africa NDVI time series dataset, and the application of the FFT noise reduction technique on these dataset. This chapter will answer the second research question in relation to the second specific objective. The results of these analyses will be presented in Chapter four, which itself is organized around the third and fourth specific objectives and its associated research questions. A similar organization is also followed in Chapter five, which presents a discussion of the results presented in Chapter four and provides summarized answers to all the research questions posed above, also in relation to the main and specific objectives. It concludes with a brief summary of the current work, its contribution to the present literature, and a number of recommendations for the direction of future avenues of research.

CHAPTER TWO

LITERATURE REVIEW

2.1 Introduction

Human activities over the years and its consequences over the environment have increased the concern over the Earth's future; environment and climate. Recently, environmental problems such as global warming and deforestation have led to the necessity of monitoring land cover and to detect changes in global and local scale. Remotely sensed data are the most widely used technique for studying this global vegetation dynamics, especially in light of climate change concerns. The International Geosphere-Biosphere Programme (IGBP) identify land-cover as a top research priority and further clarified this requirement by specifying that 1 km NOAA-AVHRR data are the logical basis for global land-cover dataset (IGBP, 1992). However, efforts to characterize vegetation phenology and extract numerical observations related to vegetation variability using per-pixel time series NDVI are hindered by noise arising from varying atmospheric conditions and sun-sensor-surface viewing geometries (Holben and Fraser, 1984; Li and Strahler, 1992; Huete *et al.*, 1999; Carreiras *et al.*, 2003; Kobayashi and Dye, 2005). For instance cloud, ozone, dust, and other aerosols generally decrease near infrared (NIR) reflectance whiles off-nadir viewing and low sun zenith angles also cause a similar effect (Gutman, 1991). Indeed, the negative bias caused by these unfavourable atmospheric conditions and anisotropic bidirectional effects are a prevalent and well recognized feature of noise in NDVI data sets. These problems tend to create data drop-outs (i.e. low NDVI values in time series) or data gaps, and make phenological markers difficult to identify (Reed *et al.*, 1994). With the growing importance of NDVI time series analyses in support of research on climate

11

change (Badeck *et al.*, 2004), biodiversity (Hurlbert and Haskell, 2003), and wildlife ecology (Hebblewhite *et al.*, 2008), there is a strong need for a more comprehensive understanding regarding noise reduction in these datasets.

2.2 The importance of Vegetation Phenology

As a crucial component in all local, regional and global level ecological dynamics, vegetation phenology has been of considerable interest to numerous branches of researches including ecology, biology, agriculture, environmental science, among others (Chen *et al.*, 2000; Schwartz *et al.*, 2002; Turner *et al.*, 2003; Ricotta *et al.*, 2003; Sakamoto *et al.*, 2005; Reeves *et al.*, 2006). Firstly, it is a driving force in the lifecycles of many organisms and plays a critical role in the timing and abundance of food supplies for insects, birds, rodents, ungulates, and many other organisms. For example, the timing of peak caterpillar abundance, which occurs after spring budburst in deciduous trees, is linked to the timing of reproduction for insectivorous bird species that rely on the abundance in this food supply to fulfill nestling nutritional requirements (Blondel *et al.*, 1993). Many ungulate breeding seasons are also timed to take advantage of peak plant growth in order to optimize offspring survival (Gaillard *et al.*, 2000; Loe *et al.*, 2005). Grizzly bear activity and movement are highly dependent upon seasonal vegetation where the spring, summer and autumn shifts in the distribution of high energy food sources influences grizzly presence over a variety of landscapes (Hobson, 2005; Munro *et al.*, 2005). Vegetation phenology also plays a part in annual cycles of insect outbreaks and disease control. For instance, it has been demonstrated that the spring production of malaria carrying mosquito larvae are highly correlated with the spring green-up of various plants in wetlands and aquatic environments (Penfound *et al.*, 1945), while desert locust breeding and migratory patterns are shown to be influenced by vegetation distribution and growth across the African desert

12

(Despland et $al.$, 2004). In addition to a notable role in biological lifecycles, the very nature of the seasonal shifts in photosynthetic active vegetation renders it an important component in the terrestrial carbon balance. By absorbing CO_2 during the photosynthetic process, green vegetation contributes to local, regional and global CO_2 fluxes and land atmosphere exchanges (Aurela et $al.$, 2001). These exchanges fluctuate throughout the year with annual cyclic shifts in vegetation phenology. Chen et $al.$, (1999) showed that while CO_2 was being released into the atmosphere during winter and early spring over an old aspen forest in Saskatchewan, Canada, maximum CO_2 absorption occurred just after leaf emergence, and then decreased gradually until the late growing season, when a rapid decrease in CO_2 uptake corresponded with leaf senescence. Such patterns are also reflected globally on much larger scales (Myneni et $al.$, 1997). The connection between vegetation phenology and the global distribution and movement of CO_2 is evident, and the link between CO_2 and global climate is well established (Hall et $al.$, 1975).

In light of the obvious need to understand vegetation phenology and its role in ecosystem dynamics, atmospheric CO_2 balance and global response to climatic shifts, its widespread incorporation into a variety of ecological, atmospheric and biological research objectives is understandable. As a means of providing repeatable, large-area views of the earth's surface and spectral responses tied to vegetation health and development, satellite derived remote sensing datasets play an increasingly integral role.

2.3 Advance Very High Resolution Radiometer (AVHRR) Sensor

Applications of Landsat data paved the way for remote sensing-based phenology and these data are still used for some applications. However, modern scientific researches

13

using satellite sensors with a more frequent repeat cycle currently dominate the field. The longest-running series of high repeat frequency sensors is the National Oceanic and Atmospheric Administration's (NOAA) advanced very high resolution radiometer (AVHRR). AVHRR instruments measure the reflectance of the earth in five relatively wide spectral bands. The first two are centered around the red (0.6 micrometres - 0.7 micrometres) and near-infrared (0.7 micrometres - 3.0 micrometres) regions, the third one is located around 3.5 micrometres, and the last two sample the thermal radiation emitted by the planet, around 11 micrometres and 12 micrometres, respectively. The NOAA satellite has equator crossing times of 0730 and 1930 local solar time (Baum *et al*, 1992).

2.3.1 Operational Procedures

NOAA has at least two polar-orbiting meteorological satellites in orbit at all times, with one satellite crossing the equator in the early morning and early evening and the other crossing the equator in the afternoon and late evening. The primary sensor on board both satellites is the AVHRR instrument. Morning-satellite data are most commonly used for land studies, while data from both satellites are used for atmosphere and ocean studies. Together they provide twice-daily global coverage, and ensure that data for any region of the earth are no more than six hours old. The swath width, the width of the area on the Earth's surface that the satellite can "see", is approximately 2,500 kilometers (about 1,500 miles). The satellites orbit between 833 or 870 kilometers (± 19 kilometers, between 516 and 541 miles) above the surface of the Earth. The highest ground resolution that can be obtained from the current AVHRR instruments is 1.1 kilometer (0.68 miles), which means that the satellite records discrete information for areas on the ground that is 1.1 by 1.1 kilometers. This smallest recorded unit is called a pixel. AVHRR data have been collected continuously since 1981.

14

2.3.2 Applications of AVHRR

The primary purpose of these instruments is to monitor clouds and to measure the thermal emission (cooling) of the Earth. These sensors have proven useful for a number of applications, including vegetation phenology, the surveillance of land surfaces, ocean state, aerosols, etc. The AVHRR data are particularly relevant to the study of climate change and environmental degradation because of the comparatively long records of data already accumulated (over 20 years). The main difficulty associated with these investigations is to properly deal with the many limitations of these instruments, especially in the early period (sensor calibration, orbital drift, limited spectral and directional sampling, etc.)

2.4 The Normalized Difference Vegetation Index (NDVI)

Regardless of the sensor used, be it Landsat Thematic Mapper, VEGETATION, AVHRR or MODIS, the majority of vegetative research studies make use of the spectral data in the form of VIs – algebraic combinations of the visible red and near-infrared spectral bands, sometimes with addition of other spectral bands, that exploit the variable spectral response of healthy vegetation across these different wavelengths (Huete et al., 2002). Green vegetation shows high absorption of visible red light for the purpose of photosynthesis by chlorophyll-containing components, while near-infrared wavelengths are largely reflected by structural cells in green leaves. This variable spectral response of healthy green vegetation to the red and near-infrared wavelengths is widely known as the 'red edge' (Myneni et al., 1995). Seasonal changes in the VIs that manipulate this relationship have been shown to closely reflect seasonal changes in the photosynthetic and structural characteristics of surface vegetation; an increase in a VI typically reflects increasing photosynthetic activity. On the basis of previous

research, a direct relationship is assumed to exist between continuous changes in surface vegetation reflectance, detected through a VI, and surface phenological development (Badeck *et al.*, 2004). Jordan's (1969) Simple Ratio Index (SRI) was one of the very first VIs to exploit these particular spectral characteristics of healthy vegetation, and is calculated by the equation:

$$SRI = DN_{NIR} / DN_{RED}$$

where DN_{NIR} and DN_{RED} are the digital numbers of a pixel in the near-infrared and red spectral bands, respectively. The simple act of ratioing these two bands works effectively toward reducing much of the inherent variation in the signal due to calibration, noise, sun angles, and atmospheric effects (Huete *et al.*, 1999).

Over the following decades, many other indices have followed the SRI, including: the Perpendicular Vegetation Index (PVI), (Jensen, 2000), Global Environment Monitoring Index (GEMI), (Myneni *et al.*, 1995), the NDVI, (Deering, 1978), the Enhanced Vegetation Index (EVI), (Huete *et al.*, 1999) and a series of soil and atmospherically-adjusted vegetation indices (Huete and Liu, 1994; Gilabert *et al.*, 2002), designed to minimize atmospheric and brightness-related soil effects (Huete *et al.*, 1988). Of these, the NDVI continues to be the most commonly used and most prevalent in the literature (Deering, 1978).

Although the NDVI time series data could be obtained from other sensors, they are commonly obtained from the "Advanced Very High Resolution Radiometer" (AVHRR) sensors, on board of the "National Oceanic and Atmospheric Administration" (NOAA) satellites. The NOAA-AVHRR sensor as stated earlier, has five detectors, two of which are sensitive to the wavelengths of light ranging from 0.55–0.70 and 0.73–1.0

16

micrometers. These two AHVRR's detectors measure the intensity of light coming off the Earth in visible and near-infrared wavelengths and quantify the photosynthetic capacity of the vegetation in a given pixel (1 square km) of land surface. In general, if there is much more reflected radiation in near-infrared wavelengths than in visible wavelengths, then the vegetation in that pixel is likely to be dense and may contain some type of forest. If there is very little difference in the intensity of visible and near-infrared wavelengths reflected, then the vegetation is probably sparse and may consist of grassland, tundra, or desert.

Nearly all satellite Vegetation Indices employ this difference formula to quantify the density of plant growth on the Earth i.e. near-infrared radiation minus visible radiation divided by near-infrared radiation plus visible radiation. The result of this formula is called the Normalized Difference Vegetation Index (NDVI). As depicted in Figure 2.1 below, calculations of NDVI for a given pixel always result in a number that ranges from minus one (-1) to plus one (+1) without any green leaves having a value close to zero. A zero means no vegetation and close to +1 (0.8 - 0.9) indicates the highest possible density of green leave (Myneni *et al.*, 1999; Huete *et al.*, 1999). This is written mathematically as:

$$NDVI = \frac{(DNNIR - DNRED)}{(DNNIR + DNRED)}$$

where DNNIR and DNRED are the digital numbers of a pixel in the near-infrared and red spectral bands, respectively (Myneni *et al.*, 1995; Huete *et al.*, 1999)

17
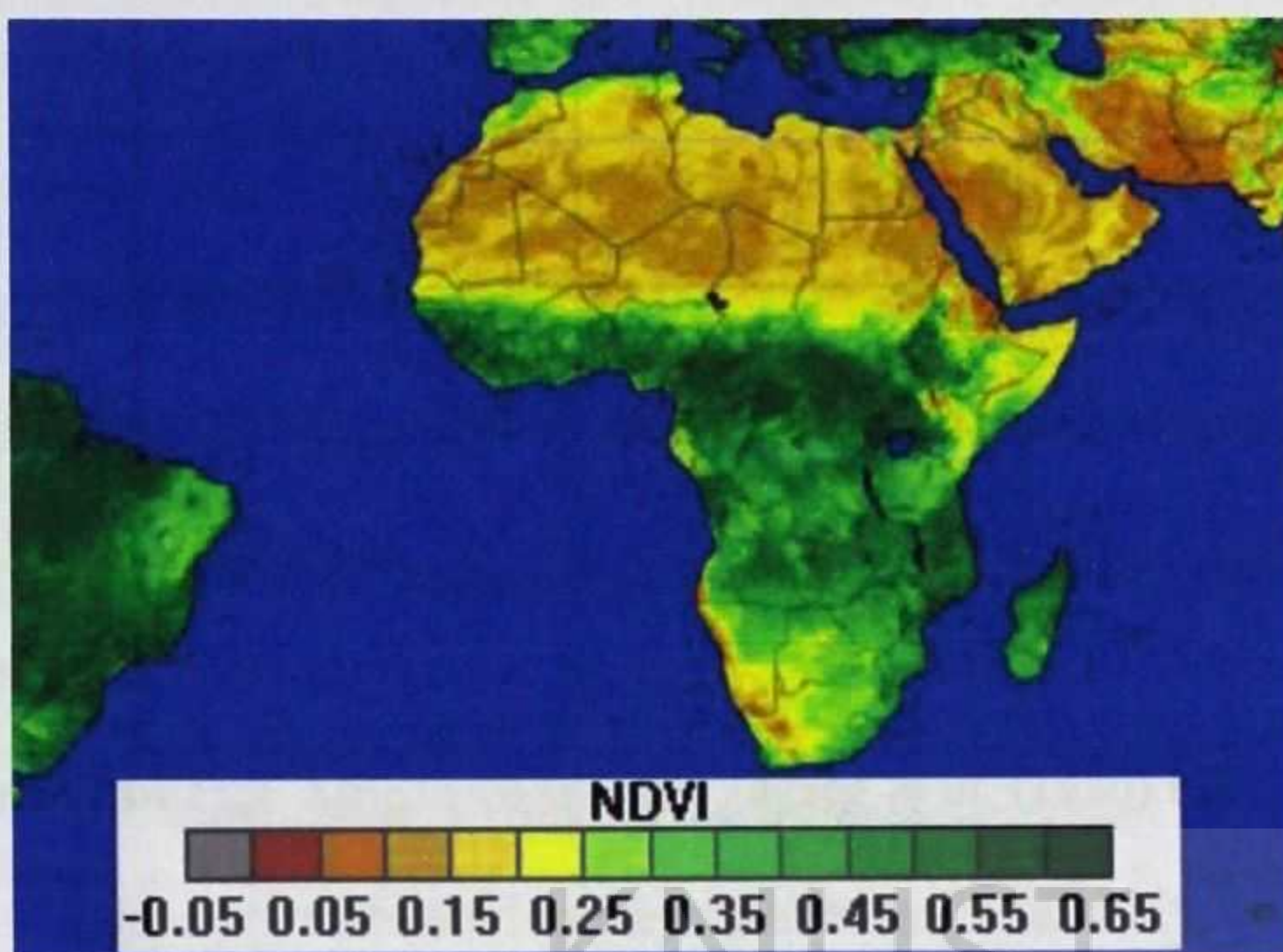
Figure 2.1: Leaf Colour and corresponding NDVI Values (Source: Tucker *et al.*, 2005)

2.4.1 Applications of NDVI

Time series of NDVI often employed as per-pixel series of NDVI over time are particularly useful for phenological research, since they provide a means to capture time-sensitive phenological shifts and vegetation developmental stages. NDVI increases and decreases with annual cycles of surficial vegetation green-up and senescence, and much of the research involving NDVI incorporates multi-temporal data sets for this reason.

Some of the first large-area applications of NDVI to the study of vegetation phenology were undertaken in the mid-1980s, beginning with a number of studies employing the globally available AVHRR imagery to examine phenological shifts across the African continent. For instance, in a global examination of AVHRR imagery, Justice *et al.* (1985) demonstrated the value of this daily, coarse-resolution data for phenological research and vegetation monitoring at varying scales and across several continents. They described general phenological patterns over Africa, highlighting known areas of drought, generated phenological profiles for a variety of vegetation types across South

18

America, West Africa and South Asia, compared information extraction from AVHRR data sets at varying spatial resolutions, and illustrated the potential of these data for climate change research (Justice *et al.*, 1985). Following this work, Townshend and Justice (1986) plotted NDVI profiles for a number of vegetation types across Africa using AVHRR, and compared the years 1983 and 1984 to highlight inter-annual variability in seasonal dynamics across the continent in a qualitative analysis. Similarly, in a regional study of East African vegetation, Justice *et al.* (1986) used NDVI profiles to study the relationship between bushland phenology and rainfall events, and to estimate growing season length.

Phenological research employing multi-temporal NDVI data sets continued to grow through the 1990's, and included the phenological classification of global vegetation types (Lloyd, 1990), modelling phenological profiles and biophysical characteristics of agricultural crops (Fischer, 1994a), deriving important phenological events from NDVI time series (Reed *et al.*, 1994), studying the relationship between NDVI and surface temperature during various phenological stages in crops (Gupta *et al.*, 1997), comparing satellite-derived start of season with modelled phenology (Schwartz and Reed, 1999), and the linking of vegetation phenology with long distance biota movement (Gage *et al.*, 1999), among many others. Interest continues to expand, with more recent research employing NDVI for phenological investigations including the study of growing season length derived from NDVI across differing climatic zones of China (Chen *et al.*, 2000), the modelling of phenological transition dates for vegetation monitoring (Zhang *et al.*, 2003), an examination of intra-seasonal dynamics in Alaskan tundra (Jia *et al.*, 2004), the linking of spring phenology to precipitation and temperature in a study of climate change (Zhang *et al.*, 2004), the detection of rice crop planting, heading, and harvesting using NDVI (Sakamoto *et al.*, 2005), and a study of the effects of inter-seasonal rainfall

variation in the dry savannah of Namibia (Wagenseil and Samimi, 2006). The long-term, continued popularity of the NDVI for studying vegetation phenology and the utility of NDVI time series for such studies provides the impetus for the current research.

2.4.2 Limitations of NDVI

In spite of its prominent usage in phenological research, NDVI time series are prone to noise and error from a number of sources. While much of this is dealt with as effectively as possible in more recent NDVI data sets, such as those provided by the MODIS sensor, older data sets particularly those from the AVHRR can be significantly affected. As enumerated in the previous chapter, much of the variation in NDVI multi-temporal imagery unrelated to surface vegetation phenology is due to atmospheric effects and to varying sun-sensor-surface angle geometries.

Atmospheric scattering and absorption due to cloud cover, water vapour, dust, ozone, and other aerosols present in the atmosphere change daily and generally depress NDVI estimates, potentially causing under estimations of vegetation biomass (Gutman, 1991; Viovy et al., 1992; Huete et al., 1999). Holben (1986) explained, for example, that high-frequency variability in water vapour and aerosols, along with cloud cover, cause much of the false lows in NDVI estimations by decreasing near-infrared reflectance. Water vapour is shown to decrease NDVI by approximately 0.02 units, and aerosols by 0.06 to 0.12 units, depending on solar and viewing angles. Goward et al., (1991) described some of these effects as they pertain to the AVHRR, stating that satellite-derived NDVI estimates can be up to 30% lower than corresponding ground-based estimates due to atmospheric attenuation. Cloud effects are particularly prevalent in tropical regions, where extended periods of cloudiness and aerosol contamination from

biomass burning are commonly encountered (Carreiras *et al.*, 2003; Kobayashi and Dye, 2005).

In terms of sun-sensor-surface geometries, daily variations in sensor view and solar zenith angles, in addition to the anisotropic nature of vegetated surfaces, result in bidirectional reflectance effects, which can, themselves, vary with vegetation type (Gutman, 1991). Holben and Fraser, (1984) demonstrated this in their simulations of varying viewing and illumination angles across an AVHRR scan line, concluding that off-nadir viewing angles and low sun angle during the winter season often decreased NDVI estimates. False highs estimates could also occur in the extreme forward-scanning angles (Gutman, 1991). Li and Strahler (1992) explained how variations in vegetative structural characteristics (e.g. shape) and plant density between different vegetation communities resulted in varying bidirectional effects across land covers. These effects add to undesirable high-frequency fluctuations in NDVI time series that are unrelated to surface phenology. Two additional sources of error that are more specific to the NDVI itself are (i) a tendency for saturation over high biomass areas and (ii) background soil effects (Huete *et al.*, 1997). For instance, Holben and Fraser (1984), in studying the use of NDVI data sets for land cover stratification, reported more difficulty in discriminating between high density green-leaf cover types than between low density green-leaf cover types because of the difficulty with saturation. Huete *et al.*, (2002) also remarked on the lower range of NDVI values over higher biomass land covers than over lower biomass land covers. On the other hand, Holben (1986) noted problems in assessing vegetation cover over the Sahara desert where vegetation can be sparse, and suggested that background soil mineralogy was a contributing factor due to sparse vegetation. As Huete *et al.*, (1988) explained this could have been be due to the addition of near-infrared scattering from soil surfaces to that of green plant surfaces,

21

contributing to unrepresentative (i.e. inaccurate) NDVI estimates. In response to this contamination, a variety of soil-adjusted vegetation indices and enhanced vegetation indices have been developed that attempt to account for these saturation and background effects (Huete *et al.*, 1988; Huete *et al.*, 1999). While these alternative indices may be improvements in these specific respects, the normalizing nature of the NDVI renders it less sensitive to atmospheric and topographic effects than those alternatives, which themselves require more sensor noise removal than does the NDVI (Huete *et al.*, 2002). For longer-term studies employing NDVI data sets, satellite orbital drift due to atmospheric drag and degradation in sensor calibration over time can also be additional causes of error and inaccuracy in NDVI estimates (Gutman, 1991). These factors are often accounted for in more currently-available data sets (Running *et al.*, 1994) and are not of concern in the current study.

Despite the issues of noise and error in NDVI data sets, it remains popular for the remote sensing of vegetation phenology. This popularity is no doubt due to its availability through a multitude of sensors, variety of scales (e.g. 250 meters to 16 kilometres resolution), daily to monthly composites (Pettorelli *et al.*, 2005), and the ease of calculation. It is because of this popularity and the resultant widespread use that inform the decision to adapt it for this research.

2.4.3 Noise Reduction in NDVI Time Series

As emphasized earlier, multi-temporal NDVI data sets, often employed as per-pixel NDVI time series, are commonly used in the study of vegetation phenology through remote sensing. Of prevalent concern in such applications is the considerable temporal variation resulting from varying atmospheric and bidirectional effects unrelated to phenological changes. As a result, a wide variety of noise reduction techniques have

been applied to these data sets. The two most outstanding assumptions that form the basis for these noise reduction strategies are that; (i) low frequency seasonal variation in NDVI is directly related to changes in surface vegetation phenology, whereas (ii) high frequency (e.g. daily or sometimes weekly) fluctuations in NDVI are not generally related to phenological shifts, but rather, reflect short-term variations in atmospheric conditions and sun-sensor-surface view angle geometries (van Dijk *et al.*, 1987). Another less common but still popular assumption that forms the basis of various noise reduction techniques is the recognition that much of the noise in NDVI time series is found in the form of spurious lows. That is, because the presence of water vapour and aerosols in the atmosphere lowers the detection of near-infrared reflectance by the satellite, these NDVI values tend to decrease (Holben, 1986). It is therefore often assumed that higher NDVI observations are generally the most accurate, and noise reduction techniques thus aim to preserve the upper envelope of NDVI values in a times series.

One of the most popular and simplest methods for reducing this noise in NDVI time series is through multi-temporal compositing (Goward *et al.*, 1991, Chen *et al.*, 2003, Kobayashi and Dye, 2005). Various methods of compositing exist, but they each involve selecting the most desirable date or NDVI value for any given period of time in a time series, based on some specified criterion for that pre-defined period of time, and generally rely on all three of the assumptions listed above (van Dijk *et al.*, 1987, Swets *et al.*, 1999, Carreiras *et al.*, 2003). Ideally, in this way, each pixel is represented by the most accurate NDVI observation from within the composite period, and daily or sometimes weekly fluctuation resulting from cloud and aerosol contamination and bidirectional reflectance effects, hence unrelated to surface phenology, are removed, while the low frequency phenological shifts occurring at the surface are retained in the

signal. The length of the composite period generally ranges from weekly to monthly. While it is recognized that longer composite periods result in better noise reduction, they also limit the extraction of phenological information from time series because of a decreased sensitivity to the timing of phenological transitions with a coarser temporal resolution (Viovy *et al.*, 1992, Chen *et al.*, 2003).,Compositing is most often done using the maximum value compositing (MVC) method described in Holben, (1986), where the highest NDVI value for a given composite period is selected to represent that period, as this is assumed to reflect the most cloud-free, aerosol-free, near-nadir view observation. The reduction in atmospheric and bidirectional effects in NDVI time series resulting from the use of the MVC method has been clearly demonstrated (Cihlar, *et al.*, 1997, Maxwell *et al.*, 2002, Chen *et al.*, 2003). Other temporal compositing strategies includes the constrained view angle MVC (CV-MVC) used in compositing MODIS vegetation index products (Huete *et al.*, 2002 and the maximum value interpolated compositing method, Taddei, (1997) and Cabral *et al.*, (2003). However, because of its simplicity and popularity, the MVC method is the means through which most NDVI data sets are provided to users as precomposited data sets (e.g. SPOT VEGETATAION, AVHRR and MODIS NDVI products).

Nevertheless it should be recognized that despite the smoothing effects of temporal compositing, residual atmospheric and bidirectional effects often still exist in an NDVI time series, particularly in regions of prevalent cloud cover or at higher latitudes where sun and sensor view angles can be large (Carreiras *et al.*, 2003). For this reason, further noise reduction is often performed on composited NDVI time series, and this forms the focus of this thesis. It is therefore appropriate to state that the noise reduction techniques described below all pertain to composited NDVI data sets.

2.5 Techniques employed in reducing noise in composited NDVI dataset

The majority of composited NDVI time series noise reduction strategies can be placed into one of two categories: filtering or function-fitting. The filtering type rely on properties of the original data points and a set of rules to replace each data value by a linear combination of a set of nearby values (Jönsson and Eklundh, 2006).The function fitting type on the other hand involve the construction of a new NDVI time series that is fitted to the overall trends in the original profile, that may pass through some, but often few, of the original data points, and that can be described using a function. Filters aim to minimize the high-frequency noise while retaining the desired signal in the times series. The filtering techniques often incorporate more of the original data in their result, which are not generally as smooth as those produced through function-fitting (van Dijk *et al.*, 1987). On the other hand, function-fitting techniques can produce spurious oscillations that distort the time series, while filters do not (Chen *et al.*, 2004). In both cases, however, the aim is to detect the desired, low-frequency signal that reflects surface vegetation phenology while minimizing or removing the undesirable, high-frequency noise related to variable atmospheric conditions and bidirectional effects (van Dijk *et al.* 1987).

2.5.1 Filtering Techniques

As in the case of function-fitting methods, a wide variety of filtering techniques has been used to reduce noise in NDVI time series, and they range from simple moving means to more complex multi-step procedures. In an example of the former, van Dijk *et al.*, (1987) presented four separate filters for noise reduction: a running weighted mean filter, a running median filter, the 4253H-twice filter and the 3RSSH-twice filter. The first two are straightforward. They simply apply a running window in which the

weighted average or median of the values in the window directly before and after the value of interest, replaces the value of interest (van Dijk *et al.*, 1987). The third filter, 4253H-twice, applies a series of running median filters with windows of four, two, five and three, followed by a running weighted mean filter to an NDVI time series. The residuals of the filtering are then also filtered in this manner and then re-added to the filtered data, hence the 'twice' in the name of the filter (Velleman, 1980). In this way, not only is noise in the time series reduced but trends in the original data are also maintained. The fourth, the 3RSSH-twice filter, iteratively runs a running median filter with a window of three to the time series until no additional changes are made, splits and interpolates resulting flat sections of the time series, then runs the weighted mean filter and same residual noise reduction step described above (Tukey, 1977). While different from the 4253H-twice filter, the 3RSSH-twice filter is designed to function in a similar manner. In applying these filters to data sets covering agricultural fields in Iowa, U.S. and west central Thailand, van Dijk *et al.*, (1987) demonstrated the applicability of simple filtering techniques to reducing noise in VI data sets over a variety of land cover types. Despite their simplicity and evident usefulness, these filters are not applied elsewhere for noise reduction in VI time series, except for the 4253H-twice filter, which is used for noise reduction in other applications (e.g. Cowan and Odell, 1990).

Viovy *et al.*, (1992) proposed another filtering noise reduction technique for use on daily NDVI time series dataset called the Best Index Slope Extraction (BISE). Through the use of set thresholds and a 'sliding period' the procedure searches forward within this sliding period from the first date of the time series, accepting values higher than preceding ones as long as they are within a set 'noise' threshold, and accepting a decrease only if it is followed by a period of gradual increase. In this way, it accounts

not only for gradual changes in surface vegetation, but also sudden changes brought on by fire, deforestation, or crop harvest, which are followed by a period of vegetative regeneration, and can thus be differentiated from spurious drops in NDVI (Viovy *et al.* 1992). Interpolation is used to fill NDVI observations between acceptable points. White *et al.*, (1997) used this technique to reduce noise in a multi-temporal NDVI data set for use in producing a continental phenology model for portions of North America, while Jia *et al.*, (2004) reduced noise with the BISE in an NDVI data set to examine phenological patterns in the Alaskan tundra, and Wang *et al.*, (2004) also used BISE-filtered NDVI to study the seasonally dynamic relationship between satellite-and ground-based observations. Lovell and Graetz, (2001) presented a revised BISE procedure adapted for use on composited, as opposed to daily NDVI data sets. They applied this successfully to a multi-year NDVI time series covering the Australian continent.

In a more complex procedure, Chen *et al.*, (2004) presented a simplified least-squares-fit convolution based on the technique described by Savitzky and Golay, (1964), in which the convolution represents a weighted moving mean filter with the weights given as a polynomial of a particular degree. The method iteratively fits a new NDVI time series to the original data points until certain conditions are met (e.g. spurious lows are removed, etc.) and the resulting time series is filtered. Chen *et al.*, (2004) applied this method to a multi-temporal NDVI data set covering portion of south-eastern Asia and a variety of land cover types, reducing the effects of atmospheric conditions and bidirectional effects in the data. Jönsson and Eklundh, (2004) also applied an adjusted Savitzky-Golay method to NDVI time series in Africa, which is then used to extract a variety of phenological information, including patterns of spring green-up across the

27

continent. Though more complicated than many other filtering techniques, the Savitzky-Golay filter provides a flexible approach to noise reduction.

In a less complex attempt at removing noise, Kobayashi and Dye, (2005) performed a simplified atmospheric correction on an NDVI data set using the atmospheric correction technique described in Rahman and Dedieu, (1994). This technique involves the application of a set of semi-empirical formulas to describe the various interactions of solar radiation with atmospheric components, but deals only with atmospheric contamination in NDVI time series. Cihlar *et al.*, (1997) proposed an alternative noise reduction procedure, referred to as the atmospheric, bidirectional and contamination corrections of Canadian Centre for Remote Sensing, (ABC3). Consisting of nine different steps, this process involves a number of atmospheric corrections, including that described by Rahman and Dedieu, (1994), angular (i.e. bidirectional) corrections and the linear interpolation of missing or contaminated observations (Cihlar *et al.*, 1997). Cihlar *et al.*, (2004) presented a revised, improved version of the ABC3 procedure, applying the algorithm to multi-temporal data sets covering the Canadian landmass. The success of the technique was demonstrated by Cihlar *et al.*, (1997, 2004).

Another filter that shows promise is Ma and Veroustraete's, (2006) mean-value iteration (MVI) filter. Based on the assumption that each observation in the NDVI time series will closely approximate the mean of the previous and following observations, the MVI filter iteratively compares the average of the previous and following NDVI observations with the observation of interest, replacing it with this average where the appropriate conditions are met (Ma and Veroustraete, 2006). In other words, where the NDVI value of interest differs too much from its neighbours, it is replaced by the mean of their values. The application of this method to NDVI data sets covering north-western China illustrated its usefulness in minimizing time series noise (Ma and

28

Veroustraete, 2006). The basic principle behind the MVI filter is also seen in the noise reduction techniques used by Chen *et al.*, (2000) and Xiao *et al.*, (2002). In the former, if the NDVI at each point in the time series was lower than the mean of the observations immediately before and after it, it was replaced with this mean; in the latter, dates identified as contaminated by cloud were replaced by the mean of the preceding and succeeding NDVI values. While the method of Chen *et al.*, (2000) may deal with both atmospheric and bidirectional effects, only atmospheric effects are accounted for in the method of Xiao *et al.*, (2002).

Another alternative filtering technique was presented by Kang *et al.*, (2005), who applied a temporal and spatial interpolation scheme to cloud-contaminated pixels in a multi-temporal data set. While the application of this technique did not actually involve NDVI time series, it could be applicable to such data sets. The method comprises a spatial interpolation first, in which pixels identified as cloudy for a particular date are replaced with a new interpolated value from surrounding cloud-free pixels (Kang *et al.*, 2005). If no cloud-free pixels are available for that date, for that pixel, temporal interpolation from previous cloud-free or interpolated dates is performed. Kang *et al.*, (2005) successfully applied this method to data sets covering a portion of the northwestern U. S., but concede that it is only applicable in cases where sufficient cloud-free data exist for the interpolation.

2.5.2 Function - Fitting Techniques

Function - fitting is the process of constructing a curve, or mathematical function, which has the best fit to a series of data points, possibly subject to constraints. Function - fitting can involve either interpolation, where an exact fit to the data is required, or smoothing, in which a "smooth" function is constructed that approximately fits the data.

A related topic is regression analysis, which focuses more on questions of statistical inference such as how much uncertainty is present in a curve that is fit to data observed with random errors. Fitted curves can be used as an aid for data visualization, to infer values of a function where no data are available, and to summarize the relationships among two or more variables.

Amongst the various function-fitting strategies employed in the noise reduction of NDVI time series, the application of the Fast Fourier transform is one of the most popular. This is a mathematical technique used in a variety of disciplines to separate dataset into its various frequency components (Jensen, 1996), in this case temporal frequencies. Fourier analysis is based on the concept that an infinite series of sine and cosine functions can be used to represent a function at every point in an interval (van Dijk et al., 1987). By generating a new NDVI time series with the appropriate temporal signal through the combination of various sine and cosine functions, Fourier-based strategies generally produces the smoothest NDVI time series.

In one of the first applications of Fourier-based techniques to noise reduction for NDVI time series, Sellers et al., (1994) presented a method involving a series of steps to produce a product called FASIR-NDVI. This consists of (i) Fourier wave Adjustment, (ii) Solar zenith angle adjustment, (iii) Interpolation of missing data, and (iv) Reconstruction of NDVI data. This first step fits a Fourier series through the original NDVI time series using a robust least-squares procedure, based on the assumption that, (a) NDVI time series should vary smoothly at any given point, and (b) major sources of error only decrease NDVI. Sellers et al., (1994) used the noise-reduced data to derive a variety of vegetative parameters for use in global biophysical monitoring efforts. Similarly, DeFries and Townshend, (1994) derived global phenology-based land cover classes using NDVI time series function-fitted with the Fourier transform of Sellers et

30

al., (1994). Wang *et al*, (2004) also applied this adjusted Fourier transform described in Sellers *et al.*, (1994) to temporally downscale a composited NDVI dataset to daily NDVI observations, whereas Wang *et al.*, (2005b) employed the same method to reduce residual cloud effects and deal with missing data values in a number of multi-temporal NDVI datasets.

While the purpose of the method of Seller *et al.*, (1994) is mainly for noise removal, the Fast Fourier Transform (FFT) technique presented in Menenti *et al.*, (1993) was used for both noise removal and for helping to map differences in vegetation development (e.g. variability in growth cycle, late or early growing seasons) across Zambia. They explained that the resulting Fourier components (i.e. amplitude and phase) can be used to quantitatively describe spatial and temporal patterns of vegetation phenology (Menenti *et al.*, 1993). The FFT and similar approaches have also been used in a number of other applications, including the mapping of uni-modal and bi-modal seasonal dynamics and rates of NDVI change across Africa (Olsson and Eklundh, 1994), the study of vegetation phenology and classification of vegetation types across Brazil (Andres *et al.*, 1994), and the mapping of vegetation in South Africa through phenological parameters (Azzali and Menenti, 2000). Moody and Johnson, (2001) employed a similar, discrete Fourier Transform (DFT) to study inter-annual phenological variation and classify vegetation types in southern California, while Wagenseil and Samimi, (2006) demonstrated the relationship between precipitation and vegetation phenology in a dry savannah environment in Namibia through the Fourier analysis of a multi-temporal NDVI data set.

Verhoef *et al.* (1996) presented an alternate Fourier-based technique called the Harmonic Analysis of NDVI Time Series (HANTS) algorithm which uses the predefined, most significant frequencies expected in a time series profile and harmonic

31

components to apply a least-squares function-fitting procedure to the data. Unlike the above Fourier analyses, this technique does not require observations to be equidistant in time, and is therefore more flexible in its application, but does involve the setting of several parameters and more time for processing (Roerink *et al.*, 2000; Verhoef *et al.* 1996). Roerink *et al.*, (2000) employed the HANTS algorithm to reduce noise and error in an NDVI data set covering Europe, demonstrating the successful removal of cloud contamination. Similarly, Jakubauskas *et al.*, (2001 and 2002) demonstrated the application of Fourier-based harmonic analysis of NDVI time series in characterizing seasonal changes and vegetative cover change detection in the southern Great Plains of the United States. By separating a signal into several multi-resolution temporal components, they allow for the localized removal of undesirable frequencies and retention of desirable, time-varying signals (Li *et al.*, 2000; Fang *et al.*, 2004). Sakamoto *et al.*, (2005) applied a wavelet transform technique to NDVI time series for the purpose of noise reduction and for the subsequent extraction of rice planting, heading and harvesting dates at several locations across Japan, concluding that it showed superior performance over Fourier-based time series noise reduction. Using a similar wavelet transform technique, Sakamoto *et al.*, (2006) processed NDVI data to map the spatial distribution of various rice cropping systems across the Mekong Delta in south-eastern Asia. More recently, Lu *et al.*, (2007) proposed an alternative wavelet-based method for noise reduction in NDVI time series which involves the use of quality flags and blue band reflectance. They found the method to perform well over a portion of eastern China when compared to alternative approaches, including a Fourier-based technique (Lu *et al.*, 2007). Other wavelet transform applications to vegetation phenology include the removal of unwanted variation in investigations of El Nino/Southern Oscillation effects on inter-annual comparisons (Li *et al.*, 2000), noise

reduction in ground-based spectral vegetation curves (Schmidt *et al.*, 2003, 2004), the reduction of noise in NDVI time series through wavelet transforms for the detection of invasive tropical plant species across the United States (Bruce *et al.*, 2006), and the wavelet-based noise reduction of NDVI time series for the prediction of seasonal foraging conditions in southern Texas (Alhamad *et al.*, 2007).

In addition to Fourier-and wavelet-based noise-reduction strategies, a number of linear and non-linear regression techniques have also been applied. For instance, Swets *et al.*, (1999) presented a weighted least-squares windowed linear regression approach that performs a series of best-fit linear regressions for each observation in the time series, averages these and interpolates between the resulting new points to generate a continuous NDVI signal. The algorithm is upwardly biased to account for much of the noise causing decreased NDVI estimations (Swets *et al.*, 1999). This method has been applied by Ricotta *et al.*, (2003) who used noise-reduced NDVI time series to study the impact of climate variability on grassland species abundance in the U.S. Great Plains, and by Reed, (2006), who used a noise-reduced NDVI dataset covering North America to analyse 20-year trends in vegetation phenology across the continent.

In an asymmetrical Gaussian function-fitting approach to NDVI time series noise reduction, Jönsson and Eklundh, (2002) fit simple local nonlinear Gaussian model functions to sets of NDVI observations. These were then combined into global functions designed to represent the full NDVI profile while preserving higher NDVI values over lower ones. Jönsson and Eklundh, (2002 and 2004) both demonstrated the successful extraction of phenological information from a noise-reduced time series covering the African continent, mapping the regional distribution of spring green-up dates and annual phenological amplitude. Verbesselt *et al.*, (2004) used this method to help reduce noise in time series for use in the study of drought in South Africa, while

33

Olofsson *et al.*, (2007) reduced noise with the asymmetrical Gaussian function-fitting before using it to model vegetation biomass production across Scandinavia.

Beck *et al.*, (2006) presented a similar function-fitting procedure, a double logistic function-fitting, whereby NDVI time series were modelled as a function of time using six parameters comprising of (i) winter NDVI (ii) maximum NDVI during the growing season (iii) a rising curve inflection point (iv) a falling curve inflection point (v) the rate of increase at the former inflection point and (vi) the rate of decrease at the latter inflection point. This was designed for applications at high-latitude environments because it accounts for winter NDVI and the effects of snow. Beck *et al.*, (2006) applied the method to an NDVI data set covering northern Scandinavia, deriving spring and autumnal phenological transition dates for the area. This method was further employed by Beck *et al.*, (2007) to create an NDVI data set covering Norway, Sweden and Finland, for use in future vegetation and climate studies, including the mapping and monitoring of regional phenological transitions.

While designed more for phenological information extraction from EVI time series rather than noise reduction, Zhang *et al.*, (2003) introduced a Piecewise Logistic regression function that reduces noise and smooth time series as it extracts measures of phenology. In this procedure, periods of increasing or decreasing values are identified, and logistic functions are first fit to each period, and then combined to describe the entire EVI profile (Zhang *et al.*, 2003). Zhang *et al.*, (2004) employed this method to reduce noise in and detect a number of phenological transition dates across the northern hemisphere, studying their link to surface temperatures and climate variability. Pañuelas *et al.*, (2004) also used this method for deriving spring green-up from time series data and linking it to patterns of rainfall and water availability in Spain. In investigating the effects of atmospheric circulation patterns on vegetation variability in Siberia, Vicente-

34

Serrano *et al.*, (2006) used the procedure described by Zhang *et al.*, (2003) to process their multi-temporal NDVI data set.

Spline-based function-fitting methods have not been employed that much. But Wang *et al.* (2005a and 2005b) applied it to interpolate missing observations (removed because of poor quality) in both LAI and NDVI time series. However, the application of a new NDVI time series noise reduction technique involving a high-order spline-based function-fitting procedure was presented by Bradley *et al.*, (2007). The procedure comprises a complex set of steps that include the use of harmonic and polynomial components to derive average annual phenology, and a spline fit to describe long term inter-annual variability in a time series, the details of which are described in Hermance, (2007) and Hermance *et al.*, (2007). Using this function-fitting technique, Bradley *et al.*, (2007) analyzed an NDVI data set covering the Great Basin region of the U.S. and examined spring green-up dates across a number of years for various land cover types, illustrating regional inter-annual variability in phenological transition dates.

2.5.3 Combination of Filtering and Function - Fitting Techniques

Knight *et al.*, (2006) described a multi-step noise reduction process for MODIS NDVI time series that involves both filtering and function-fitting techniques. First, anomalous spikes or drops in the dataset are identified using an empirically-derived threshold value, designed to detect sudden increases or decreases that are followed by a return to values near those of previous data points. These are removed and the data points flagged. Secondly, using MODIS quality flags, data values of unacceptable quality are identified, removed, and flagged (Knight *et al.*, 2006). In the third and final step, a Fourier transform is used to separate noise from the desired temporal signal in the data and produce a fitted curve, the values of which are used to replace the deleted and

35

flagged values from previous steps. The resulting time series are then applied in a multi-temporal land cover classification of a study area covering eastern portions of North Carolina and Virginia. By incorporating both filtering and function-fitting techniques in their process, Knight *et al.*, (2006) were able to exploit the advantages of both types of methods, while minimizing their respective disadvantages. However, the setting of initial thresholds and a minimum quality flag for selecting pixels for replacement can be highly subjective.

2.6 Time Series Analysis

In signal processing, statistics, pattern recognition, econometrics, mathematical finance, weather forecasting, earthquake prediction, control engineering and communications engineering, a time series is a sequence of data points, measured typically at successive time instants spaced at uniform time intervals either secondly, minutely, hourly, daily, weekly, monthly, quarterly, yearly, etc. Usually the intent is to discern whether there is some pattern in the values collected so as to extract meaningful statistics and other characteristics of the data to date.

The usage of time series models is twofold; i.e. (i) to obtain an understanding of the underlying forces and structure that produced the observed data, and (ii) fit a model that will be used for forecasting, monitoring, assessing and analyzing the data. The analysis of time-series data has been employed for many purposes including: (i) to describe characteristics of the data; (ii) to explain variance of any variable associated to surrogate variables; (iii) to predict a variable beyond the time span and (iv) to control processes (Chatfield, 1984).

An observed time series can be decomposed into three components; the trend (long term direction), the seasonal (systematic, calendar related movements) and the irregular

36

(unsystematic, short term fluctuations). Most time series analysis technique involves some form of filtering out noise in order to make the pattern more salient.

2.7 Trend Analysis

In some fields of study, the term "trend analysis" has more formally defined meanings. In this field of study, trend analysis is the practice of collecting data and attempting to spot a pattern, or trend, in the data. Although trend analysis is often used to predict future events, it could also be used to estimate uncertain events in the past. Trend analysis is based on the idea that what has happened in the past gives an idea of what will happen in the future. There are three main types of trends. These are short, intermediate and long term trend.

According to Box and Jenkins, (1976) there are no proven "automatic" techniques to identify trend components in time series data. However, as long as the trend is consistently increasing or decreasing, analysis and future predictions of such data becomes easy. If the time series data contain considerable noise or error, then the first step in the process of trend identification is smoothing. Smoothing always involves some form of local averaging of data such that the nonsystematic components of individual observations cancel each other out. The most common technique is moving average smoothing, which replace each element of the series by either the simple or weighted average of the surrounding elements (Box and Jenkins, 1976; Velleman and Hoaglin, 1981). Medians can also be used instead of means. The main advantage using the median as compared to moving average smoothing is that its results are less biased by outliers (within the smoothing window). Thus, if there are outliers in the data (e.g. due to measurement errors), median smoothing typically produces smoother or at least more "reliable" curves. However, the main disadvantage of median smoothing is that in

the absence of clear outliers it may produce more "jagged" curve than moving average and does not allow for weighting.

2.8 Fourier Analysis

Satellite measurements of land cover are often disturbed by noise caused by the atmosphere, sensor instability or orbit deviations. In order to derive interpretable characteristics from a noisy pattern, atmospheric transmission models, Modtran or 6S (Wolfe and Zissis, 1993) and geocoding methods can be applied. Alternatively, Fourier analysis can be deployed. Fourier or harmonic analysis is a mathematical technique to decompose a complex static signal into a series of individual cosine waves, each characterized by a specific amplitude and phase angle. Several authors have successfully applied Fourier analysis in analysing time series of AVHRR NDVI imagery (e.g. Azzali and Menenti, 2000; Roerink and Menenti, 2000; Moody and Johnson, 2001; Jabubauskas et al., 2001and 2002).

As a matter of fact, a process that repeats itself every t seconds can be represented by a series of harmonic functions whose frequencies are multiples of a base frequency. This series of harmonic functions is called a Fourier series. Assume the process can be described by a function F (t). The usual form of the Fourier series is (Pipes and Harvill, 1971):

$$f(x) = a_0 + \sum_{n=1}^{\infty}\left(a_n \cos\frac{n\pi x}{L} + b_n \sin\frac{n\pi x}{L}\right) \ldots\ldots\ldots (1)$$

The constant term in equation (1) is always equal to the mean value of the equation, e.g. the mean NDVI value in a series of satellite imagery. Equation (1) can be written in different forms, following basic mathematical laws (Pipes and Harvill, 1971). In this

38

research it was decided to transfer equation (1) to a form that only contains cosine terms to facilitate interpretation. Equation (1) can therefore be written as

$$f(x) = a_0 + \sum_{n=1}^{\infty} \left(c_n \cos\frac{n\pi x}{L} - \emptyset n \right) \ldots\ldots\ldots (2)$$

Equation (2) now has a desirable form with only cosine terms. The signal is decomposed in a series of cosine terms, each with its own amplitude (c_n) and phase angle ($\emptyset_n$), and a constant term (a_0). When a signal is described using Fourier analysis the values for the coefficients c_n need to be found. An algorithm to recover those coefficients from a discrete signal is the FFT. In this case we are analysing a discrete signal of 36 samples (NDVI images) with a fixed interval of ten days and the FFT is used to find values for the Fourier coefficients c_n. The result of the FFT is a complex vector, and its real part contains the coefficients of (a_0) and its imaginary part contains the coefficients of (b_n) of equation (1). The coefficients c_n of equation (2) can be derived from (a_0) and (b_n) by calculating the length of the vector. There are a few limitations to the FFT related to the underlying mathematics. Firstly, in order to correctly recover a signal from the Fourier transform of its samples, the signal must be sampled with a frequency of at least twice its bandwidth (the Nyquist frequency). Secondly, only static waves can be analysed using the FFT, which means that both the amplitude and phase of the individual terms must be constant over time.

The frequencies, which are recovered by the FFT, are given by

$$f_k = \frac{k}{n}f_s \ldots\ldots\ldots (3)$$

where f_k is the frequency of the kth term, n is the number of samples and f_s is the sampling frequency. In this case the smallest frequency that can be recovered from the

time series is 2.778 * 10^{-3} (1/36 * 1/10), which is equal to a period of 360 days. The total variance of the Fourier series can be calculated from the amplitude values (Davis, 1986) through:

$$\text{Total variance} = \sum_1^n \frac{(amplitude)^2}{2} \quad \ldots\ldots\ldots (4)$$

The percentage variance of each individual term can then be calculated by dividing its contribution by the total.

CHAPTER THREE

MATERIALS AND METHOD

3.1 Introduction

The following chapter describes the methods used to complete an empirical FFT analysis on time series NDVI for assessment of vegetation patterns in Ghana. Figure 3.4 and 3.5 presents a flowchart outlining these methods and the principal steps involved. The procedures and steps summarized in Figure 3.5 are each described in the sections and subsections presented below. First, a description of the study area, located in Sub - Sahara Africa, Ghana, is given in section 3.1, followed by explanations of the acquisition and pre-processing of the time series multi-temporal NDVI dataset employed in the research.

3.2 The Study Area

The study area, Ghana, depicted in Figure 3.1 is located in Sub - Sahara Africa. It extends for a maximum of 672 km from north to south and lies within latitudes 4.5°N and 11°N, and 536km from west to east and lies within longitude 3°W and 1°E. It is bounded to the west (668 km) by Cote d' Ivoire, to the north (548 km) by Burkina Faso, to the south (877 Km) by the Gulf of Guinea and the Atlantic Ocean and to the east (668 km) by the Republic of Togo (Clifford *et al*, 2000). It has a total area of 238,500 square kilometres (or 92,090 square miles) and an estimated population of 25 million, (2010 census data) drawn from more than one hundred ethnic groups - each with its own unique language. English, is the official language, a legacy of British colonial rule. The country's economy is dominated by agriculture, which employs about 40 percent of the working population.
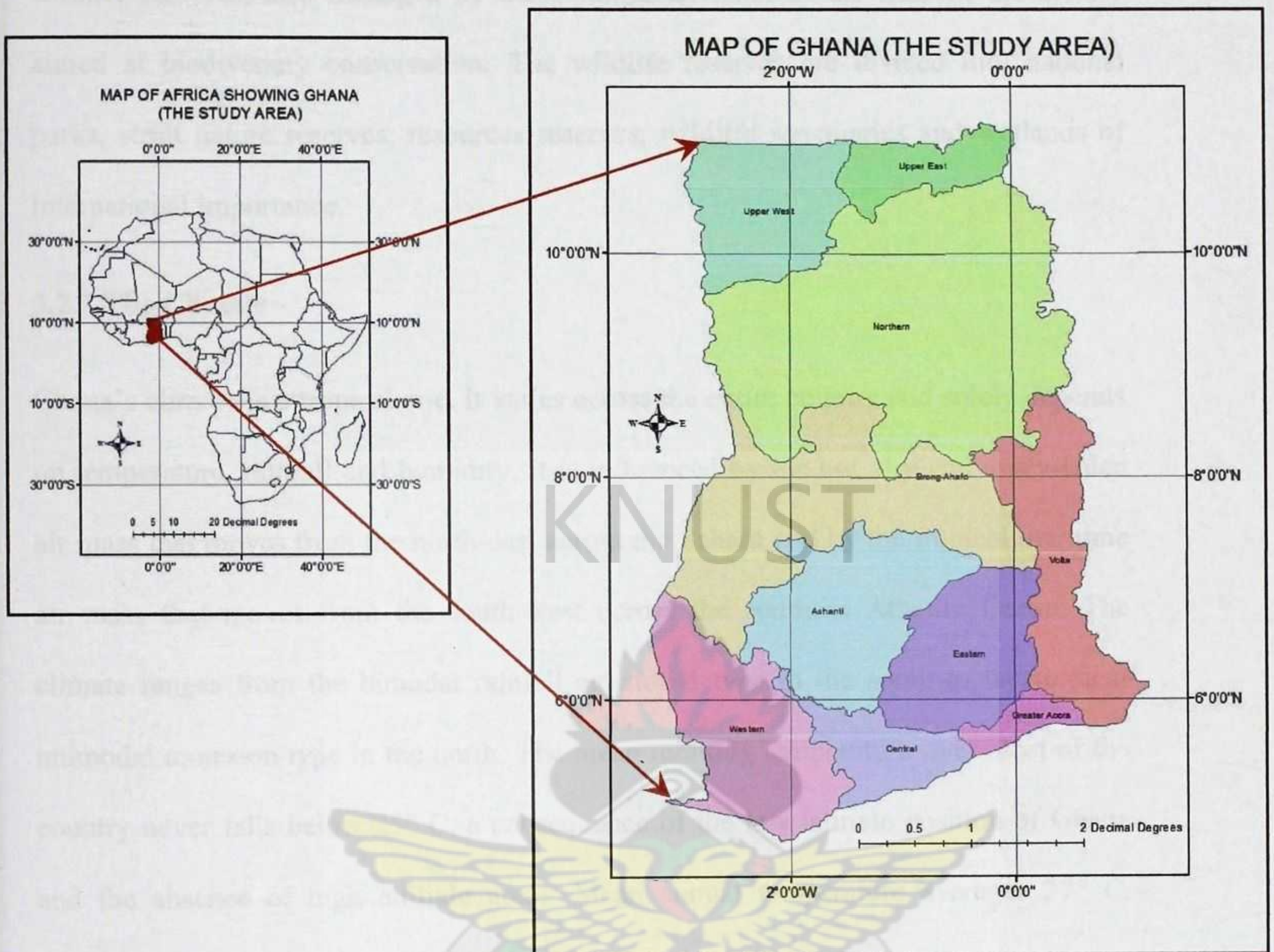
Figure 3.1: The map of Africa (left) showing the map of Ghana (right), (The Study Area)

3.2.1 Protected Areas

There are two main categories of protected areas in Ghana. These are (i) the forest reserves and (ii) the wildlife reserves. The forest reserves, managed by the Forest Services Division of the Ministry of Lands and Natural Resources (MLNR), are forest areas where controlled extractive activities such as logging are permitted. However, in the last years, the Forestry Service Division has re-designated 29 of the forest resources as Globally Significant Biodiversity Areas. These areas have been found to have a high concentration of biological resources that are of global conservation importance. The

42

wildlife reserves, also managed by the Wildlife Division of the MLNR, are clearly aimed at biodiversity conservation. The wildlife reserves are divided into national parks, strict nature reserves, resources reserves, wildlife sanctuaries and wetlands of international importance.

3.2.2 The Climate

Ghana's climate is a tropical one. It varies across the entire country and solely depends on temperature, rainfall and humidity. It is influenced by the hot, dry and dusty-laden air mass that moves from the north-east across the Sahara and by the tropical maritime air mass that moves from the south-west across the southern Atlantic Ocean. The climate ranges from the bimodal rainfall equatorial type in the south to the tropical unimodal monsoon type in the north. The mean monthly temperature over most of the country never falls below 25° C, a consequence of the low latitude position of Ghana and the absence of high altitude areas. Mean annual temperature averages 27° C. Absolute maxima approach 40° C, especially in the north, with absolute minima descending to about 15° C. In the coastal areas, where the modifying influence of the sea breeze is felt, the annual range of temperature sometimes falls between 15°C and 16°C. In the interior of the coastal areas, the range becomes higher, thus about 17°C to 19°C (Dickson and Benneh, 1988; Benneh et al., 1990). Ghana has two fundamental seasons, the wet and dry. During summer in the northern hemisphere, the monsoon winds pushes northward across the country from the southwest. These warm air masses carried by the winds bring torrential rains and thunder storms. This normally occurs between April and September, with July- August being the peaks in most areas. This is the Rainy Season. The Axim area, located in the southwest tip of Ghana receives the highest amount of this rain throughout the whole year (Dickson and Benneh, 1988; Benneh et al., 1990).

In the dry season, the northeast trade winds from the northern hemisphere travel across to the south, bringing dry and dusty warm air from the Sahara desert. In most cases, the northern parts of Ghana could hit maximum temperatures of about 32°C (89.6F). This also normally occurs between late November and late March, with December and January being the peaks. This is the period called the Harmattan Season (Dickson and Benneh, 1988; Benneh et al., 1990).

3.2.3 Topography and Soils

The topography of Ghana as shown in figure 3.3 is mainly undulating with most slopes being less than 5% and many not exceeding 1%. It consists mostly of low plains in the south-central area with almost half of the country lying less than 152 meters (499 ft) above mean sea level. The highest elevation, 883 meters (2,897ft) above mean sea level is located at Mount Afadjato in the Akwapim-Togo Ranges. The 537 kilometers (334 mi) coastline is mostly a low, sandy shore backed by plains and scrub and intersected by several rivers and streams, most of which are navigable only by canoe. A tropical rain forest belt, broken by heavily forested hills and many streams and rivers, extends northward from the shore, near the Côte d'Ivoire frontier. This area produces most of the country's cocoa, minerals, and timber. North of this belt, the country varies from 91 to 396 meters (299 to 1,299 ft) above mean sea level and is covered by low bush, park-like savanna, and grassy plains. Despite the general undulating nature of the terrain, about 70% of the topography suffers from moderate to severe soil erosion (Boateng, 1998) with a high degree of gully erosion occurring in the Savannah zones along the north and south, and to some extent along the west. Most of these soils are developed on thoroughly weathered parent materials, with alluvial soils (Fluvisols) and eroded shallow soils (Leptosols) common to all the ecological zones and are plagued with inherent or human induced infertility (MoFA, 1998). The soils in the Forest zone are

grouped under Forest Oxysols and Forest Acid Gleysols. They are porous, well drained and generally loamy and are distinguished from those of the Savannah zones by the greater accumulation of organic matter in the surface resulting from higher accumulation of biomass. They occur in areas underlain by various igneous, metamorphic and sedimentary rocks, which have influenced the nature and properties of the soil (MoFA, 1998). Soils of the Savannah zones, especially in the interior Savannah, are low in organic matter (less than 2% in the topsoil), have high levels of iron concretions and are susceptible to severe erosion (MoFA, 1998).
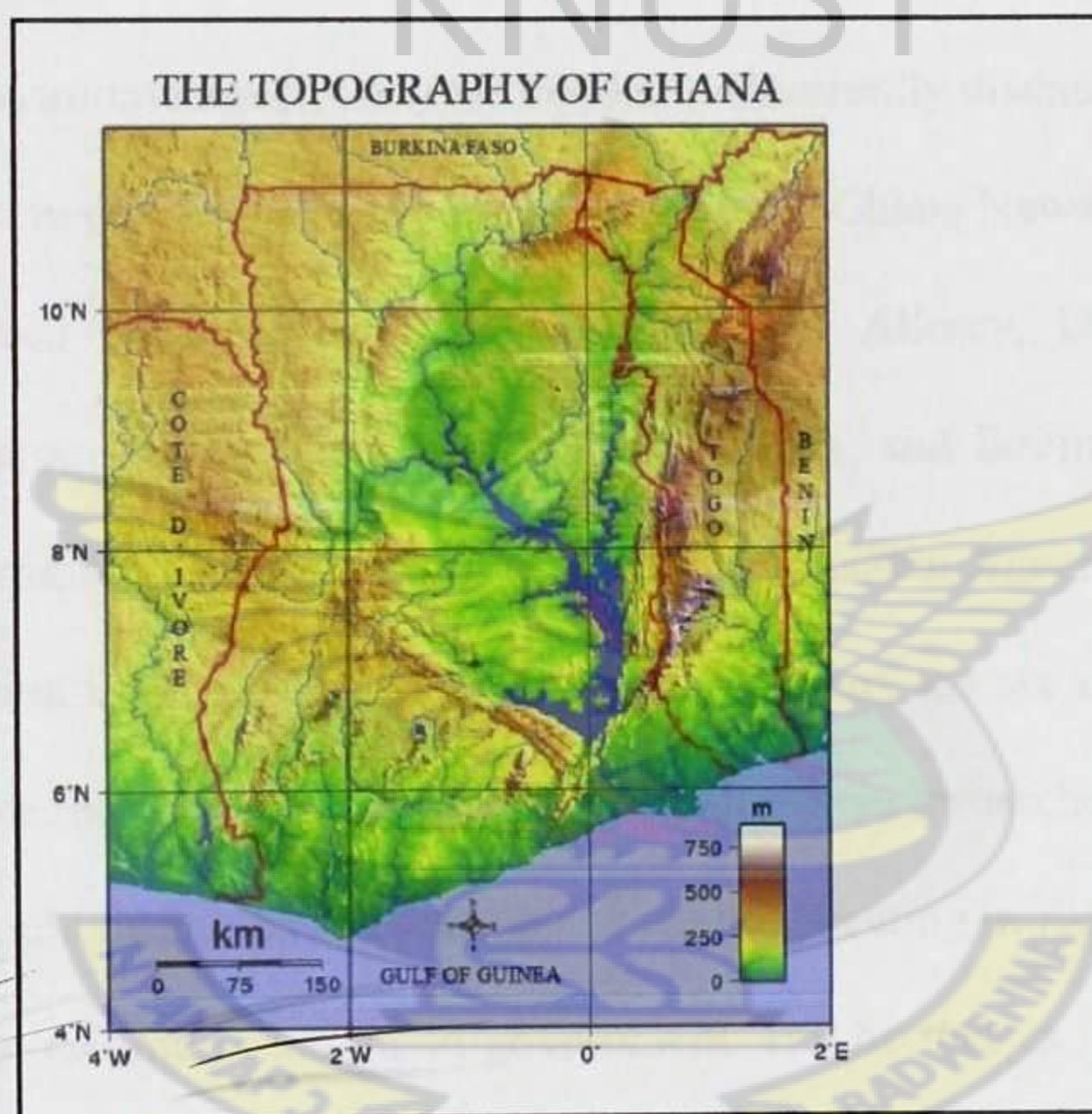
Figure 3.2: The topography of Ghana (Source: Oppong-Anane, 2001)

3.2.4 Agriculture

Agriculture is the backbone of the Ghanaian economy and a major foreign exchange earner. It contributes about 35% to the Gross Domestic Product (GDP), employs 55% of the population on a formal and informal basis and contributes about 45% of all export earnings (Ghana National Commission for UNESCO Report, 2010). The country produces a variety of crops in various climatic zones which range from dry savanna to

wet forest and which run in east west bands across the country. The agriculture sector is made up of five major sub sectors, including food crops, livestock, fisheries, cocoa and forestry. The food crops made up yams, grains, cocoa, oil palms, kola nuts, and timber, form the base of Ghana's economy. Agriculture is predominantly practiced on smallholder, family-operated farms using rudimentary technology to produce about 80% of the total output. The production is primarily rain-fed, and has therefore been very unpredictable (Ghana National Commission for UNESCO Report, 2010).

3.2.5 The Agro - Ecological Zones

Scientist, ecologist, environmentalist, and researchers, are currently discussing the issue of dividing Ghana into twelve major agro - ecological zones (Ghana News Agency, 21st Sept. 07). The research conducted and headed by Albert Allotey, Department of Geography and Resource Development, University of Ghana, and Emmanuel Techie-Obeng, Senior Programme Officer of the Environmental Protection Agency (EPA) said with the fast degradation in the ecological system of the country the six zones were no longer viable and hence the need to review it. According to these researchers, the names of the 12 new ones would be agreed to by a team of experts meeting in Accra to discuss the research and make recommendations to government. But be that as it may, Ghana for now still remains divided into six agro - ecological zones. Shown in the Figure 3.3 below, these zones includes the following (i) Closed Forest, (ii) The Strand and Mangrove Swamp, (iii) Semi - Deciduous Forest, (iv) Coastal Shrub and Grassland (Coastal Savanna), (v) Guinea Savannah and (vi) Sudan Savannah (Dickson and Benneh, 1988). Because the names of these six agro - ecological zones keep changing and most often not explanatory enough, the names of the vegetation types (refer to appendix i) adopted by the EPA in the 2000 vegetation map of Ghana as shown in Figure 3.4 was applied in this research.
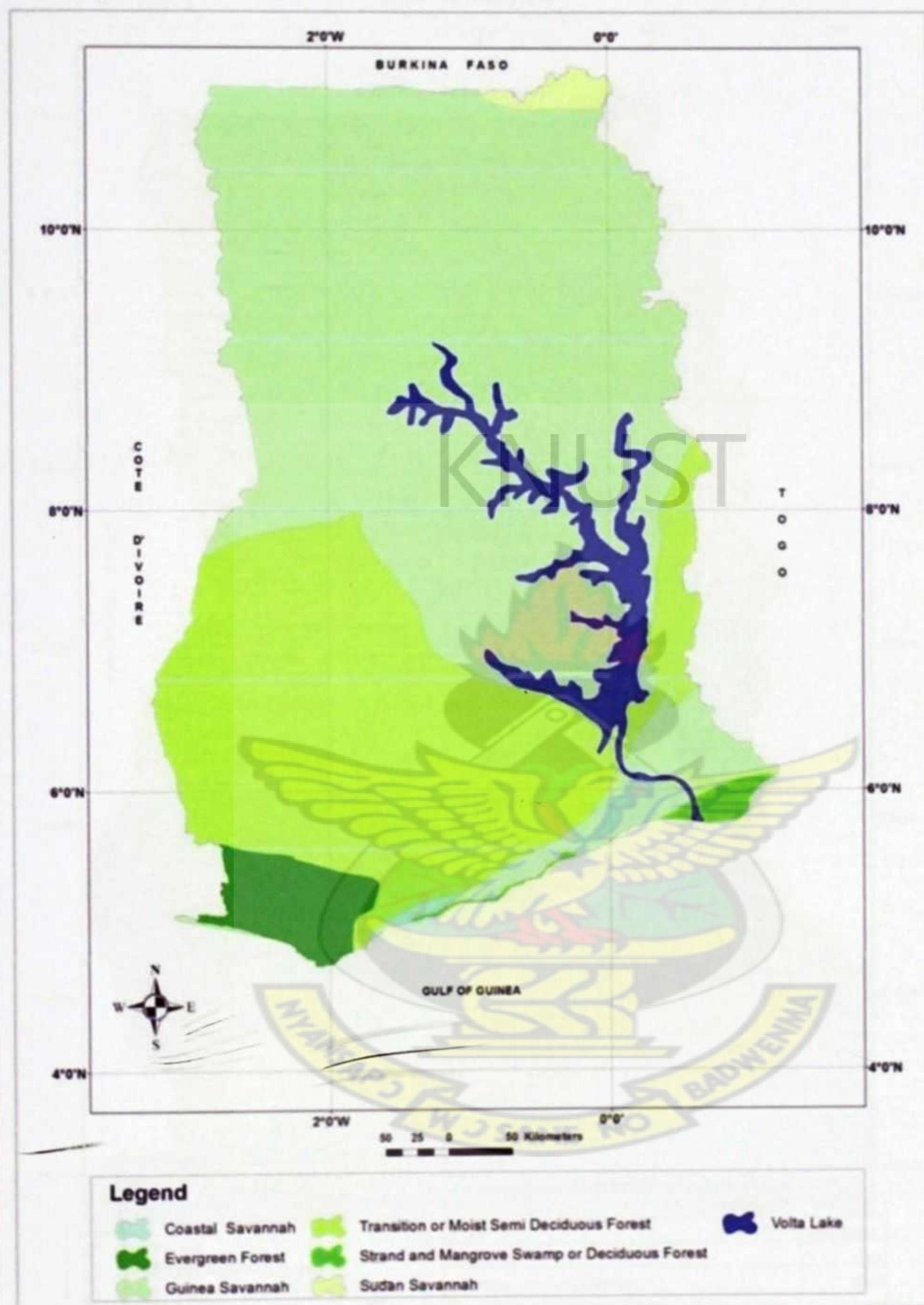
46

THE SIX AGRO - ECOLOGICAL ZONES OF GHANA

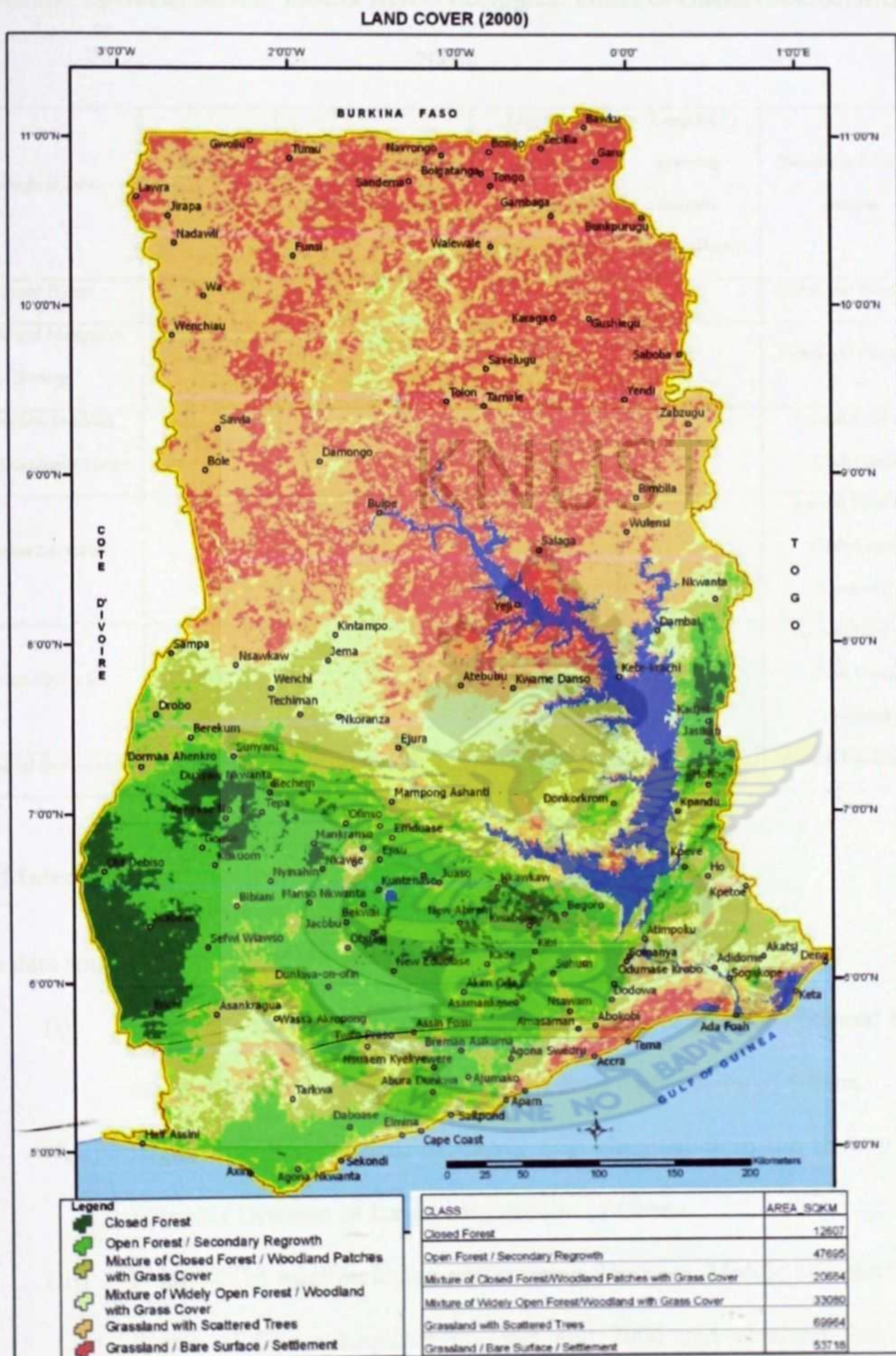Figure 3.3: The Six Agro-Ecological Zone of Ghana (Source: Dickson and Benneh (1988))

Figure 3.4: 2000 Vegetation Map of Ghana (Source: EPA Report (2001))

48

Table 3.1: Characteristics of the Six Agro - Ecological Zones of Ghana (Source: SRID, 2001)

Ecological Zone	Rainfall (mm/year)	Average Percentage of Total Area (%)	Length of growing seasons Major (Days)	Length of growing seasons Minor (Days)	Dominant Land use system
Closed Forest	2200	3	150 – 160	100	Forest and Plantation
Strand and Mangrove Swamp	1500	3	150 – 160	90	Forest and Plantation
Transition or Moist Semi Deciduous Forest	1300	28	200 – 220	60	Annual Food and Cash Crops
Guinea Savannah	1100	63	180 – 200		Annual Food and Cash Crops, Livestock
Sudan Savannah	1000	1	150 – 160		Annual Food and Cash Crops, Livestock
Coastal Savannah	800	2	100 -110	60	Annual Food Crops,

3.3 Materials

The data sources for this study include the following:

(i)   Hard copy topographic maps of Ghana at scale of 1:50000 obtained from the Survey and Mapping Division of Lands commission of Ghana.

(ii)   Digital topographic map of Ghana also obtained from the Survey and Mapping Division of Lands commission of Ghana.

(iii) Landsat TM satellite image representing Southern, Middle and Northern Sector of Ghana acquired in 1996 and 2006 and obtained from the Centre for Remote Sensing and Geographic Information Systems (CERGIS), University of Ghana, Accra, Ghana.

49

(iv)   Sokkia L1 GPS data of some randomly elected location within the study area.

(v)   10 - day composite NOAA - AVHRR NDVI dataset acquired from Global Inventory Modeling and Mapping Studies (GIMMS) for Africa and covering the period 1987 to 2006.

(vi)   2000 land cover land use map of Ghana, generated by the Centre for Remote Sensing and Geographic Information System (CERGIS), University of Ghana.

3.4 Method

3.4.1 Geometric Correction

Geometric correction was performed on the NDVI datasets and the TM satellite images in order to assign them to their correct position on the earth's surface. Out of the several resampling methods that could be used to rectify remotely sensed images, and to co-register them to a coordinate system, the nearest neighbour method was selected to resample the satellite images in order to assign them to the WGS 84 coordinate system.

3.4.2 Extraction of the Region of Interest, Ghana

The region of interest, Ghana, was extracted using ArcMap 10.0 software. A shapefile of Ghana extracted from a shapefile of Africa with WGS 84 coordinate system and downloaded from the internet was used to clip the entire Africa NDVI datasets. These NDVI datasets prior to the clipping was georeferenced using the WGS84 shapefile Africa map. Values of the NDVI images of Ghana obtained after the extraction was reduced from an 8-bit digital number (DN) to NDVI values between 0 and 1 according to the following equation by the World Data Centre for Remote Sensing of the

Atmosphere; For 2 <= DN <= 183: NDVI = (DN-2)*0.0022099 - 0.2, where DN = 0 is equivalent to water, DN = 1 represents anomaly less than -0.2, DN = 184 represents anomaly more than 0.2 and DN = 185 is equivalent to no data.

The datasets were checked and corrected for NDVI values between 0 and 1 in order to prevent negative NDVI values that normally complicate the application of the FFT algorithm. Two separate NDVI averages of Ghana each based on ten years were calculated in ArcMap using the Raster Math in the 3D Analyst Tools. This is shown if Figure 3.4 below. Finally average NDVI images representing 1996 (i.e. 1987 -1996, 360 images) and 2006 (i.e. 1997 -2006, 360 images) were used for the study.
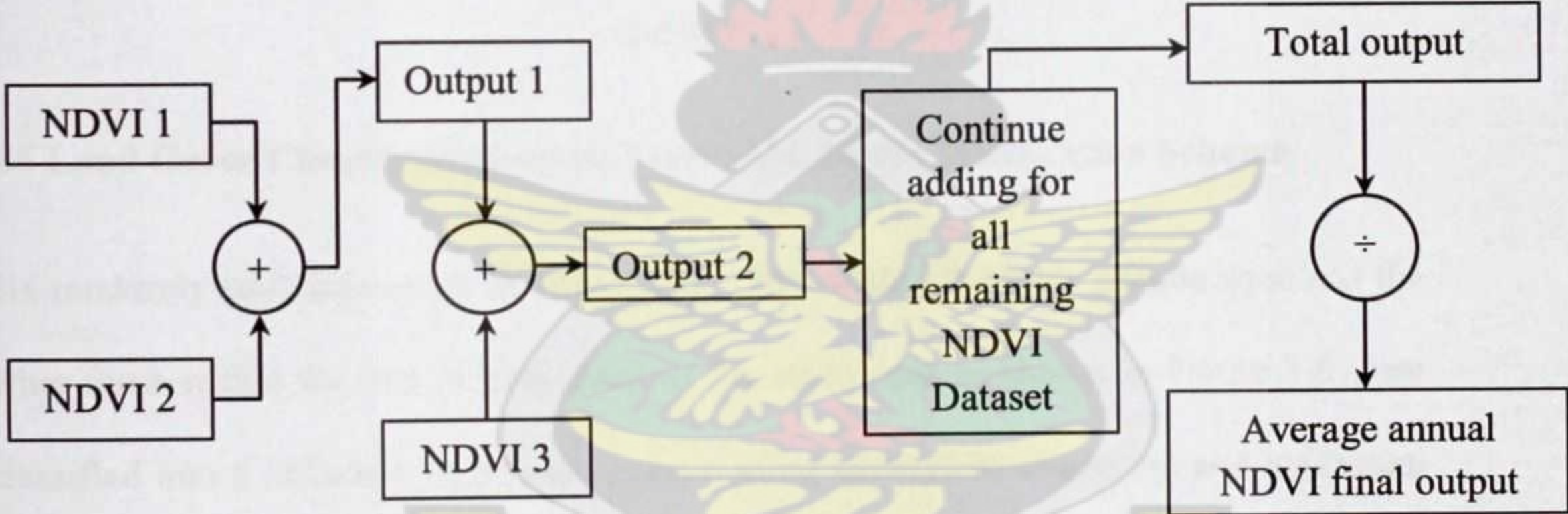
Figure 3.5: Flow chart of NDVI averages in ArcMap

3.4.3 Image Noise Reduction using FFT

Before using these average NDVI images representing 1996 and 2006 to derive the vegetation zone variables, it was necessary to, as a focus of this research, reduce any inherent noise effect. The FFT tool in Erdas imagine 2010 was used to perform this task under the Convolution Spatial Enhancement option using a 3X3 Low-Pass filter. The transformation was performed as an enhancement in the frequency domain, then

51

returned to the original spatial domain by using the Inverse Fourier Transform tool. This procedure is illustrated in figure 3.5 above.

Figure 3.6: Diagram Summarizing the FFT application. (Provides answer to research question 2)

3.5 Land Cover Classification using Vegetation Zone Classification Scheme

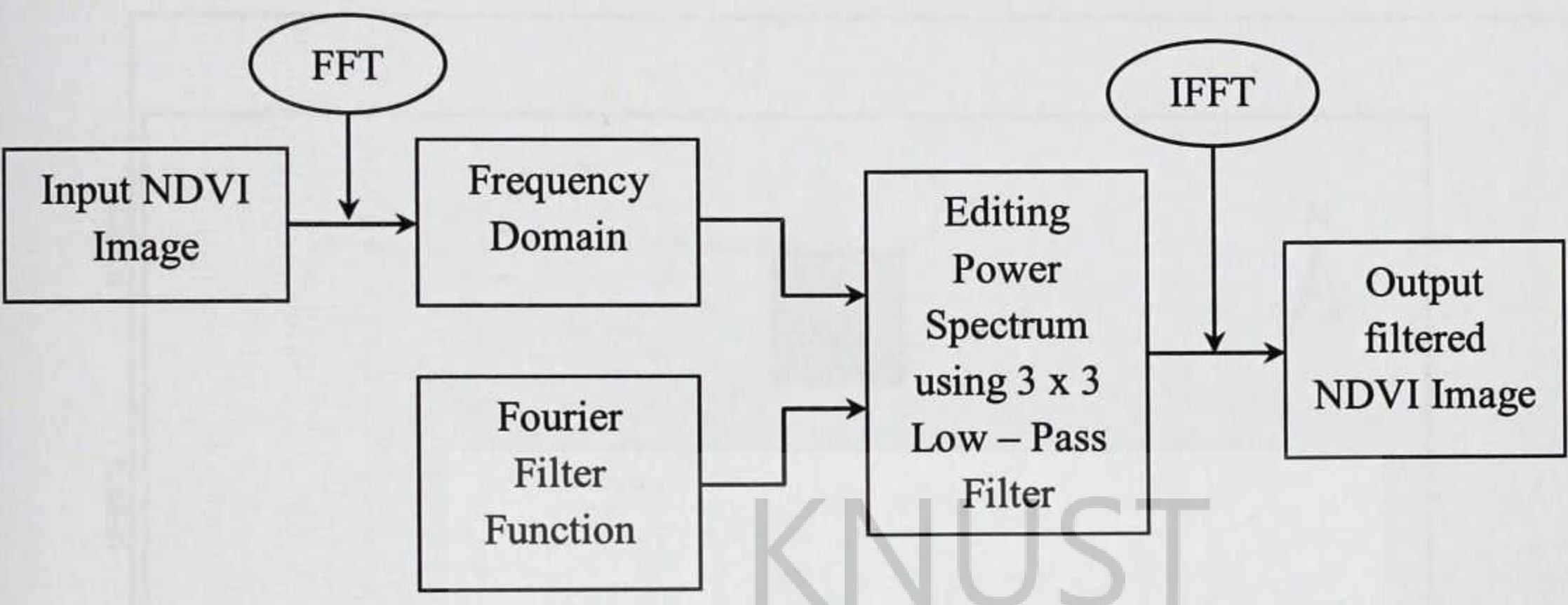Six randomly selected scenes of TM images, three within the high latitude zone and the other three within the low latitude zone of the study area as shown in Figure 3.6 were classified into 6 different Vegetation pattern using supervised clustering and maximum likelihood classifications algorithm in Erdas Imagine. "Ground truth" data were obtained from three sources. (i) 2000 land cover land use map, generated by the Centre for Remote Sensing and Geographic Information System (CERGIS), University of Ghana, (ii) topographic map of Ghana, also generated by the Survey and Mapping Division of Lands Commission and (iii) Global Positioning System data of some arbitrary selected points.

This information was used for selection of training signatures in the NDVI images by determining which pixel of the vegetation zone of the TM image matches that of the NDVI dataset. The scheme for the classification of the TM image into various

vegetation zones was derived from the main vegetation formations as described by
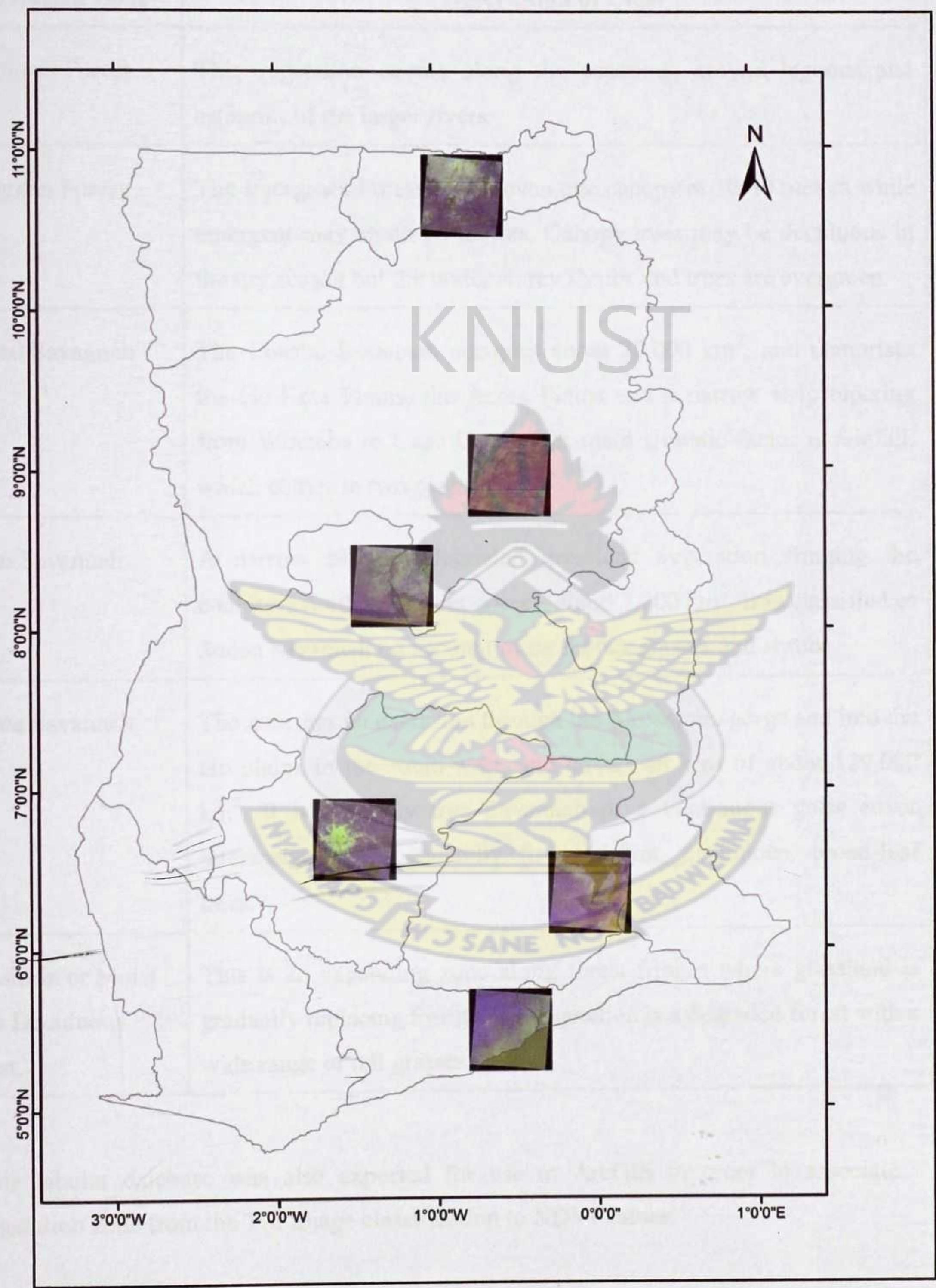
Benneh et al. (1990).

Figure 3.7: The six randomly selected scenes of TM images

Table 3.2: Vegetation Zone Classification (Source; Benneh *et al.* (1990))

Vegetation Zone	Description of Class
Deciduous Forest	This vegetation occurs along the coastline, around lagoons and estuaries of the larger rivers.
Evergreen Forest	The Evergreen Forest has an even tree canopy at 30-40 metres while emergent may attain 60 metres. Canopy trees may be deciduous in the dry season but the under storey shrubs and trees are evergreen.
Coastal Savannah	The Coastal Savannah occupies about 20,000 km^2, and comprises the Ho-Keta Plains, the Accra Plains and a narrow strip tapering from Winneba to Cape Coast. The main climatic factor is rainfall, which comes in two peaks.
Sudan Savannah	A narrow strip of degraded grassland vegetation fringing the country's northern border corner, about 7,200 km^2. It is classified as Sudan Savannah on account of its shorter grasses and shrubs.
Guinea Savannah	The zone has an extension through the Akosombo gorge and into the Ho plains in the south-west, and covers an area of about 129,000 km^2. It is typically tree Savannah or a continuous grass cover interspersed with generally fire resistant, deciduous, broad-leaf trees.
Transition or Moist Semi Deciduous Forest.	This is an expanding zone along forest fringes where grassland is gradually replacing forest. The vegetation is a degraded forest with a wide range of tall grasses.

This tabular database was also exported for use in ArcGIS in order to associate vegetation zone from the TM Image classification to NDVI values.

3.6 Data Analyses

Results from the Vegetation Zone were used to create a georeferenced tabular database based on class mapping of Vegetation Zone data to NDVI values. As stated earlier, this tabular database was exported for use in ArcGIS in order to associate Vegetation Zone Classification of the TM images to NDVI values calculated. This was used to reclassify the NDVI maps of Ghana into the various Vegetation Zone Maps of Ghana in accordance with the Vegetation Map produced by the EPA in 2000. The total area occupied by each respective vegetation class was digitally computed for using the image processing software (Erdas Imagine) and the visualization of the vegetation map made by using ArcGIS.

3.7 Accuracy Assessment

To ensure that the information derived from the classification was of high quality and to deduce meaningful indications on thematic correctness, the classified NDVI maps were assessed for accuracy using classification matrix table and Cohen's kappa. In the assessment, the classified NDVI image and "ground truth data" were compared. The relationship between these two sets of information was summarized in two ways (i) Contingency matrix, which describes the comparison of the remote sensing derived classification map and "ground truth" reference data (ii) kappa statistics, which provides a measure of agreement between the classified remotely sensed data and "ground truth" reference data. Overall accuracy and class-specific user and producer accuracies were calculated for each of the resultant six vegetation zone classes. Producer's accuracy was obtained by taking the number of points classified correctly for a class and divides it by the number of ground reference points in that class, while

55

user's accuracy was the number of points classified correctly for a class divided by the number of points classified as that class.

Table 3.3: Classification Error Matrix for 2006 vegetation zone

Classified Data	Reference Data						
	Grassland with Scattered Trees	Grassland / Bare Surface / Settlement	Mixture of Closed and Open Forest	Closed Forest	Open Foerst / Secondary Regrowth	Mixture of widely Open Forest / Woodland	Row Total
Grassland with Scattered Trees	60	0	6	0	0	0	66
Grassland / Bare Surface / Settlement	0	2	0	0	0	0	2
Mixture of Closed and Open Forest	2	0	32	3	0	0	37
Closed Forest	1	0	1	7	0	0	9
Open Forest / Secondary Regrowth	0	0	0	0	4	0	4
Mixture of widely Open Forest / Woodland	0	0	0	0	0	2	2
Column Total	63	2	39	10	4	2	120

56

Table 3.4: Accuracy Total

Class Name	Reference Total	Classified Total	Number Correct	Producers Accuracy	Users Accuracy
Grassland with Scattered Trees	63	66	60	95.24%	90.91%
Grassland / Bare Surface / Settlement	2	2	2	100.00%	100.00%
Mixture of Closed and Open Forest	39	37	32	82.05%	86.49%
Closed Forest	10	9	7	70.00%	77.78%
Open Forest / Secondary Regrowth	4	4	4	100.00%	100.00%
Mixture of widely Open Forest / Woodland	2	2	2	100.00%	100.00%
Column Total	120	120	107		

Overall Classification Accuracy = 89.17%

Kappa statistics

Overall Kappa statistics = 0.8204

Table 3.5: Conditional Kappa for each category

Class Name	Kappa
Grassland with Scattered Trees	0.8086
Grassland / Bare Surface / Settlement	1.0000
Mixture of Closed and Open Forest	0.7998
Closed Forest	0.7576
Open Forest / Secondary Regrowth	1.0000
Mixture of widely Open Forest / Woodland	1.0000

CHAPTER FOUR

RESULTS AND DISCUSSIONS

4.1 Introduction

The results of the analysis described above are presented in this chapter. It lays more emphasis on the vegetation dynamism of Ghana produced from the NDVI dataset from 1986 to 2006. Vegetation maps representing 1996 (i.e. 1987 -1996), and 2006 (i.e. 1997 -2006) were produced after the analysis. These were visually assessed for vegetation classes and the associated changes during the 10-year period.

4.2 Extracted average NDVI dataset for Ghana

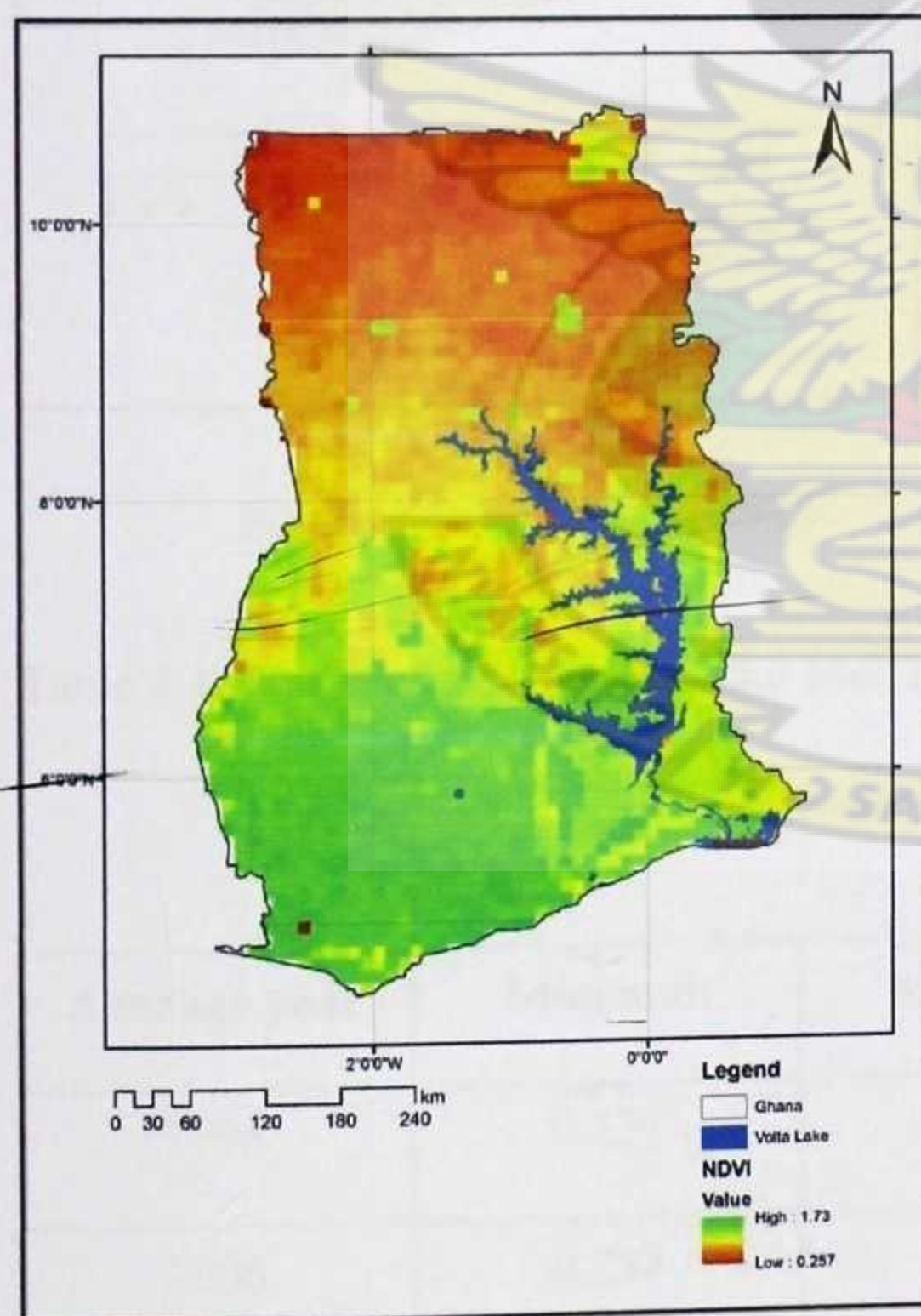Figure 4.1 and figure 4.2 represent the extracted average NDVI dataset for Ghana, the study area.
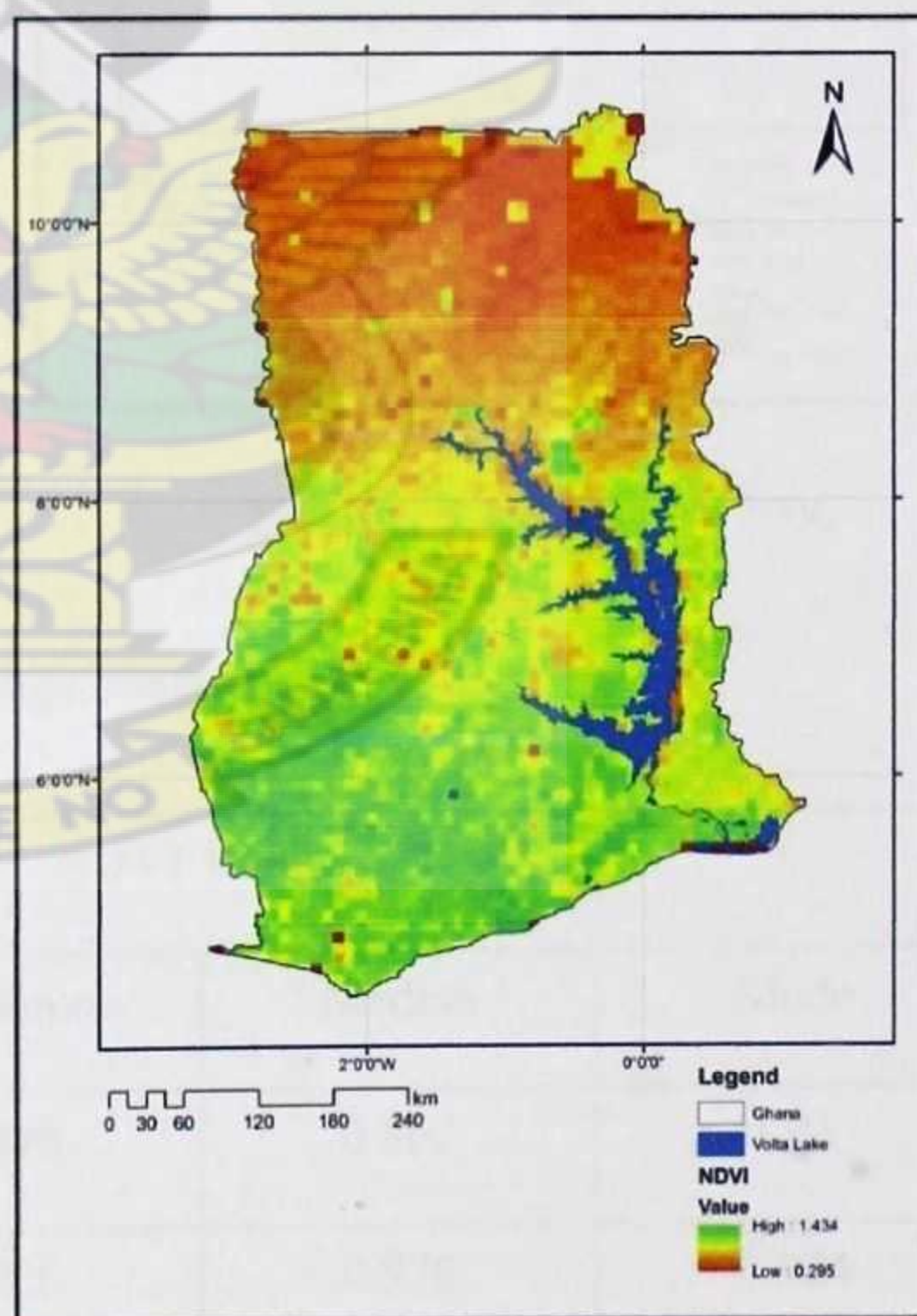
Figure 4.1: NDVI 1996   Figure 4.2: NDVI 2006

4.3 NDVI images of Ghana after applying the FFT algorithm

Figure 4.3 and figure 4.4 shows the NDVI images of Ghana after applying the FFT algorithm. The Statistics information from each image is shown in table 4.1 below.

Figure 4.3: FFT NDVI 1996   Figure 4.4: FFT NDVI 2006
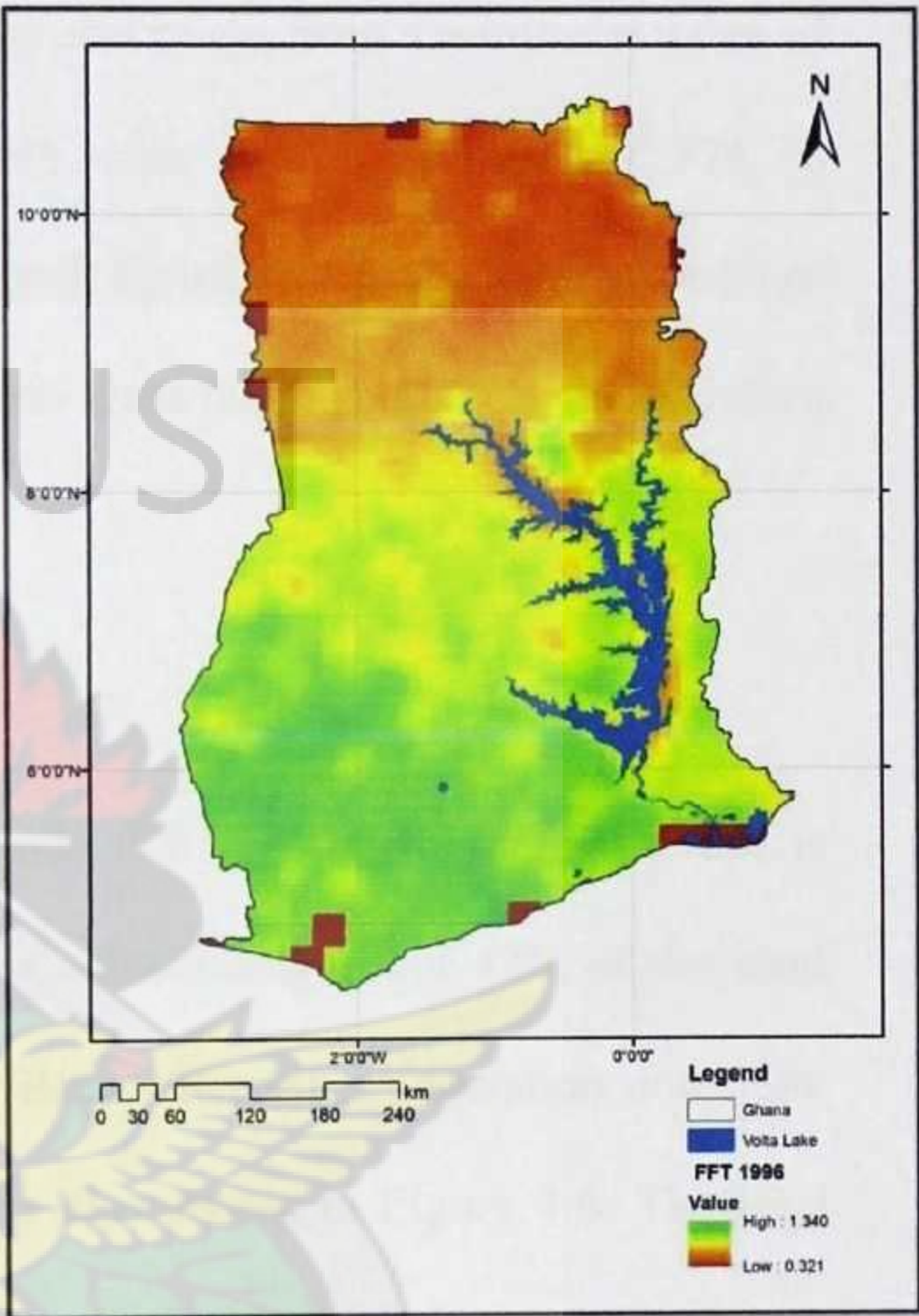
Table 4.1: Statistics information from each average image

Average year	NDVI Values			
	Minimum	Maximum	Median	Mode
1996	0.321	1.340	0.862	1.25
2006	0.257	1.726	0.978	0.924

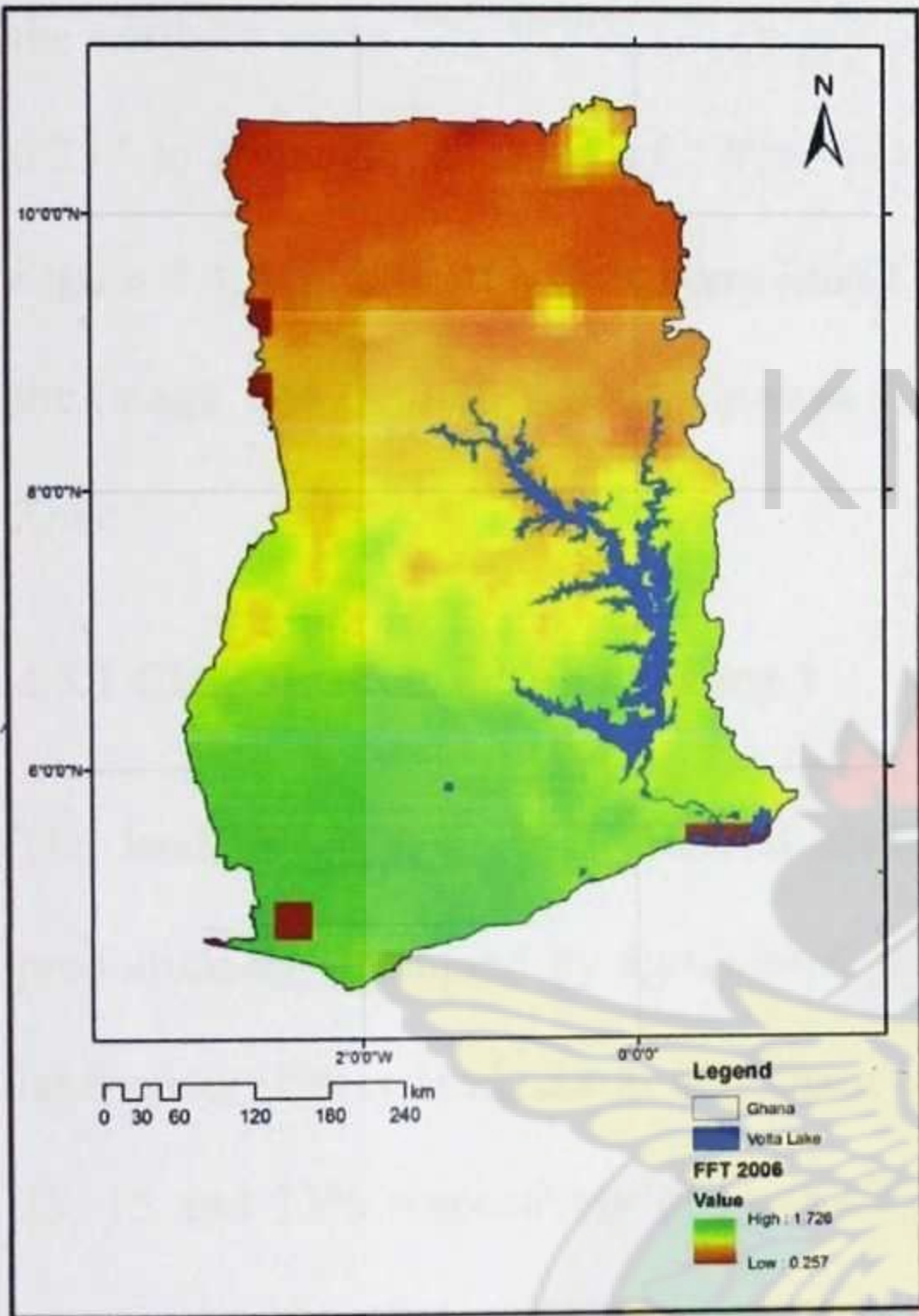The NDVI values of Figure 4.3 ranges from a minimum value of 0.321 to a maximum value of 1.340. The median value is 0.52 with mode 0.776. Visual observation of this figure indicates high NDVI values within the south western part of the study area. This decreases gradually, spreading through the central areas and dropping significantly in the northern zone. The NDVI values of Figure 4.4 also range from a minimum value of 0.257 to a maximum value of 1.726. The median value is 0.52 with mode 0.776. In Figure 4.4, high NDVI values were found to be well distributed in the southern part of the image, decreasing gradually through the central areas that also drop in the Northern Zone.

4.3.1 Classification Result of Scene 1

The land cover in scene 1, located above latitude 008° as shown in Figure 4.5, is predominantly occupied by agricultural activities, constituting about 47% of the total land cover. Grass land, shrub and Open Water Bodies/Riverine Vegetation constitute 25, 15 and 13% respectively of the total land as also shown in Figure 4.6. The total acreage occupied by each land cover class is depicted in Table 4.2 below.
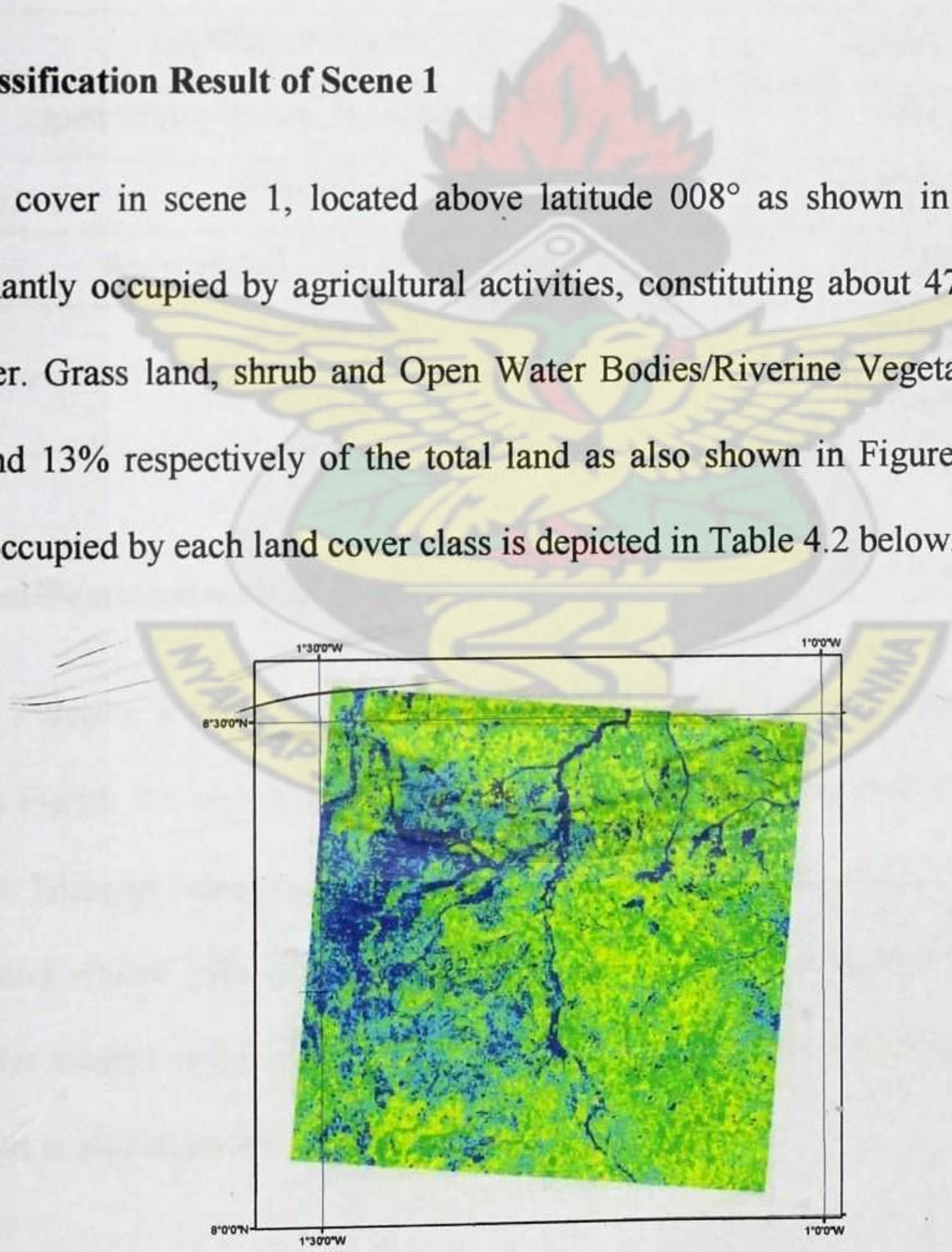

Figure 4.5: Supervised classification of scene 1

Figure 4.6: Legend of the land cover distribution of scene 1

Table 4.2: The total area occupied by each land cover class in scene 1

LANDCOVER CLASS	AREA (HA)
Open Water Bodies/Riverine Vegetation	34090.02
Grass Land	69264.72
Agricultural and Fallow Areas	127544.49
Shrub Land	39942.99
TOTAL	270842.22

4.3.2 Classification Result of Scene 2

Figure 4.7 depict a classified scene above latitude 008°N. The classification result shown in Figure 4.8 shows dominance of agricultural activities with 45% of the total land cover being occupied by agricultural and fallow areas. The land is made up of 20% of grassland whiles 19% is occupied by Shrubs. The remaining 16% is occupied by open water bodies and riverine vegetation. The total acreage occupied by each land cover class is also depicted in Table 4.3 below.

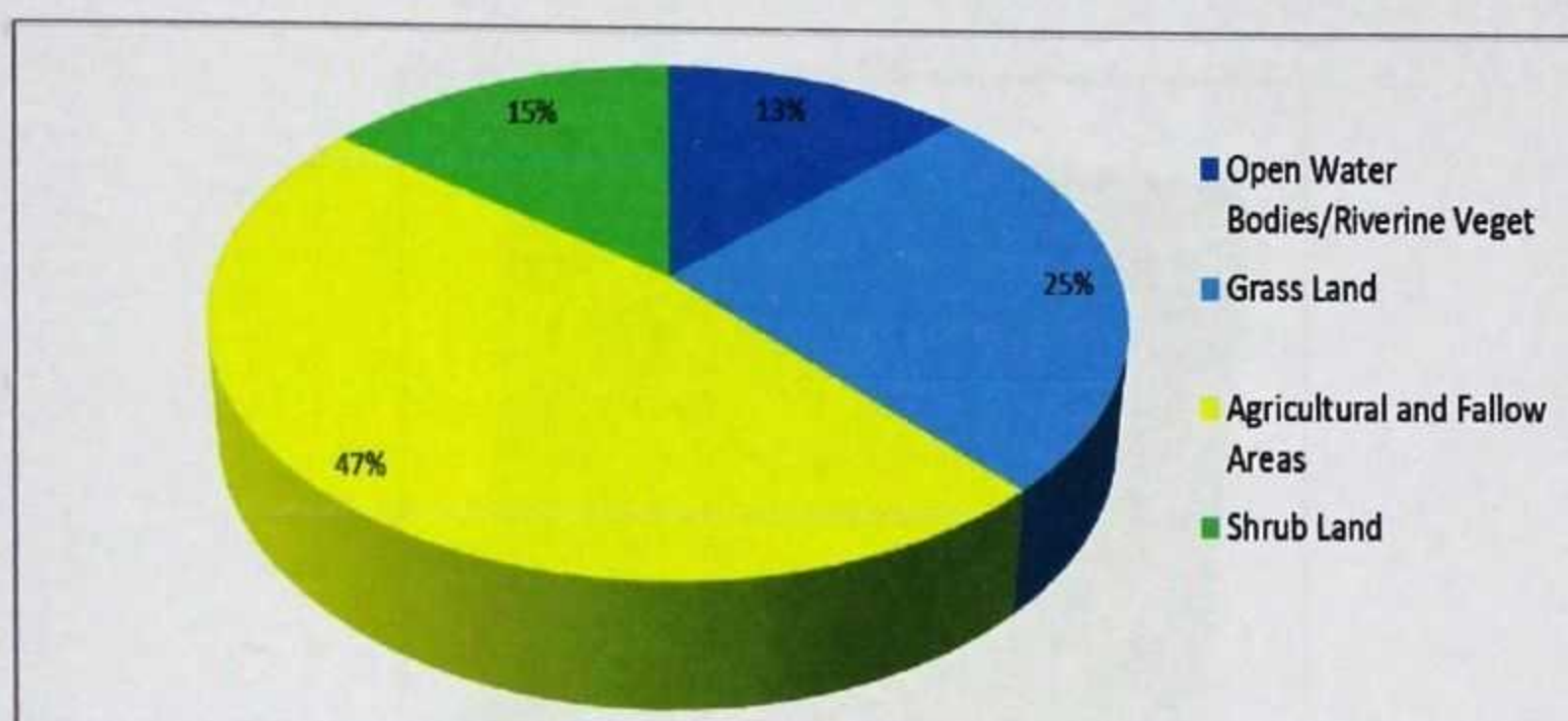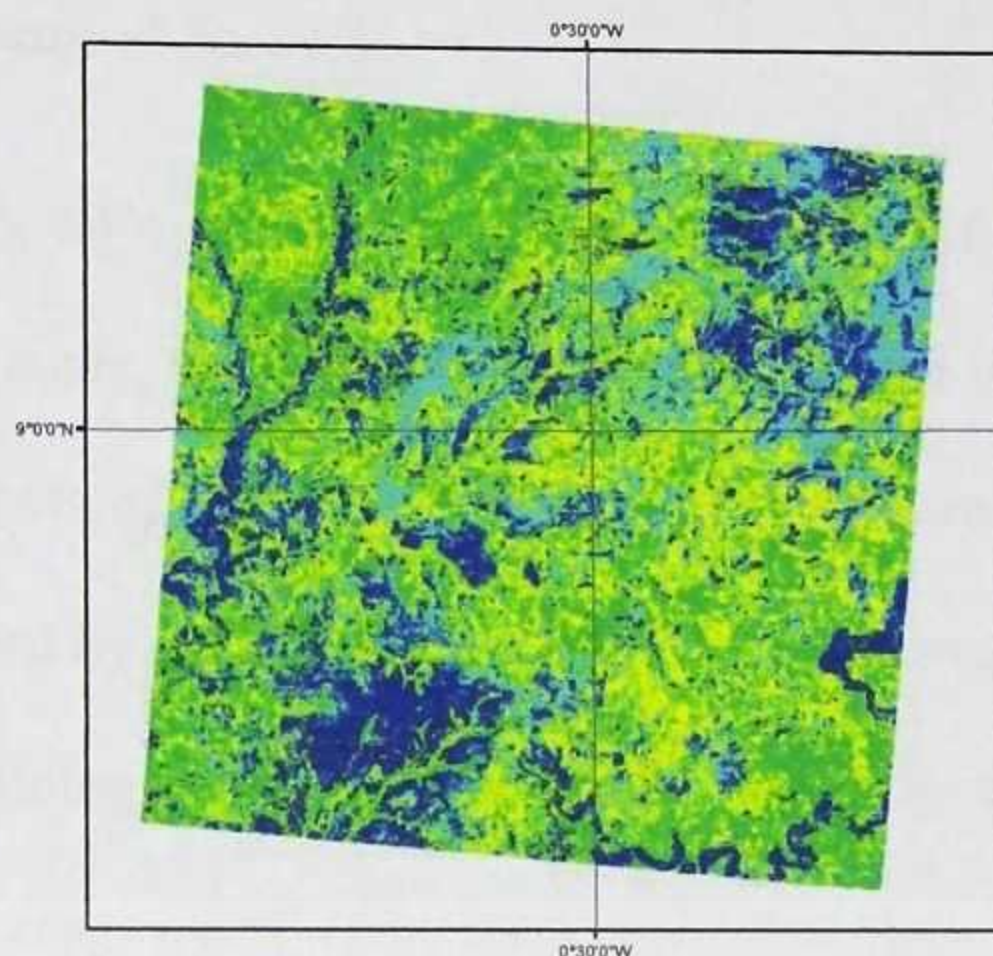Figure 4.7: Supervised classification of scene 2

Figure 4.8: Legend of the land cover distribution of scene 2

Table 4.3: The total area occupied by each land cover class in scene 2

LANDCOVER CLASS	AREA (HA)
Open Water Bodies/Riverine Vegetation	43334.16
Grass Land	54167.71
Agricultural and Fallow Areas	121877.34
Shrub Land	51459.32
TOTAL	270838.53

4.3.3 Classification Result of Scene 3

In scene 3 (Figure 4.9), 34% of the total land area (ie, 91336.41 Ha) is covered by agricultural and fallow lands. Shrubs cover 65867.76 Ha of the land forming 24% of the total land area, while 26% of the land (71384.94 Ha) is covered by grass. Of the total land area 10% is covered by open water bodies and riverine vegetation. As represented in figure 4.10, the remaining 6% of the land consist of built up areas. Depicted in Table 4.4 below is the total acreage occupied by each land cover class.

This scene shows land cover co-dominated by grassland, shrub and agricultural lands. Agricultural activities are mainly of the grass family and they include crops like maize, millet, guinea corn. This makes these regions typically a continuous grass cover interspersed with generally fire resistant, deciduous, broad-leaf trees forming the shrub cover. In the most luxuriant form, the shrubs show varying completeness of canopy. The grasses associated with the land cover are not uniform but differ according to a change in land cover type and latitude. This is an expanding zone along forest fringes where grassland is gradually replacing forest. The grassy background of the zone is invariably dominated by *Andropogon gayanus* with *Hyparrhenia* and *Schizachyrium* as co-dominants in some areas. The tree cover includes *Butyrospermum, Khaya, Ceiba, Pterocarpus, Parkia, Anogeissus, Diospyros* and *Adansonia*. This zone of the study area is classified as the Savannah Zone. The vegetation is a degraded forest with a wide range of tall grasses. Among the surviving forest relics are *Antiaris, Phyllanthus* and *Elaeis*. While *Borassus, Lophira, Daniellia, Lonchocarpus, Pterocarpus, Burkea* and *Parkia* represent the Savannah intrusions. Table 4.4 shows the total acreage occupied by each land cover class.

63

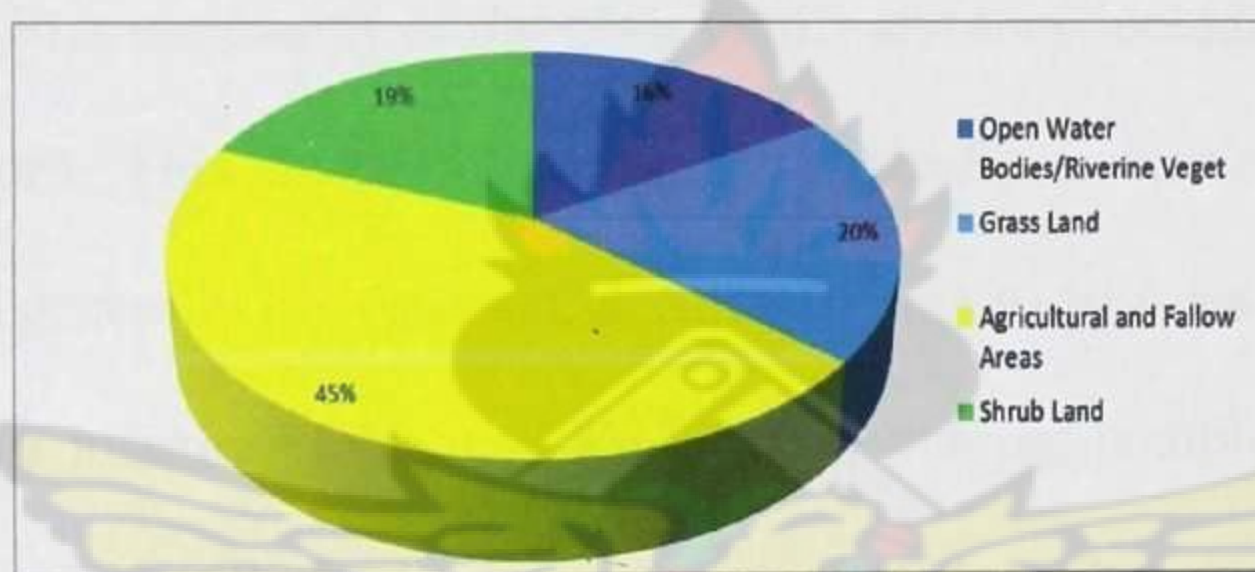Figure 4.9: Supervised classification of scene 3

Figure 4.10: Legend of the land cover distribution of scene 3

Table 4.4: The total area occupied by each land cover class in scene 3

LANDCOVER CLASS	AREA (HA)
Open Water Bodies/Riverine Vegetation	27441.9
Grass Land	71384.94
Agricultural and Fallow Areas	91336.41
Shrub Land	65867.76
Built-Up Areas	14770.08
TOTAL	270801.09

4.3.4 Classification Result of Scene 4

The situation, however, changes in the lower latitudes as shown in Figure 4.11 of scene 4 below. The classified scene as shown in Figure 4.12 shows that 17% of the total scene constitutes built-up/bare areas while agricultural land makes up only 12% of the scene. Majority of the scene is, however, covered with 40% of forest and 29% of degraded forest. The Forest land cover class is made up of natural forest and forest plantation with other life-forms obviously suppressed. Table 4.5 shows the total acreage occupied by each land cover class.
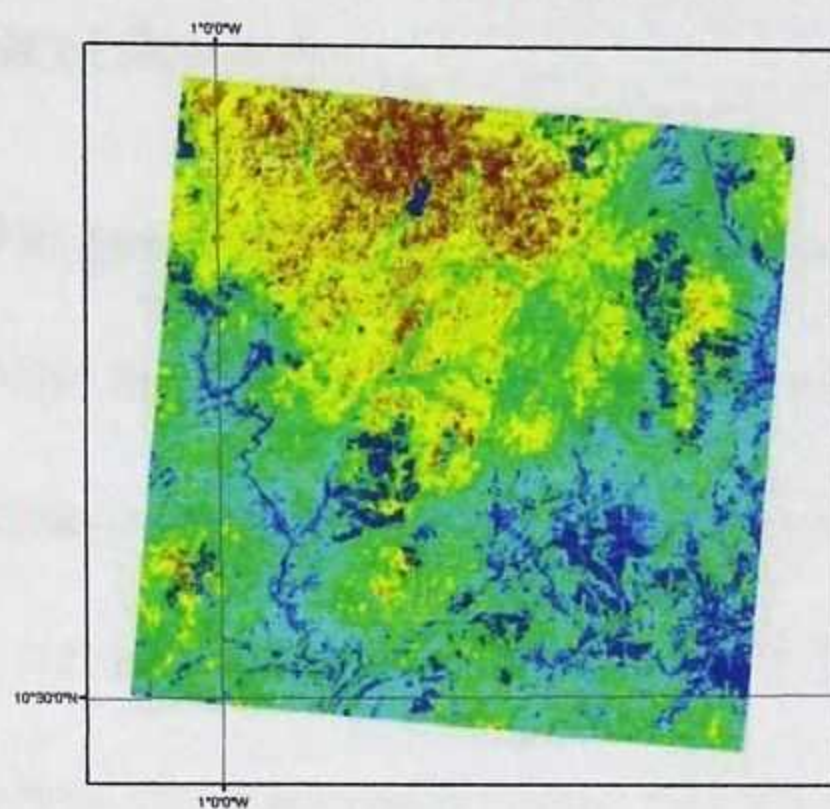

Figure 4.11: Supervised classification of scene 4

Figure 4.12: Legend of the land cover distribution of scene 4

65

Table 4.5: The total area occupied by each land cover class in scene 4

LANDCOVER CLASS	AREA (HA)
Water	84960.36
Built-Up/Bare Areas	15218.1
Forest	92286.27
Degraded Forest	62453.07
Agricultural Land	15920.73
TOTAL	270838.53

4.3.5 Classification Result of Scene 5

In Figure 4.13 also of the lower latitude, forest areas make up 34% of the total land cover while degraded forest makes up 23%. The built-up/bare areas and agricultural land makes up only 6% each. This is shown in Figure 4.14 below. Shown below is the total acreage occupied by each land cover class in Table 4.6.
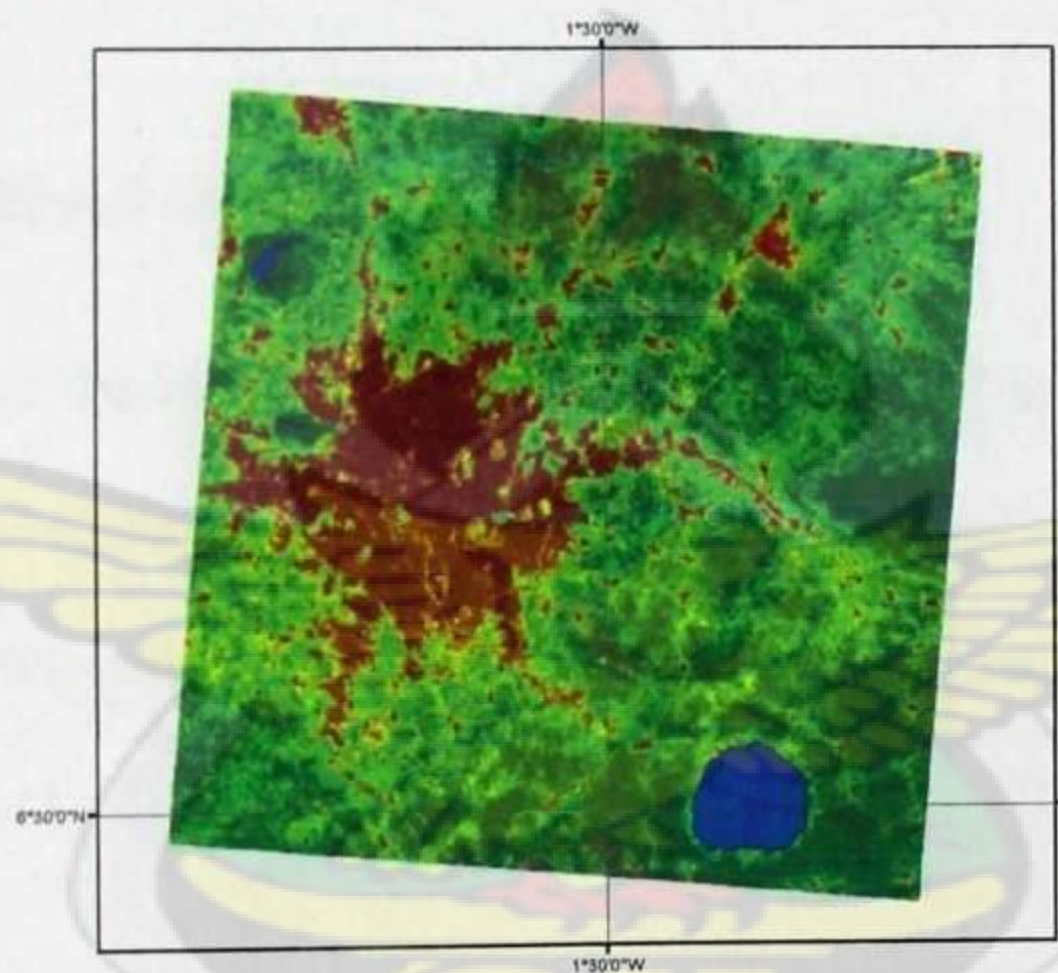

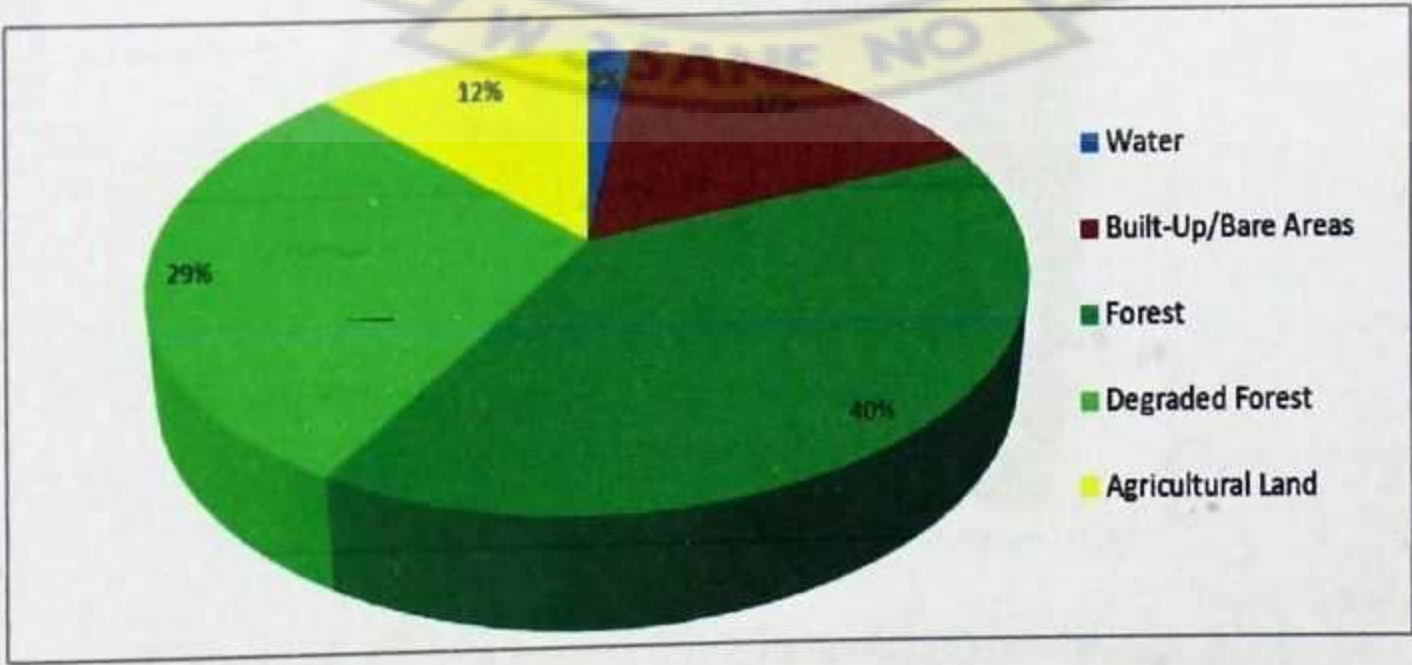Figure 4.13: Supervised classification of scene 5

Figure 4.14: Legend of the land cover distribution of scene 5

Table 4.6: The total area occupied by each land cover class in scene 5

LANDCOVER CLASS	AREA (HA)
Water	5186.61
Built-Up/Bare Areas	46355.04
Forest	106871.04
Degraded Forest	79730.73
Agricultural Land	32695.11
TOTAL	270838.53

4.3.6 Classification Result of Scene 6

As shown from the classification of this lower latitude scene (Figure 4.15), most people living within this area are located in between the forest zone and the water bodies. From Figure 4.16 below, the forest zone occupies 26% of the total land cover. The degraded forest covers 18%, whiles 5% makes up the agricultural land. The 25% left is for built-up/ bare areas.

The vegetation is a degraded forest with a wide range of tall grasses. Among the surviving forest relics are *Antiaris, Phyllanthus* and *Elaeis*. While *Borassus, Lophira,*

Daniellia, *Lonchocarpus*, *Pterocarpus*, *Burkea* and *Parkia* represent the Savannah intrusions. Similarly, among the grasses, the humid zone representatives include *Pennisetum purpureum* and *Panicum maximum*, while the subhumid zone species include *Andropogon gayanus*, *A. tectorum*, *Hyperthelia* and *Hyparrhenia* spp. Table 4.7 shows the total acreage occupied by each land cover class in this scene.
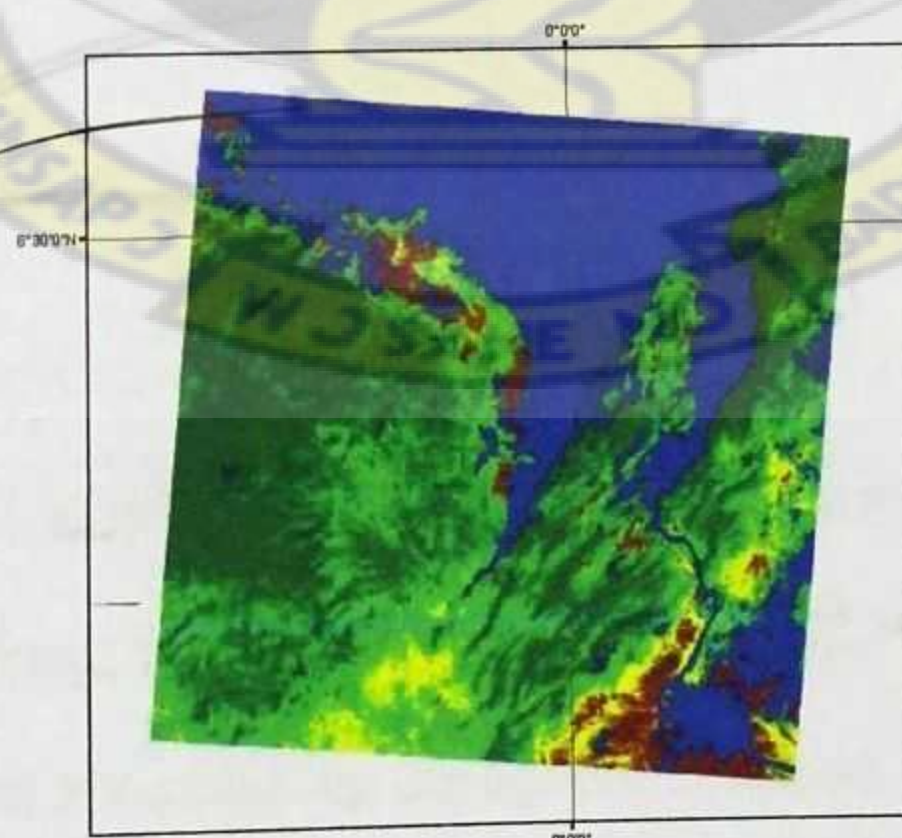

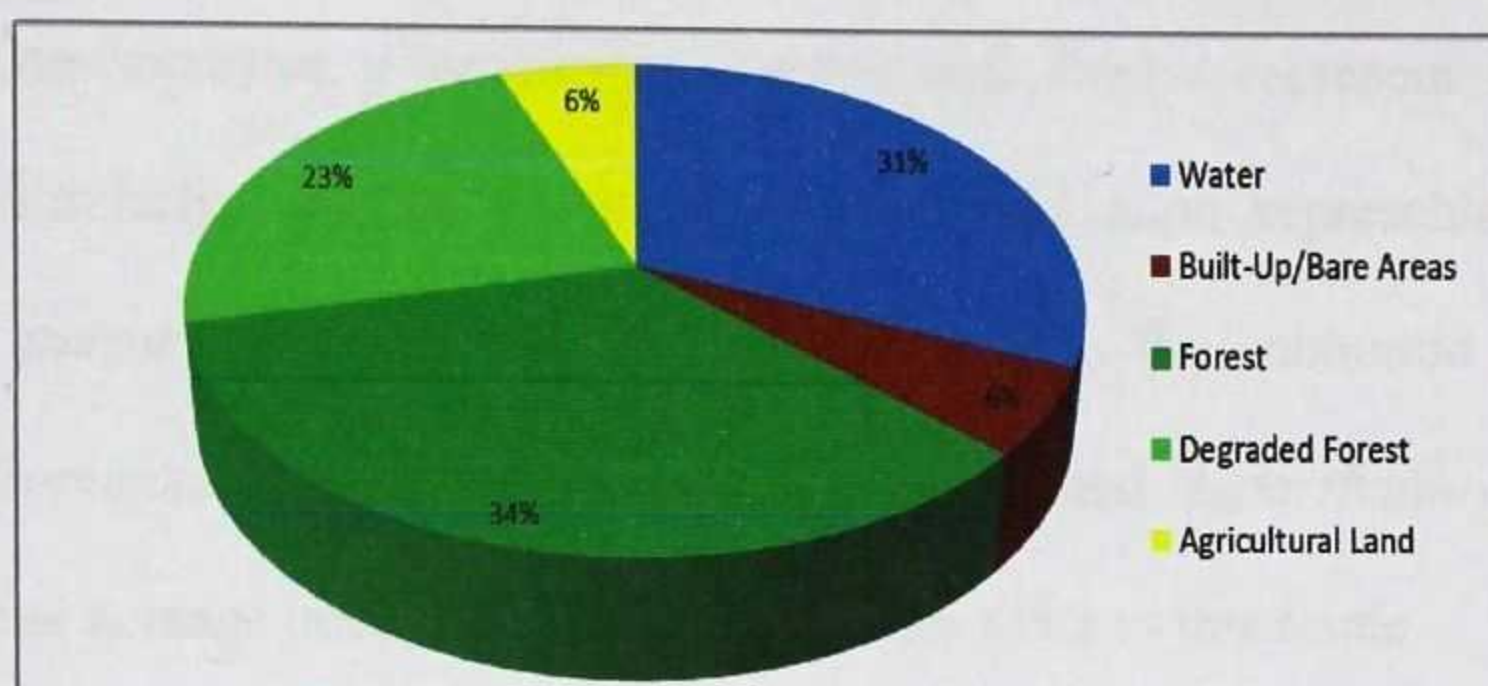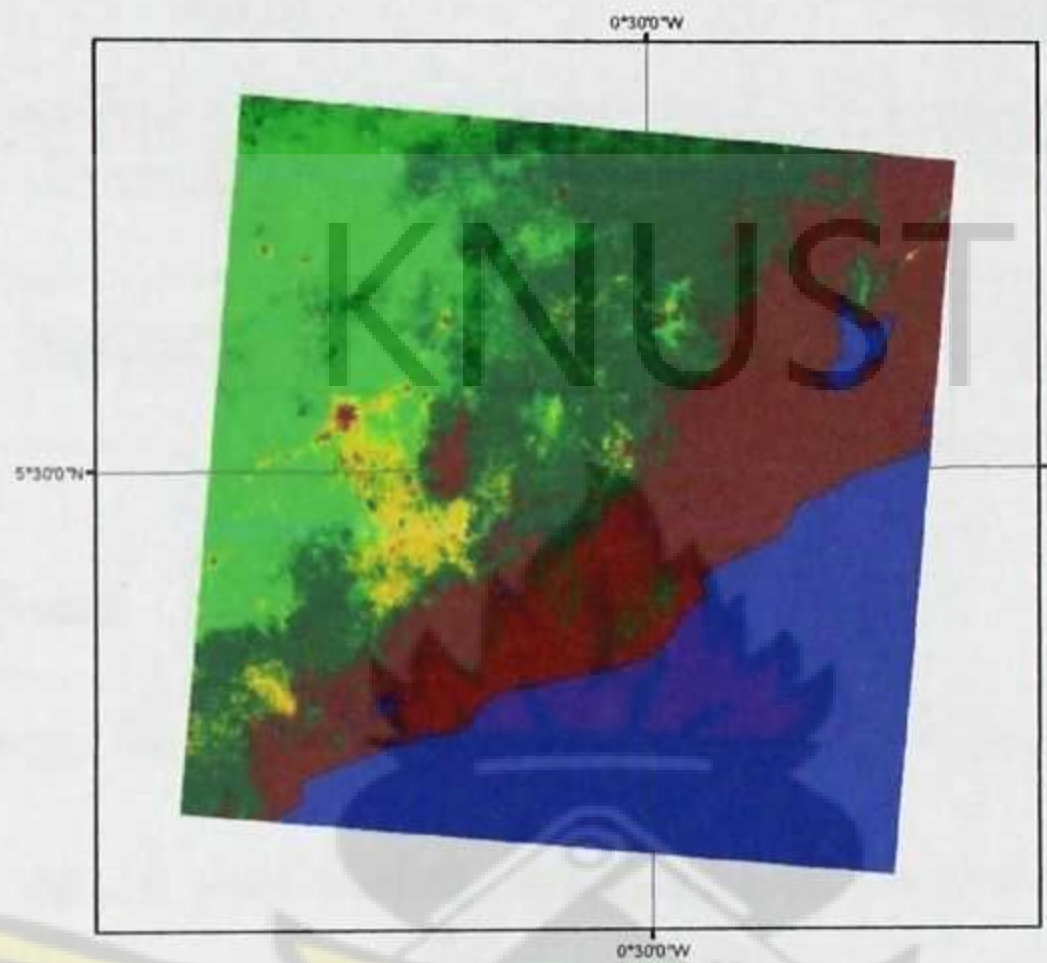Figure 4.15: Supervised classification of scene 6
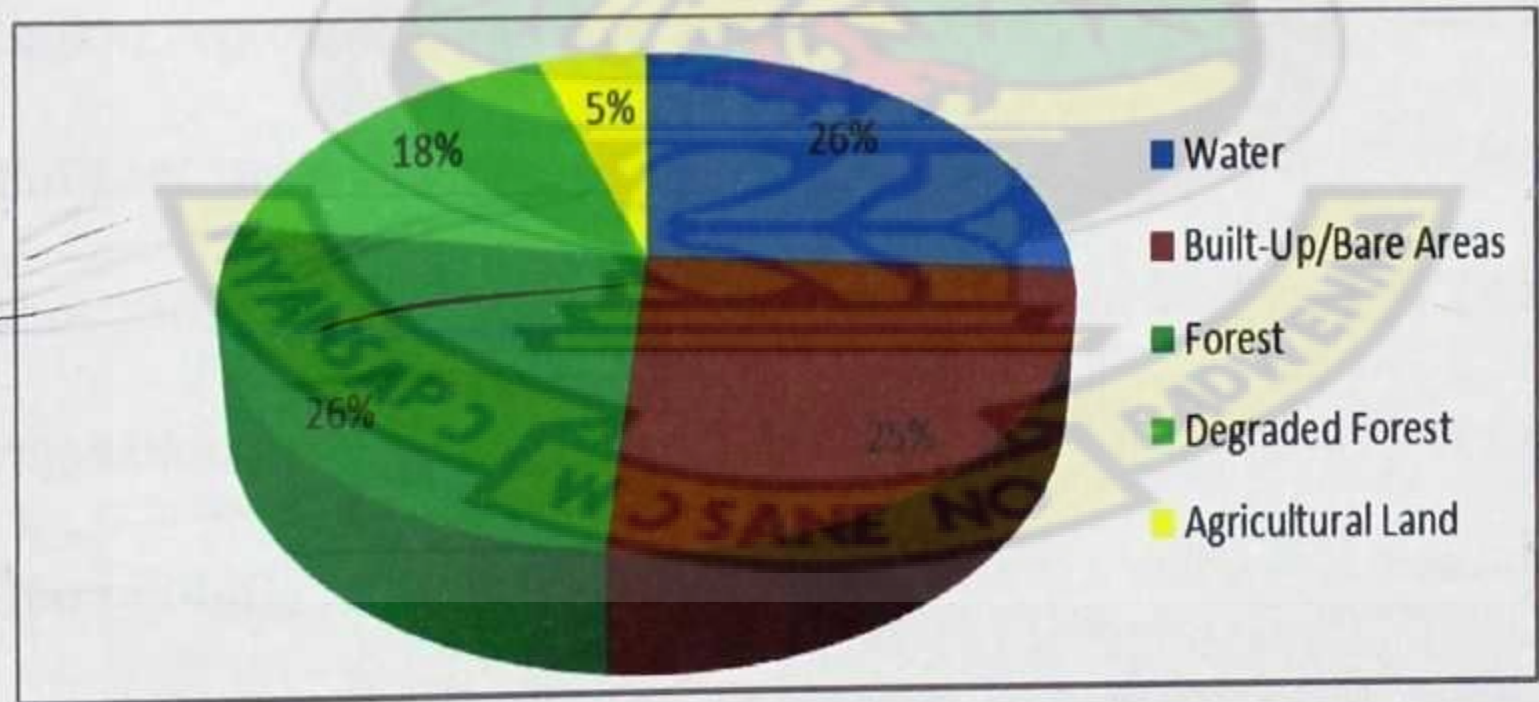
Figure 4.16: Legend of the land cover distribution of scene 6

Table 4.7: The total area occupied by each land cover class in scene 6

LAND COVER CLASS	AREA (HA)
Water	70815.6
Built-Up/Bare Areas	68093.82
Forest	70811.64
Degraded Forest	47899.89
Agricultural Land	13166.1

4.4 The Vegetation Trend

The two vegetation maps for 1996 and 2006 produced were visually assessed for land cover changes during the 10 year period. The comparison shows an alarming change over the 10-year period. The dark green patches within the Western Region, central part of the Eastern Region, southern part of Brong Ahafo region and the northern part of the Volta Region represent Closed or Evergreen Forest. This vegetation type in 1996 covered significant areas than in 2006. In 1996, the total area of Evergreen Forest occupied about 13011.56 km², equivalent to 5.47% of the land area of Ghana. In 2006, that same vegetation type reduced to about 12087.32 km², or 5.08% of the country's land area. Open Forest / Secondary Regrowth also saw a reduction from 49523.41 km² representing 20.83% of the land area of Ghana to 38625.23 km² also representing 16.25% of the land area of Ghana. This is largely due to the traditional slash and burn method of agriculture, logging, and annual wildfires. In addition, the recently commissioned open cast mining including the expansion of cocoa and other crop farms also represents some of the secondary drivers responsible for such decline in this vegetation zone. In 1996, although mining activities in the western region, specifically

the Tarkwa area resulted in the cutting and fragmentation of the Mixture of Closed and Open Forest, this vegetation type rather increased from 22,103.23 km^2 representing 9.30% of Ghana's land area to 36,259.78 km^2 representing 15.25% of the land area of Ghana in 2006. Mixture of Widely Open Forest or Woodland reduced from 33,172.45 km^2 representing 13.95% of the land area of Ghana in 1996 to 22,008.79 km^2 also representing 9.26% of the land area in Ghana respectively in 2006. This reduction could have also accounted for the increase in the Open Forest / Secondary regrowth. Grassland with Scattered Trees occupying the Northern, Upper East and Upper West Regions including some parts of the Volta and Brong Ahafo Regions saw a drastic reduction from 71,234.23 km^2 representing 29.96% of the total land area of Ghana to 53,668.17,km^2 also representing 22.57% of Ghana's total land area. Although there were remarkable decreases in five of the vegetation types from 1996 to 2006, the most noticeable change is the major increase in the Grassland, Bare Surface and Settlement within the entire study area. This vegetation type increased from about 48,703.12 km^2 to 75,098.71 km^2 representing an increase of 26,395.59 km^2; (ie 54.20 %). The land cover and land use conversion during the 10 year period indicates drastic transformation of the landscape from a variety of vegetation types to agricultural dominated landscapes. This transformation has fragmented the landscape into patches of forest/woodland, reducing habitat suitability for many types of wildlife. This degradation is attributed to charcoal production and cattle grazing activities initiated by cattle herdsmen. According to farmers in these settlements, the major challenge to agriculture is soil compaction arising from groups of cattle between 200 and 500 trampling the land as they move about to graze. The unsuitable compacted soils compelled most of the farmers to move to more fertile woody vegetation lands for

farming. These statistics are simplified in table 4.8 and the bar chart in Figure 4.15 below.

Table 4.8: The area/percentage occupied by each vegetation type in 1996 and 2006

VEGETAION TYPE	1996		2006	
	Area (km^2)	%	Area (km2)	%
Closed or Evergreen Forest	13011.56	5.47	12087.32	5.08
Mixture of Closed and Open Forest	22103.23	9.30	36259.78	15.25
Open Forest / Secondary Regrowth	49523.41	20.83	38625.23	16.25
Mixture of Widely Open Forest / Woodland	33172.45	13.95	22008.79	9.26
Grassland with Scattered Trees	71234.23	29.96	53668.17	22.57
Grassland / Bare Surface / Settlement	48703.12	20.49	75098.71	31.59
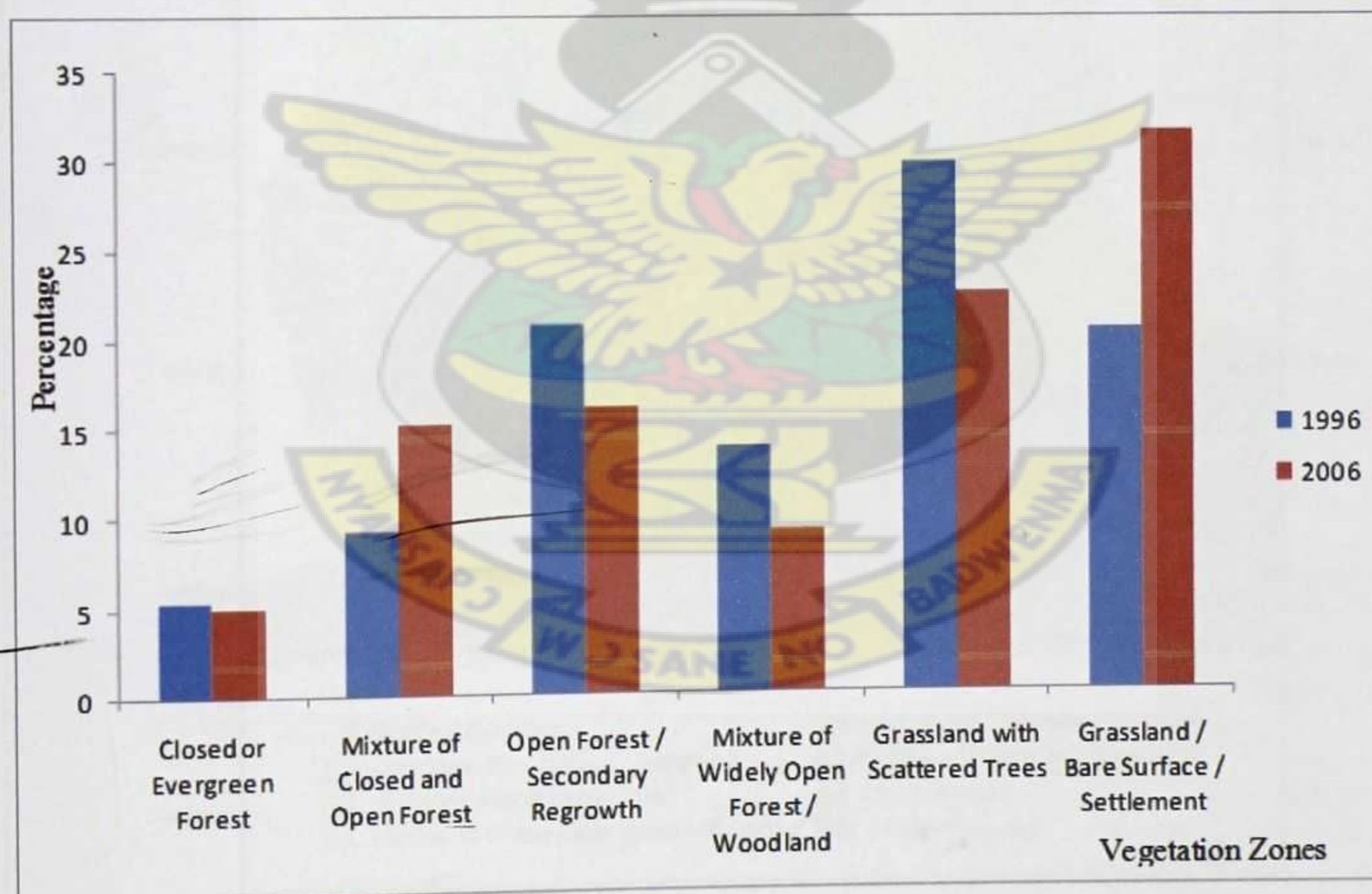
Figure 4.17: The percentage of the various vegetation types in 1996 and 2006

71
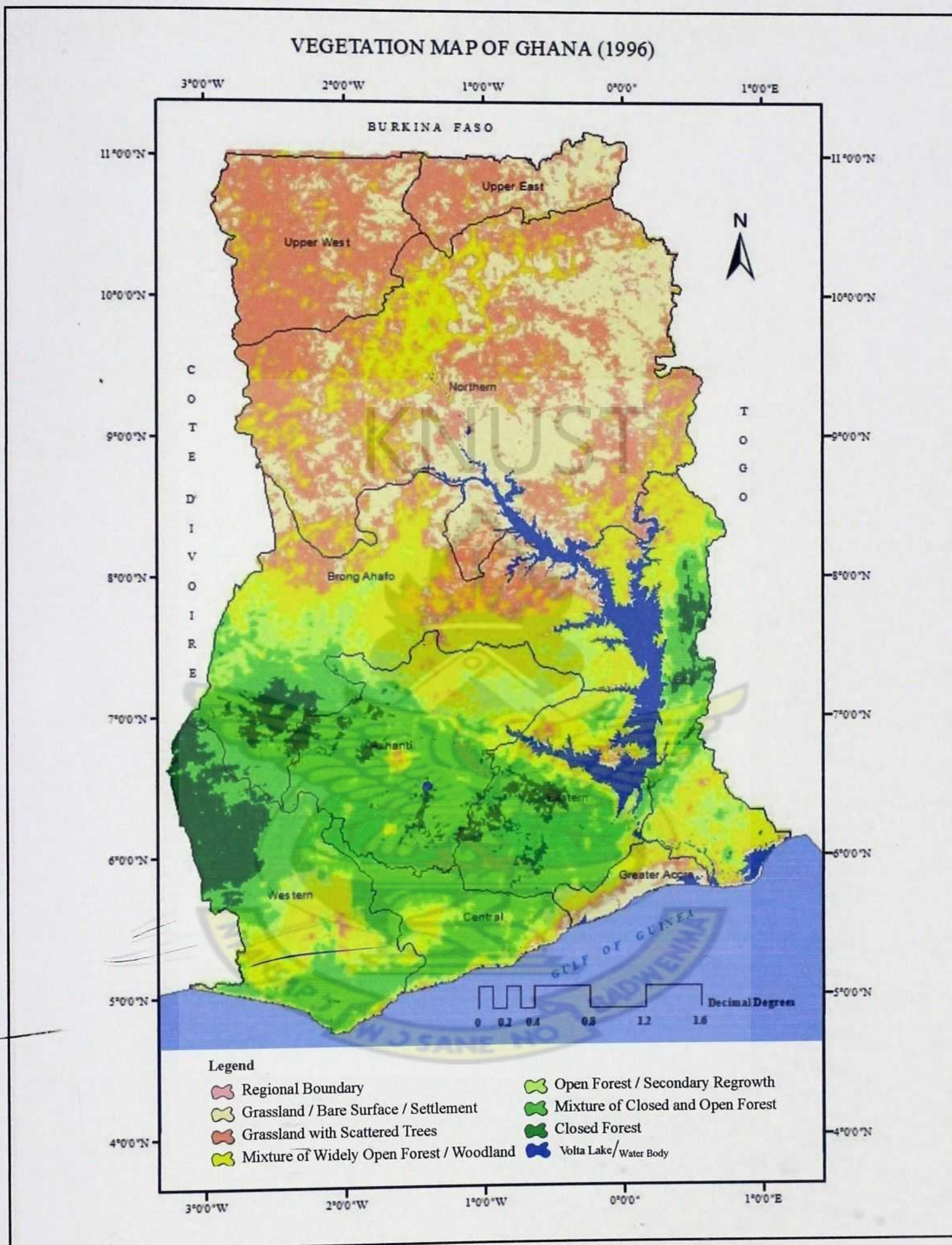
Figure 4.18: The Final FFT Vegetation Map of Ghana (1996)
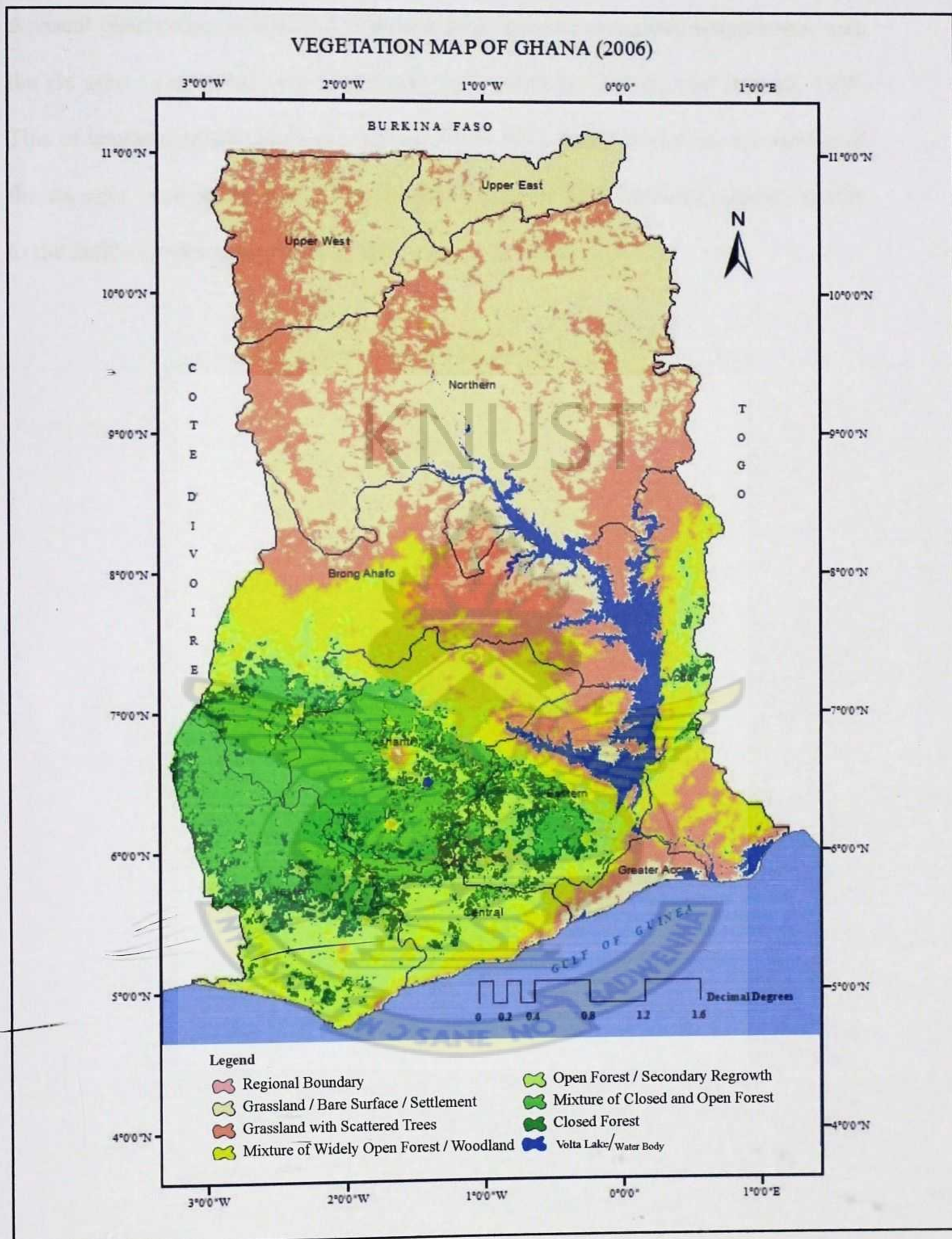
Figure 4.19: The Final FFT Vegetation Map of Ghana (2006)

A visual observation of both the 1996 and 2006 shows a complete disagreement with the six agro - ecological zones of Ghana propounded by Dickson and Benneh, 1988. This of course emphasizes the importance of the need for the re-zoning and naming of the six agro - ecological zones. The vegetation map of 1996, however, appears similar to the 2000 vegetation map produced by the EPA of Ghana.
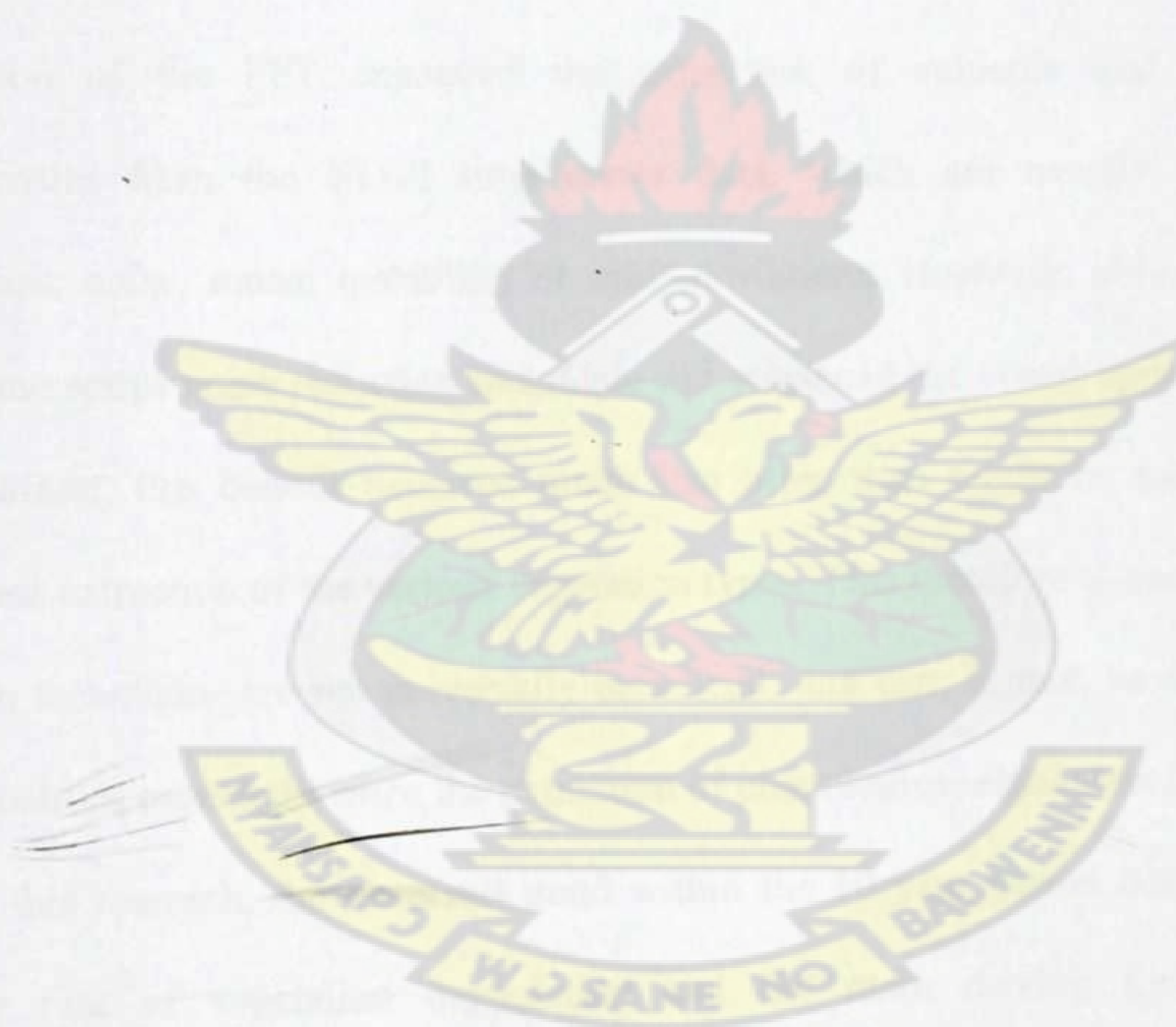
CHAPTER FIVE

CONCLUSION AND RECOMMENDATIONS

5.1 Conclusion

5.1.1 Summary of the Study

The study outlines the result obtained over 10 years through the analysis of FFT noise reduction technique on NDVI time series for the assessment of vegetation pattern in Ghana. Analysis of NDVI time series proves to be a valuable tool for studying complex vegetation patterns in inaccessible and data-scarce regions. The derived results support a conclusion that areas with high value in AVHRR NDVI represent green vegetation. Application of the FFT enhanced the extraction of valuable and interpretable characteristics from the NDVI time series data, which are usually disturbed by atmospheric noise, sensor instability or orbit deviations. However, although the FFT NDVI time series noise reduction technique did enhanced the visual appearance of the NDVI dataset, this benefit occurred much less often than might be assumed in the subsequent extraction of the various vegetation types. This therefore suggests that noise reduction techniques are not universally beneficial, and can, in fact, be detrimental in some situations especially when the extraction of phenological signatures is the ultimate goal. In this research, the observed trend within the 10 year period demonstrated an alarming rate of vegetation degradation and the main driving forces probably responsible for this drastic change were investigated using verbal discussions. Key themes for the discussions were on the bio-data of respondents, biophysical environment, human induced land cover changes and indicators of land degradation in the respective ecological zones. The idea for gathering such data was to understand some of the human contributing factors to the degradation and hence offer the necessary and appropriate recommendations as regards the alarming rate of change.

75

5.2 Recommendation

5.2.1 Vegetation zones that require urgent attention

Although all the six vegetation types deserve some sort of attention as far as land degradation is concerned, the Grassland vegetation requires urgent and immediate attention. These zones are considered crucial because of the fact that large parts of the population living in these zones depends on the land for crop cultivation and animal farming as the basic source of their livelihood. The Mixture of Closed and Open Forest is equally a priority zone that also requires some intervention even though it increased in acreage from 1996 to 2006. At the moment this zone serves as the corridor between the Closed or Evergreen Forest and the Grassland vegetation. Any rapid transformation of this ecological zone to a degraded land may quickly replace the existing Closed or Evergreen Forest when logging and farming actives expand over the entire forest ecological zone.

5.2.2 Interventions

As much as the Grassland ecological zones may be considered as degrading and becoming arid lands, there are still some parts of these ecological zones that are occupied by open and closed canopy woodlands and as such have the potential of being developed to forest lands. The protection of such vegetation is a collective responsibility of every Ghanaian and hence every citizen more importantly those living in the northern territory should be a guardian of the remaining trees and be inspired to plant many more trees. Even though some people argue that trees take too long to grow, it is better to plant a tree today and harvest it in 50 years than not to plant today and be forced to plant it in 50 years and end up using it after 100 years or more from now. As the old Greek proverb says, "a society grows great when old men plant trees whose shade they know they shall never sit in".

5.2.3 Future Study

Future studies should not only focus on the application of any noise reduction techniques on the NDVI time series dataset for the production of vegetation phenology but also look at the possibility of generating a GIS Database model for Early Warning System.

REFERENCES

Alhamad, M. N., Stuth, J. and Vannucci, M., 2007, Biophysical modelling and NDVI time series to project near-term forage supply: spectral analysis aided by wavelet denoising and ARIMA modelling. *International Journal of Remote Sensing*, **28**, 2513-2548

Andres, L., Salas, W. A. and Skole, D., 1994, Fourier analysis of multi-temporal AVHRR data plied to a land cover classification. *International Journal of Remote Sensing*, **15**, 1115-1121.

Anyamba, A. & Eastman, J. R. (1996): Interannual variability of NDVI over Africa and its relation to El Niño/Southern Oscillation. *International Journal of Remote Sensing* **17**(13): 2533-2548.

Aurela, M., Touvinen, J.-P. and Lauila, T., 2001, Net CO2 exchange of a subarctic mountain birch system. *Theoretical and Applied Climatology*, **70**, 135-148.

Azzali, S. and Menenti, M., 2000, Mapping vegetation-soil-climate complexes in southern Africa using temporal Fourier analysis of NOAA-AVHRR NDVI data. *International Journal of Remote Sensing*, **21**, 973-996.

Badeck, F. W., Bondeau, A., Böttcher, K., Doktor, D., Lucht, W., Schaber, J. and Sitch, S., 2004, Responses of spring phenology to climate change. *New Phytologist*, **162**, 295 309.

Badhwar, G. D., Carnes, J. G. and Austin, W. W., 1982, Use of Landsat-derived temporal profiles from corn-soybean feature extraction and classification. *Remote Sensing of Environment*, **12**, 57-79.

Baum, Bryan A. and Wielicki, Bruce A. (1992), On the retrieval and analysis of multilevel clouds. International Conference on Clouds and Precipitation, 11th, Montreal, Quebec, Canada, 17-21 August 1992. National Aeronautics and Space Administration (NASA), NASA Center for AeroSpace Information (CASI), Technical Reports Server. pp. 12

Beck, P. S. A., Atzberger, C., Høgda, K. A., Johansen, B. and Skidmore, A. K., 2006, Improved monitoring of vegetation dynamics at very high latitudes: a new method using MODIS NDVI. *Remote Sensing of Environment*, **100**, 321-334.

Beck, P. S. A., Jönsson, P., Høgda, K. A., Karlsen, S. R., Eklundh, L., and Skidmore, A. K., 2007, A ground-validated NDVI dataset for monitoring vegetation dynamics and mapping phenology in Fennoscandia and the Kola peninsula. *International Journal of Remote Sensing*, **28**, 4311-4330.

Benneh, G., Agyepong, G. T. and Allotey, J. A., 1990. Land degradation in Ghana. Food Production and Rural Development Division. Commonwealth Secretariat, Marlborough House. Pall Mall. London.

Blondel, J., Dias, P.C., Maistre, M. and Perret, P., 1993, Habitat heterogeneity and life history variation of the Mediterranean blue tits (*Parus caeruleus*). *Auk*, **110**, 511-520.

Boateng, E., 1998. Proceedings of Workshop a Land Use Planning. FAO Land Use Planning Project. TCP/GHA/67/6715/A.

Box, G. E. P. and Jenkins, G.M., 1976. Time Series Analysis. Forecasting and Control (revised edition), Holden Day, San Francisco. as a predictor for Biomas, Primary productivity and Net CO2 flux, vegetation 80 : 71 – 89.

Bradley, B. A., Jacob, R. W., Hermance, J. F., Mustard J. F., (2007). "A curve fitting procedure to derive inter-annual phenologies from time series of noisy satellite NDVI data." *Remote Sensing of Environment*, **106** (2), 137-145.

Bruce, L. M., Mathur, A. and Byrd, J. D. JR., 2006, Denoising and wavelet-based feature extraction of Modis multi-temporal vegetation signatures. *GIScience and Remote Sensing*, **43**, 67-77.

Cabral, A., DE Vasconcelos, M. J. P., Pereira, J. M. C., Bartholomé, E. and Mayaux, P., 2003, Multi-temporal compositing approaches for spot-4 vegetation. *International Journal of Remote Sensing*, **24**, 3343-3350.

Carreiras, J. M. B., Pereira, J. M. C., Shimabukuro, Y. E. and Stroppiana, D., 2003, Evaluation of compositing algorithms over the Brazilian Amazon using SPOT-4 VEGETATION data. International Journal of Remote Sensing, 24, 3427-3440.

Chatfield, C. 1984. The Analysis of time-series: an Introduction. *Chapman and Hall*, London.

Chen, J., Jönsson, P., Tamura, M., GU, Z., Matsushita, B. and Eklundh, L., 2004, A simple method for reconstructing a high-quality NDVI time-series data set based on the Savitzky-Golay filter. *Remote Sensing of Environment*, **91**, 332-344.

Chen, P. Y., Srinivasan, R., Fedosejevs, G., and Kiniry, J. R., 2003, Evaluating different NDVI composite techniques using NOAA-14 AVHRR data. *International Journal of Remote Sensing*, **24**, 3403-3412.

Chen, W. J., Black, T. A., Yang, P. C., Barr, A. G., Neumann, H. H., Nesic, Z., Blanken, P. D., Novak, M. D., Eley, J., Ketler, J. and Cuenca, R., 1999, Effects of climate variability on the annual carbon sequestration by a boreal aspen forest. *Global Change Biology*, **5**, 41-53.

80

Chen, X., Tan, Z., Schwartz, M. D. and XU, C., 2000, Determining the growing season of land vegetation on the basis of plant phenology and satellite data in Northern China. *International Journal of Biometeorology*, **44**, 97-101.

Cihlar, J., Latifovic, R., Chen, J., Trishchenko, A., Du, Y., Fedosejevs, G. and Guindon, B., 2004, Systematic corrections of AVHRR image composites for temporal studies. *Remote Sensing of Environment*, **89**, 217-233.

Cihlar, J., Ly, H., Li, Z., Chen, J., Pokrant, H. and Huang, F., 1997, Multitemporal, Multichannel AVHRR Data Sets for Land Biosphere Studies – Artifacts and Corrections. *Remote Sensing of Environment*, **60**, 35-57.

Cleland, E. E., Chuine, I., Menzel, A., Mooney, H. A., & Schwartz, M. D. (2007). Shifting plant phenology in response to global change. Trends in Ecology & Evolution, 22, 57–365.

connections with climate. *International Journal of Remote Sensing*, **24**, pp. 3595–3609.

Coppin, P., Jonckheere, I., Nackaerts. K., Muys. B., and Lambin, E., (2004). "Digital change detection methods in ecosystem monitoring: a review." *International Journal of Remote Sensing*, **25**(9), 1565-1596.

Cowan, F. L. and OdelL, G. H., 1990, More on estimating tillage effects: reply to Dunnell and Yorston. *American Antiquity*, **55**, 598-605.

Davis, J. C., 1986, Statistics and Data Analysis in Geology, 2nd edn (New York: Wiley).

Deering, D. W., 1978, Rangeland reflectance characteristics measured by aircraft and spacecraft sensors. Ph.D. Dissertation, Texas A & M University, College Station, TX, 338 pp.

Defries, R. S. and Townshend, 1994, NDVI-derived land cover classifications at a global scale. *International Journal of Remote Sensing*, **15**, 3567-3586.

Despland, E., Rosenberg, J. and Simpson, S. J., 2004, Landscape structure and locust swarming: a satellite's eye view. *Ecography*, **27**, 381-391.

Dickson, K. B. and Benneh, G., 1988. A new geography of Ghana. Longman Group UK Limited. Longman House, Burnt Mill, Harlow, Essex, England.

Dougill, A. and Trodd, N., 1999, Monitoring and modelling open savannas using multisource information: analyses of Kalahari studies. *Global Ecology and Biogeography*, **8**, 211-221.

Eastman, J. R., and Fulk, M. (1993). Long sequence time series evaluation using standardized principal components. *Photogrammetric Engineering and Remote Sensing*, **59**(8), 1307-1312.

EPA (2001). Districts Consultative Workshop On Drought And Desertification. Reports, EPA, Accra

Evans, J. P., and Geerken, R. (2006). Classifying rangeland vegetation type and coverage using a Fourier component based similarity measure. *Remote Sensing of Environment*, **105**, 1-8.

Fang, H. T. and Huang, D. S., 2004, Noise reduction in lidar signal based on discrete wavelet transform. *Optics Communications*, **233**, 67-76.

Fischer, A., 1994a, A model for the seasonal variations of vegetation indices in coarse resolution data and its inversion to extract crop parameters. *Remote Sensing of Environment*, **48**, 220-230.

Gage, S. H., Isard, S. A. and Colunga-g., M., 1999, Ecological scaling of aerobiological dispersal processes. *Agricultural and Forest Meteorology*, **97**, 249-261.

82

Gaillard, J. M., Festa-bianchet, M., Yoccoz, N. G., Loison, A. and Toigo, C., 2000, Temporal variation in fitness components and population dynamics of large herbivores. *Annual Review of Ecology and Systematics*, **31**, 367-393.

Gilabert, M. A., González-piqheras, J., García-haro, F. J. and Meliá, J., 2002, A generalized soil-adjusted vegetation index. *Remote Sensing of Environment*, **82**, 303-310.

Goward, S. N., Markham, B. and Dye, D., 1991, Normalized Difference Vegetation Index measurements from the Advanced Very High Resolution Radiometer. *Remote Sensing of Environment*, **35**, 257-277.

Gupta, R. K., Prasad, S., Sesha Sai, M. V. R. and Viswanadham, T. S., 1997, The estimation of surface temperature over an agricultural area in the state of Haryana and Panjab, India, and its relationship with the Normalized Difference Vegetation Index (NDVI), using NOAA-AVHRR data. *International Journal of Remote Sensing*, **18**, 3729-3741.

Gurgel, H. C., and Fereira, N. J. (2003). Annual and interannual variability of NDVI in Brazil and its connections with climate. *International Journal of Remote Sensing*, **24**(18), 3595–3609.

Gutman, G. G., 1991, Vegetation indices from AVHRR: an update and future prospects. *Remote Sensing of Environment*, **35**, 121-136.

Hall, C. A. S., Ekdahl, C. A. and Wartenberg, D. E., 1975, A fifteen-year record of biotic metabolism in the Northern Hemisphere. *Nature*, **255**, 136-138.

Hebblewhite, M., Merrill, E., and McDermid, G. J. (2008). A multi-scale test of the forage maturation hypothesis in a partially migratory ungulate population. *Ecological Monographs*, **78**, 141–166.

83

Hermance, J. F., 2007, Stabilizing high-order, non-classical harmonic analysis of NDVI data for average annual models by damping model roughness. *International Journal of Remote Sensing*, **28**, 2801-2819.

Hermance, J. F., Jacob, R. W., Bradley, B. A. and Mustard, J. F., 2007, Extracting phenological signals from multi-year AVHRR NDVI time series: framework for applying high-order annual splines with roughness damping. *IEEE Transactions on Geoscience and Remote Sensing*, **45**, 3264-3276.

Hird, J. N., and McDermid, G. J. (2009). Noise reduction of NDVI time series: An empirical comparison of selected techniques. *Remote Sensing of Environment*, **113**, 248–258.

Grizzly Bears in the Foothills Model Forest. In *Foothills Model Forest Grizzly Bear Research Program 1999-2003 Final Report*, G. B. Stenhouse and K. Graham (Eds.), pp. 32-37.

Holben, B. N., 1986, Characteristics of maximum-value composite images from temporal AVHRR data. *International Journal of Remote Sensing*, 7, 1417-1434.

Holben, B. N., and Fraser, R. S., 1984, Red and near-infrared response to off-nadir viewing. *International Journal of Remote Sensing*, 5, 145-160.

Huete, A. R. and Liu, H. Q., 1994, An error and sensitivity analysis of the atmospheric- and soil correcting variants of the NDVI for MODIS-EOS. *IEEE Transactions on Geoscience and Remote Sensing*, **32**, 897-905.

Huete, A. R., 1988, A Soil-Adjusted Vegetation Index (SAVI). *Remote Sensing of Environment*, **25**, 295-309.

Huete, A. R., Liu, H. Q., batchily, K. and Van Leeuwen, W., 1997, A comparison of vegetation indices over a global set of TM images for EOS-MODIS. *Remote Sensing of Environment*, **59**, 440-451.

Huete, A., DidaN, K., Miura, T., Rodriguez, E.P., Gao, X. and Ferreira, L.G., 2002, Overview of the radiometric and biophysical performance of the MODIS vegetation indices. *Remote Sensing of Environment*, **83**, 195-213.

Huete, A., Justice, C. and Van Leeuwen, W., 1999. *Modis Vegetation Index (MOD 13) Algorithm Theoretical Basis Document*. Version 3.

Hurlbert, A. H. and HaskelL, J. P., 2003, The effect of energy and seasonality on avian species richness and community composition. *The American Naturalist*, **16**, 83-97.

IGBP, 1992. Improved Global Data for land Applications, edited by J.R.G Townshed. IGBP Global Change Report no. 20, International Geosphere – Biosphere prograrmme, Stokholm, Sweden.

Immerzeel, W. W., Quiroz, R. A. and de Jong, S. M., 2005. Understanding precipitation patterns and land use interaction in Tibet using harmonic analysis of spot VGT-S10 NDVI time series. *International Journal of Remote Sensing*, **26**:11, 2281 — 229.

Jakubauskas, M. E., Legates, D. R. and Kastens, J. H., 2001, Harmonic analysis of time series AVHRR NDVI data. *Photogrammetric Engineering and Remote Sensing*, **67**, 461 470

Jakubauskas, M. E., Peterson, D. L., Kastens, J. H. and Legates, D. R. 2002, Time series remote sensing of landscape-vegetation interactions in the southern Great Plains. *Photogrammetric Engineering and Remote Sensing*, **68**, 1021-1030.

Jensen, J. R., 1996, Image enhancement. In *Introductory Digital Image Processing: A Remote Sensing Perspective*, edited by Clarke, K. C. (Upper Saddle River, New Jersey: Prentice Hall), pp.139-196.

Jensen, J. R., 2000, Remote sensing of vegetation. In *Remote Sensing of the Environment: An Earth Resource Perspective*, edited by K. C. Clarke (Upper Saddle River, New Jersey: Prentice Hall), pp. 333-377.

Jia, G. J., Epstein, H. E. and Walker, D. A., 2004, Controls over intra-seasonal dynamics of AVHRR NDVI for the Arctic tundra in northern Alaska. *International Journal of Remote Sensing*, **25**, 1547-1564.

Jönsson, P. and Eklundh, L., 2004, Timesat – a program for analyzing time-series of satellite sensor data. *Computers and Geosciences*, **30**, 833-845.

Jönsson, P. and Eklundh, L., 2006, Timesat – a program for analyzing time-series of satellite sensor data: Users Guide for Timesat 2.3. (*Sweden: Malmö and Lund*), 39 pp.

Jönsson, P. K. and Eklundh, L., 2002, Seasonality Extraction by Function-fitting to Time Series of Satellite Sensor Data. *IEEE Transactions on Geoscience and Remote Sensing*, **40**, 1824-1832.

Jordan, C. F., 1969, Derivation of leaf area index from quality of light on the forest floor, *Ecology*, **50**, 663-666.

Juarez, R. I. N., and Liu, W. T. (2001). FFT analysis on NDVI annual cycle and climatic regionality in Northeast Brazil. *International Journal of Climatology*, **21**, 1803–1820.

Julien, Y., Sobrino, J. A., and Verhoef, W. (2006). Changes in land surface temperatures and NDVI values over Europe between 1982 and 1999. *Remote Sensing of Environment*, **103**, 43–55.

Justice, C. O., Holben, B. N. and Gwynne, M. D., 1986, Monitoring East African vegetation using AVHRR data. *International Journal of Remote Sensing*, **7**, 14531474.

Justice, C. O., Townshend, J. R. G., Hoblen, B. N. and Tucker, C. J., 1985, Analysis of the phenology of global vegetation using meteorological satellite data. *International Journal f Remote Sensing*, **6**, 1271-1318.

Kang, S., Running, S. W., Zhao, M., Kimball, J. S. and Glassy, J., 2005, Improving continuity of modis terrestrial photosynthesis products using an interpolation scheme for cloudy pixels. *International Journal of Remote Sensing*, **26**, 1659-1676.

Knight, J. F., Lunetta, R. S., Ediriwickrema, J. and Khorram, S., 2006, Regional scale land cover characterization using MODIS-NDVI 250 m multi-temporal imagery: a phenology- based approach. *GIScience & Remote Sensing*, **43**, 1-23.

Kobayashi, H. and Dye, D. G., 2005, Atmospheric conditions for monitoring the long-term dynamics in the Amazon using normalized difference vegetation index. *Remote Sensing of Environment*, **97**, 519-525.

Lee, R., Yu, F., Price, K. P., Ellis, J. and Shi, P., 2002, Evaluating vegetation phenological patterns in Inner Mongolia using NDVI time-series analysis. *International Journal of Remote Sensing*, **23**, 2505-2512.

Li, S. Z. and Strahler, A. H., 1992, Geometric-optical bidirectonal reflectance modeling of the discrete crown vegetation canopy: effect of crown shape and mutual shadowing. *IEEE Transactions on Geoscience and Remote Sensing*, **30**, 276-292.

Li, S. Z., 2000. Modeling image analysis problems using random markov field", in Handbook of Statistics, 20. Elsevier Science, pp. 1-43.

Linderholm H. W. (2006). "Growing season changes in the last century". *Agricultural and Forest Meteorology*, **137**(1-2), 1-14.

Lloyd, D., 1990, A phenological classification of terrestrial vegetation cover using shortwave vegetation index imagery. *International Journal of Remote Sensing*, **11**, 2269-2279.

Loe, L. E., Bonenfant, C., Mysterud, A., Gaillard, J.-M., Langvatn, R., Klein, F., Calenge, C., Eragon, T., Pettorelli, N., and Stenseth, N. C., 2005, Climate predictability and breeding phenology in red deer: timing and synchrony of rutting and calving in Norway and France. *Journal of Animal Ecology*, **75**, 579.

Lovell, J. L. and Graetz, R. D., 2001, Filtering pathfinder AVHRR land NDVI data for Australia. *International Journal of Remote Sensing*, **22**, 2649-2654.

Lu, X., Liu, R., Liu J. and Liang, S., 2007, Removal of noise by wavelet method to generate high quality temporal data of terrestrial MODIS products. *Photogrammetric Engineering and Remote Sensing*, **73**, 1129-1139.

Ma, M. and Veroustraete, F., 2006a, Reconstructing pathfinder AVHRR land NDVI time-series data for the Northwest of China. *Advances in Space Research*, **37**, 835-840.

Macdonald, R. B. and HALL, F. G., 1980, Global crop forecasting. *Science*, **208**, 670-679.

Maxwell, S. K., Hoffer, R. M. and Chapman, P. L., 2002, AVHRR composite period selection for land cover classification. *International Journal of Remote Sensing*, **23**, 5043-5059.

Menenti, M., Azzali, S., and Verhoef, W., Fourier analysis of time series of NOAA-AVHHR NDVI composites to map isogrowth zones, in: Climate change research: evaluation and policy implications, book on "*Studies in Environmental Science*", Vol. 65, edited by: Zwerver, S., van Rompaey, R. S. A. R., Kok, M. T. J., and Berk, M. M., Elsevier, Amsterdam, The Netherlands, 425–430, 1995.

Menenti, M., Azzali, S., Verhoef, W. and Van Swol, R., 1993, Mapping agro-ecological zones and time lag in vegetation growth by means of Fourier analysis of time series of NDVI images. *Advances in Space Research*, **13**, (5)233-237.

Ministry of Food and Agriculture (MOFA), 1998. National Soil fertility management action plan. Director of Crop Service. Accra. Ghana.

Moody, A. and Johnson, D. M., 2001, Land-surface phonologies from AVHRR using the discrete Fourier transform. *Remote Sensing of Environment*, **75**, 305-323.

Munro, R. H. M., Price, M. H. H. and Stenhouse, G. B., 2005, The Diet of Grizzly Bears, *Ursus arctos*, in West-Central Alberta, Canada. In *Foothills Model Forest Grizzly Bear Research Program 1999-2003 Final Report*, G. B. Stenhouse and K. Graham (Eds.), pp. 11-20.

Myneni, R. B., Hall, F. G., Sellers, P. J. and Marshak, A. L., 1995, The interpretation of spectral vegetation indexes. *IEEE Transactions on Geoscience and Remote Sensing*, **33**, 481-486.

Myneni, R. B., Keeling, C. D., Tucker, C. J., Asrar, G. and Nemani, R. R., 1997, Increased plant growth in the northern high latitudes from 1981 to 1991. *Nature*, **386**, 698-702.

Myneni, R. B., Knyazikhin, Y., Zhang, Y., Tian, Y., Wang, Y., Lotsch, A., Privette, J. L., Morisette, J. T., Running, S. W., Nemani, R., Glassy, J., Votava, P., 1999. MODIS leaf area index (LAI) and fraction of photosynthetically active radiation

absorbed by vegetation (FPAR) product (MODIS) Algorithm Theoretical Basis Document, version 4.

Nikolakopoulos, K.G., 2008.Comparison of nine fusion techniques for very high resolution data. *Photogrammetric Engineering and Remote Sensing*, **74**: 647-659.

Olofsson, P., Eklundh, L., Lagergren, F., Jönsson, P. and Lindroth, A., 2007, Estimating Net Primary Production for Scandinavian forests using data from Terra/MODIS, Advances in Space Research, 39, 125-130.

Olsson, L. and Eklunh, L., 1994, Fourier series for analysis of temporal sequences of satellite sensor imagery. *International Journal of Remote Sensing*, **15**, 3735-3741.

Olsson, L., & Eklundh, L. (2001). Fourier series for analysis of temporal sequences of satellite sensor imagery. *International Journal of Remote Sensing*, **15**(18), 3735–3741.

Oppong-Anane, K., 2001. Country Pastures/ Forage Resource Profiles.

Pañuelas, J., Filella, I., Zhang, X., Llorens, Ogaya, R., Lloret, F., Comas, P., Estiarte, M. and Terradas, J., 2004, Complex spatiotemporal phenological shifts as a response to rainfall changes. *New Phytologist*, **161**, 837-846.

Parmesan C., Yohe G., (2003). "A globally coherent fingerprint of climate change impacts across natural systems" *Nature*, **421** (6918), 37-42.

Penfound, W. T., Hall, T. F. K and Hess, D., 1945, The spring phenology of plants in and around reservoirs in north Alabama with particular reference to malaria control. *Ecology*, **26**, 332-352.

Pettorelli, N., Vik, J. O., Mystrerud, A., Caillard, J. M., Tucker, C.J. and Stenseth, N. C., 2005, Using the satellite-derived NDVI to assess ecological responses to environmental change. *Trends in Ecology and Evolution*, **20**, 503-510.

Pipes, L. A. and Harvill, L. R., 1971, Applied Mathematics for Engineers and Physicists, 3rd edn (Singapore: McGraw-Hill).

Rahman, H. and Dedieu, G., 1994, SMAC: a simplified method for the atmospheric correction of satellite measurements in the solar spectrum. *International Journal of Remote Sensing*, **15**, 123-143.

Reed, B. C., 2006, Trend analysis of time-series phenology of North America derived from satellite data. *GIScience and Remote Sensing*, **43**, 24-38.

Reed, B. C., Brown, J. F., Vanderzee, D., Loveland, T. R., Merehant, J. W. and Ohlen, D. O., 1994, Measuring phenological variability from satellite imagery. *Journal of Vegetation Science*, **5**, 703-714.

Reeves, M. C., Zhao, M. and Running, S. W., 2006, Applying improved estimates of MODIS productivity to characterize grassland vegetation dynamics. *Rangeland Ecology & Management*, **59**, 1-10.

Ricotta, C., Reed, B. C. and Tieszen, L. T., 2003, The role of C3 and C4 grasses to interannual variability in remotely sensed ecosystem performance over the US Great Plains. *International Journal of Remote Sensing*, **24**, 4421-4431.

Roerink, G. J., Menenti, M. and Verhoef, W., 2000, Reconstructing cloudfree NDVI composites using Fourier analysis of time series. *International Journal of Remote Sensing*, **21**, 1911-1917.

Roerink, G. J., Menenti, M., Soepboer, W. and SU, Z., 2003, Assessment of climate impact on vegetation dynamics by using vegetation. *Physics and Chemistry of the Earth*, **28**, pp. 103–109.

Running, S. W., Justice, C. O., Salomonson, B., Hall, D., Barker, J., Kaufmann,Y. J., Strahler, A. H., Huete, A. R., Muller, J. P., Venderbilt, V., Wan, Z. M., Teillet, P., and Carneggie, D., 1994, Terrestrial remote sensing science and algorithms planned for EOS/MODIS. *International Journal of Remote Sensing*, **15**, 3587-3620.

Sakamoto, T., Van Nguyen, N., Ohno, H., Ishitsuka, N. and Yokozawa, M., 2006, Spatio temporal distribution of rice phenology and cropping systems in the Mekong Delta with special reference to the seasonal water flow of the Mekong and Bassac rivers. *Remote Sensing of Environment*, **100**, 1-16.

Sakamoto, T., Yokozawa, M., Toritani, H., Shibayama, M., Ishitsuka, N. and Ohno, H., 2005, A crop phenology detection method using time-series MODIS data. *Remote Sensing of Environment*, **96**, 366-374.

Sanz, J. J., Potti, J., Moreno, J., Merino, S. and Frías, O., 2003, Climate change and fitness components of a migratory bird breeding in the Mediterranean region. *Global Change Biology*, **9**, 461-472.

Savitzky, A. and Golay, M. J. E., 1964, Smoothing and differentiation of data by simplified least squares procedures. *Analytical Chemistry*, **36**, 1627-1639.

Schmidt, K. S. and Skidmore, A. K., 2003, Spectral discrimination of vegetation types in a coastal wetland. *Remote Sensing of Environment*, **85**, 92-108.

Schmidt, K. S. and Skidmore, A. K., 2004, Smoothing vegetation spectra with wavelets. *International Journal of Remote Sensing*, **25**, 1167-1184.

Schwartz, M. D. (1999). Advancing to full bloom: Planning phenological research for the 21st century. *International Journal of Biometeorology*, **42**, 113–118.

Schwartz, M. D. and Reed, B. C., 1999, Surface phenology and satellite sensor-derived onset of greenness: and initial comparison. *International Journal of Remote Sensing*, **20**, 3451 3457.

Schwartz, M. D., Reed, B. C. and White, M. A., 2002, Assessing satellite-derived start-of season measures in the conterminous USA. *International Journal of Climatology*, **22**, 1793-1805.

Sellers, P. J., Tucker, C. J., Collatz, G. J., Los, S. O., Justice, C. O., Dazlich, D. A. and Randall, D. A., 1994, A global 10 by 10 NDVI data set for global studies. Part 2: The generation of global fields of terrestrial biophysical parameters from the NDVI. *International Journal of Remote Sensing*, **15**, 3519-3545.Sensing, 26(20), 4485–4498.

Statistics, Research and Information Directorate (SRID). 2001. Agriculture in Ghana. Facts and figures. *Ministry of Food and Agriculture*. Accra. Ghana.

Swets, D. L., Reed, B.C., Rowland, J. R. and Marko, S. E., 1999, A weighted least-squares approach to temporal smoothing of NDVI. In *ASPRS Annual Conference, From Image to Information*, Portland, Oregon, May 17-21 1999, Bathesda, Maryland, (*American Society for Photogrammetry and Remote Sensing*).

Taddei, R., 1997, Maximum Value Interpolated (MVI): a Maximum Value Composite method improvement in vegetation index profiles analysis. *International Journal of Remote Sensing*, **18**, 2365-2370.

Townshend, J. R. G. and Justice, C. O., 1986, Analysis of the dynamics of African vegetation using the normalized difference vegetation index. *International Journal of Remote Sensing*, **7**, 1435-1445.

Tucker, C., Pinzon, J., Brown, M., Slayback, D., Pak, E., Mahoney, R., *et al*. (2005). An extended AVHRR 8 km NDVI dataset compatible with MODIS and SPOT vegetation NDVI data. *International Journal of Remote Sensing*, **26**, 4485–4498.

Tucker, C.J., 1979, Red and photographic infrared linear combination for monitoring vegetation. *Remote Sensing of Environment*, 8, pp. 127–150.

Tukey, J. W., 1977, Robust nonlinear data smoothers; theory definitions and applications. PhD thesis, Princeton University, Princeton, NJ.

Turner, D. P., Ritts, W. D., Cohen, W. B., Gower, S. T., Zhao, M., Running, S. W., Wofsy, S. C., Urbanski, S., Dunn, A. L. and Munger, J. W., 2003, Scaling Gross Primary Production (GPP) over boreal and deciduous forest landscapes in support of MODIS GPP product validation. *Remote Sensing of Environment*, **88**, 256-270.

UNESCO World Report. (2010), "Towards Knowledge Societies". UNESCO Publishing, 2010.

Van Dijk, A., Callis, S. L., Sakamoto, C. M. and Decker, W. L., 1987, Smoothing vegetation index profiles: an alternative method for reducing radiometric disturbance in NOAA/AVHRR data. *Photogrammetric Engineering and Remote Sensing*, **53**, 1059-1067.

Velleman, P. F. and Hoaglin, D. C. (1981) Applications, Basics, and Computing of Exploratory Data Analysis *Duxbury Press*, Boston, MA.

Velleman, P. F., 1980, Definition and comparison of robust nonlinear data smoothing algorithms. *Journal of the American Statistical Association*, **75**, 609-615.

Verbesselt J, Jönsson P, Lhermitte S, van Aardt J, Coppin P (2006). "Evaluating satellite and climate data derived indices as risk indicators in savanna

ecosystems." *IEEE Transactions on Geoscience and Remote Sensing*, **44**(6), 1622-1632.

Verbesselt, J., Lhermitte, S., Coppin, P., Eklundh, L. and Jönsson, P., 2004, Biophysical drought metrics extraction by time series analysis of Spot Vegetation data. In *IEEE International Geoscience and Remote Sensing Symposium, Science for Scoeity:* Exploring and Managing a Changing Planet, Anchorage, Alaska, September 20-24 2004, *(IEEE Geoscience and Remote Sensing Society).*

Verhoef, W., "Application of Harmonic Analysis of NDVI Time Series (HANTS)", in: Fourier analysis of temporal NDVI in the Southern African and American continents, edited by S. Azzali and M. Menenti, DLO-Winand Staring Centre, Report No. 108, Wageningen, 1996, pp. 19-24.

Verhoef, W., Menenti, M. and Azzali, S., 1996, A colour composite of NOAAAVHRR NDVI based on time series analysis (1981-1992). *International Journal of Remote Sensing*, **17**, 231-235.

Vicente-Serrano, S. M., Grippa, M., Delbart, N., Le Toan, T. and Kergoat, L., 2006, Influence of seasonal pressure patterns on temporal variability of vegetation activity in central Siberia. *International Journal of Climatology*, **26**, 303-321.

Viovy, N., Arino, O. and Belward, A.S., 1992, The Best Index Slope Extraction (BISE): A method for reducing noise in NDVI time-series. *International Journal of Remote Sensing*, **13**, 1585-1590.

Wagenseil, H. and Samimi, C., 2006, Assessing spatio-temporal variations in plant phenology using Fourier analysis on NDVI time series: results from a dry savannah environment in Namibia. *International Journal of Remote Sensing*, **27**, 3455-3471.

Wang, Q., Adiku, S., Tenhunen, J. and Granier, A., 2005b, On the relationship of NDVI with leaf area index in a deciduous forest site. *Remote Sensing of Environment,* **94**, 244-255.

Wang, Q., Tenhunen, J., Dinh, N. Q., Reichstein, M., Vesala, T. and Keronen, P., 2004, Similarities in ground-and satellite-based NDVI time series and their relationship to phenological activity of a Scots pine forest in Finland. *Remote Sensing of Environment,* **93**, 225-237.

Wang, Q., Tenhunen, J., Dinh, N. Q., Reiinchste, M., Otieno, D., Granier, A. and Pilegarrd, K., 2005a, Evaluation of seasonal variation of MODIS derived leaf area index at two European deciduous broadleaf forest sites. *Remote Sensing of Environment,* **96**, 475-484.

Wen, J., Su, Z., and Ma, Y., Reconstruction of a cloud-free vegetation index time series for the Tibetan plateau, *Mt. Res. Dev.,* **24**, 348–353, 2004.

White M. A., Nemani A. R., (2003). "Canopy duration has little influence on annual carbon storage in the deciduous broad leaf forest" *Global Change Biology,* **9**(7), 967-972.

White, M. A., Thornton, P. E. and Running, S. W., 1997, A continental phenology model for monitoring vegetation responses to interannual climatic variability. *Global Biogeochemical Cycles,* **11**, 217-234.

Wolfe, W. L. and Zissis, G. J. (Eds), 1993, The Infrared Handbook (Ann Arbor, MI: *Environmental Research Institute of Michigan (ERIM)*).

Xiao, X., Boles, S., Liu, J., Zhuang, D. and Liu, M., 2002, Characterization of forest types in Northeastern China, using multi-temporal Spot-4 Vegetation sensor data. *Remote Sensing of Environment,* **82**, 335-348.

Yang, W., Yang, L. and Merchant, J.W., 1997, An assessment of Avhrr/ndvi ecoclimatological relations in Nebraska, U.S.A. *International Journal of Remote Sensing*, **18**, 2161-2180.

Zhang, X., Friedl, M. A., Schaaf, C.B., Strahler, A. H., Hodges, J. C. F., Gao, F., Reed, B. C. and Huete, A., 2003, Monitoring vegetation phenology using MODIS. *Remote Sensing of Environment*, **84**, 471-475.

Zhang, X., Friedl, M. A., Schaff, C. B. and Strahler, A. H., 2004, Climate controls on vegetation phenological patterns in northern mid-and high latitudes inferred from MODIS data. *Global Change Biology*, **10**, 1133-1145.

APPENDIX I

GROUNDTRUTHING AND DESCRIPTION OF THE VARIOUS VEGETATION TYPES

1. Closed or Evergreen Forest

A visit to Enchi and Juabeso in the Western Region shows a complete inaccessible Closed or Evergreen Forest. The Forest land cover class is made up of remnant natural forest and forest plantation with other life-forms obviously suppressed. Among the surviving forest relics are Antiaris, Phyllanthus and Elaeis.
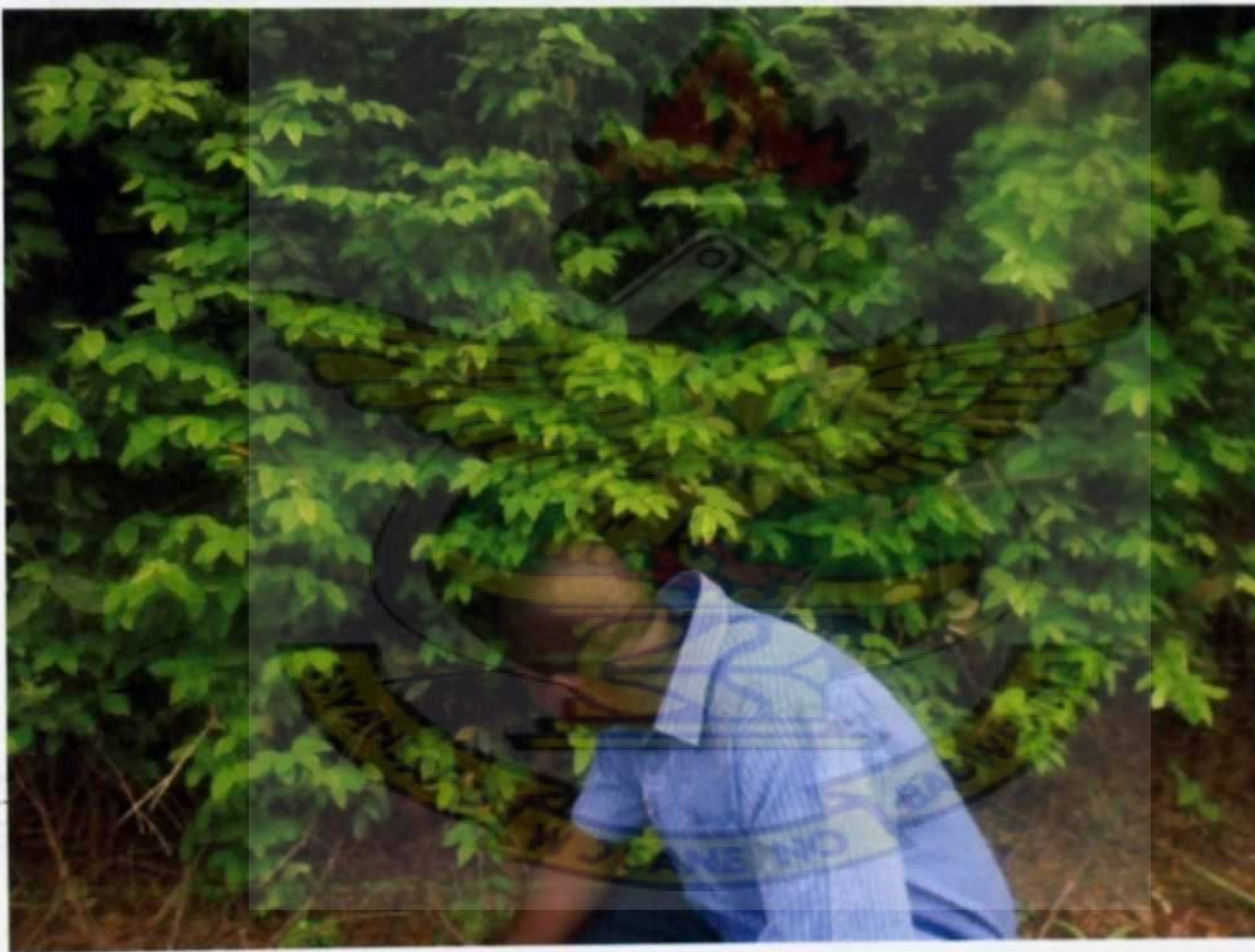

Figure 1: Observing an inaccessible closed forest at Enchi

High temperatures coupled with heavy rainfall of 1,500-2,200 mm, which is well distributed throughout the year in the zone, promotes very rapid plant growth. The zone has an even tree canopy at 30-40 metres while emergents may attain 60 metres.

2. Mixture of Closed and Open Forest

In the transitional ecological zone such as in Berekum and Drobo, the general appearance of the vegetation cover is a mixture of closed and open forest with scattered trees. As stated earlier, this zones demands great attention as it serves as the region between the savanna and the forest zones.

Figure 2: Taking GPS readings in a mixture of closed and open forest at Berekum

Canopy trees may be deciduous in the dry season but the understorey shrubs and trees are evergreen. A herbaceous layer which may include a few specialized grasses occurs over a variable portion of the forest floor. Compared to that of the Savannah zones, pasture resources in this zone are not very significant. Furthermore, ruminant livestock production is of minor importance as the area is not only dominated by food and tree crop farming but also associated, in some places, with heavy infestation of tsetse flies, the transmitter of trypanosomiasis.

3. Open Forest / Secondary Regrowth

A visit to Tainso and Suronuase showed vegetation cover that is predominantly open forest. However, forest grooves and secondary regrowth forests could be seen on some parts of the land. Major land use activities in the area are farming and cattle rearing.

Figure 3: Demonstrating an open forest vegetation type at Tainso

Degraded farmlands were identified with indicator weeds such as *Rawlings* in Tainso which indicates that the soil fertility has reached a level that cannot support the growth of crops and as such it has to be allowed to lay fallow for some time. In Suronuase much of the trees were cut to produce charcoal resulting in the current appearance of tall grasses with scattered tall trees. Canopy trees are deciduous in the dry season but the under storey shrubs and trees are evergreen. Similarly, herbaceous layer which may include a few specialized grasses occurs over a variable portion of the forest floor. Compared to that of the Savannah zones, pasture resources in this zone are not very significant.

4. Mixture of Widely Open Forest / Woodland

A visit to Nkwanta and Kpasa in the Nkwanta District showed vegetation cover that is predominantly widely open forest with woodland patches. Again, major land use activities in the area are farming and cattle rearing. Indicators of land degradation noted in this area include soil compaction due to Fulani cattle grazing activities and soil erosion during the raining season.
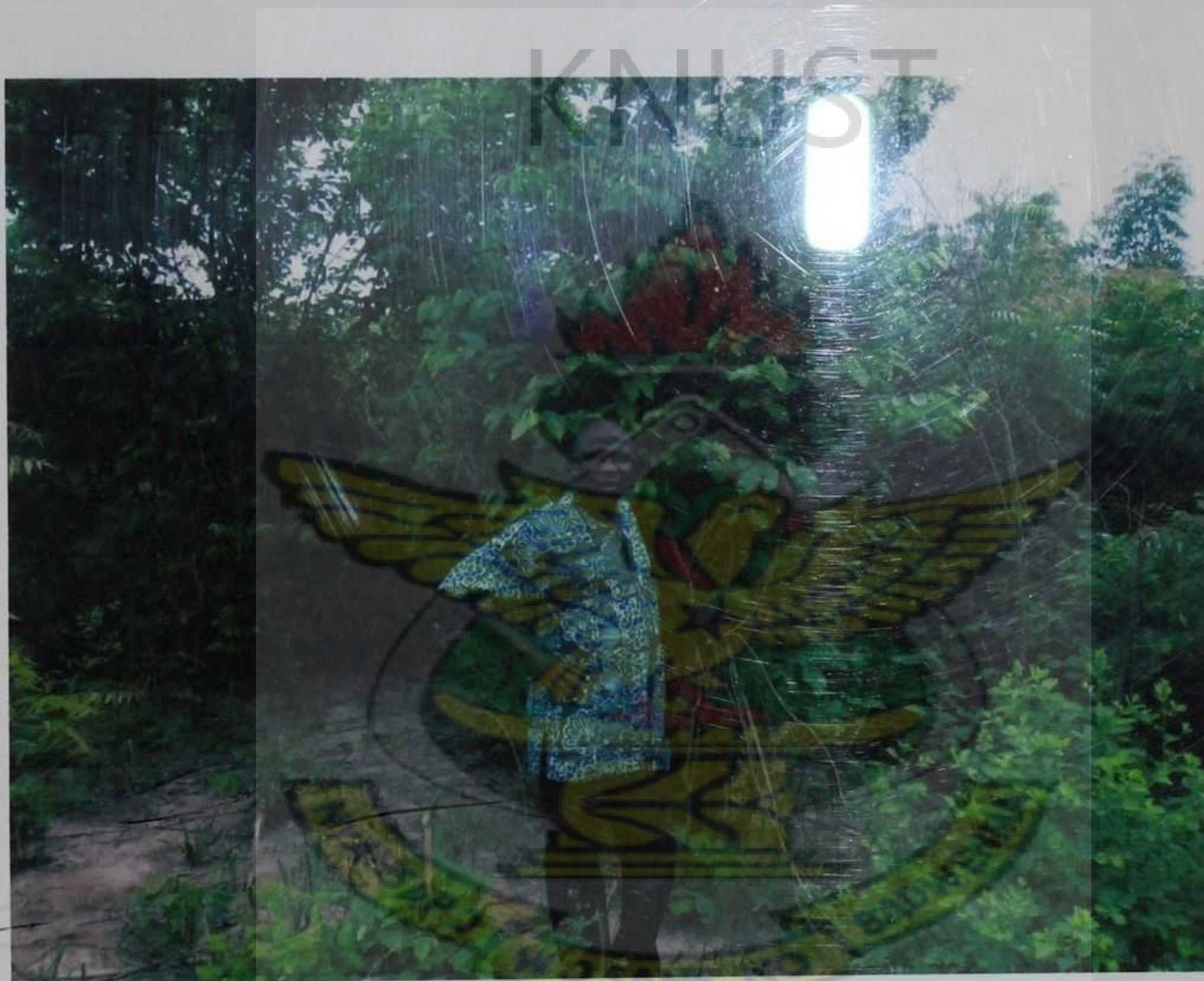

Figure 4: Showing widely open forest at Nkwanta

The residents of the area were of the opinion that even though some of them own cattle they are careful about where their cattle graze such that they do not destroy the natural environment and farms. The main climatic factor is rainfall, which comes in two peaks. March - July is the main season and September - October, the minor rainy season. The annual total rainfall is about 700 to 800 mm.

5. Grassland with Scattered Trees

A visit to Deatsawome and Medjikope in the Volta Region, showed grassland vegetation with scattered trees interspersed with isolated cases of woody vegetation cover in unsettled areas. According to the natives, much of the land degradation originated from cattle grazing activities as well as charcoal production.

Figure 5: Showing grassland vegetation type at Deatsawome

Farmers in these settlements noted that major challenge to agriculture is soil compaction arising from groups of cattle between 200 and 500 trampling the land as they move about to graze. The unsuitable compact soils compelled most farmers to move to more fertile woody vegetation lands for farming which contributed to further losses of the woody vegetation cover. Rainfall in the zones comes in one peak, which starts in April - May and builds up slowly to a height in August - September and declines sharply in October - November.

102

6. Grassland / Bare Surface / Settlement

The vegetation cover in most parts of Greater Accra Region such as Bueko, Adjen Kotoku and Oboum is most often open canopy grassland with scattered trees and uncompleted / completed structures. The inhabitant acknowledges the fact that the rapid rate of development in these areas has resulted in the increase of heat in the communities.

Figure 6: Showing grassland / bare surface vegetation type at Adjen Kotoku

The grasses associated with these zones are not uniform but differ according to soil type and moisture regime. The grassy background of the zone is invariably dominated by *Andropogon gayanus* with *Hyparrhenia* and *Schizachyrium* as co-dominants in some areas. The rainfall in this zone also comes in one peak, which starts in April - May and builds up slowly to a height in August - September and declines sharply in October - November. The total precipitation is also about 1,100 mm per annum, with a range from about 800 mm to about 1,500 mm.